DISSERTATION

RATE CONSTANT MEASUREMENT AND MECHANISTIC PROBE OF PROTONATION OF RHENIUM(III) OXO ALKYNE COMPLEXES

submitted by

Yi Han

Department of Chemistry

In partial fulfillment of the requirements

for the Degree of Doctor of Philosophy

Colorado State University

Fort Collins, Colorado

Fall 2000

COLORADO STATE UNIVERSITY

April 25, 2000

WE HEREBY RECOMMEND THAT THE DISSERTATION PREPARED UNDER OUR SUPERVISION BY YI HAN ENTITLED " RATE CONSTANT MEASUREMENT AND MECHANISTIC PROBE OF PROTONATION OF RHENIUM(III) OXO ALKYNE COMPLEXES" BE ACCEPTED AS FULFILLING IN PART REQUIREMENT FOR THE DEGREE OF DOCTOR OF PHILOSOPHY.

Committee on graduate work

Advisor

Department Head

ABSTRACT OF DISSERTATION

RATE CONSTANT MEASUREMENT AND MECHANISTIC PROBE OF PROTONATION OF RHENIUM(III) OXO ALKYNE COMPLEXES

Separated and somewhat broadened peaks were found for their protonated derivatives when $Re(O)(Et)(MeC{\equiv}CMe)_2$ and $Re(O)(Me)(MeC{\equiv}CMe)_2$ were treated with acids below room temperature. The upper limit of the rate constant for the protonation of $Re(O)(Et)(MeC{\equiv}CMe)_2$ by CF_3SO_3H was estimated to be 120 $M^{-1}s^{-1}$ at -15 °C, much slower than a diffusion-controlled one.

The protonation of oxo (iodo)(η^2-2,7-nonadiyne) rhenium(III), (**1**), was studied thoroughly in order to determine the rate constants. Strong acids were needed to protonate the terminal oxo ligand. Crystals of the final product, $Re(I)(CH_3CN)_3(CH_3C{\equiv}C(CH_2)_3CC{\equiv}CH_3)(BF_4)_2$, (**3**), were obtained from protonation with $HBF_4{\bullet}(CH_3)_2O$ in CH_3CN/CH_2Cl_2 mixed solution, so that the X-ray structure of **3** could be determined.

A two-step consecutive protonation of the terminal oxo ligand, A→B→C, was observed when the reaction of **1** with CF_3SO_3H in acetonitrile was monitored by a rapid scan stopped-flow apparatus at low temperature. Both steps proved to be second order, first in [**1**] and in [CF_3SO_3H]. The second order rate constants were of the order of 10^1 $M^{-1}s^{-1}$ at -40 °C, much slower than the diffusion-controlled one. Rearrangements involved

in the protonation were modeled by the reaction of **1** with $B(C_6F_5)_3$, a model for protonation at oxo ligand.

Two intermediates, X and Y, were found when complex **1** was treated with CF_3SO_3H. In low temperature ^1H NMR spectra the observed first-order rate constants for the conversion of X and Y to **3**, obtained from exponential fitting of the experimental data, showed no correlation with acid concentration.

A mechanistic scheme was proposed to account for all the experimental findings. A seemingly simple proton transfer can be very complicated.

Yi Han
Department of Chemistry
Colorado State University
Fort Collins, CO 80523
Fall 2000

ACKNOWLEDGMENT

I am grateful to my parents for their support and understanding. We haven't met in almost seven years since I came here to pursue my degree in chemistry. They always encourage me in their letters and telephone calls. I miss them. I thank Dr. Jack Norton for giving me the opportunity to work in his research group. I learned a lot from him, chemistry and hard working. Many past group members helped me in my research. Dr. Nikolaos Spetseris gets me started on my research project. Dr. Philipp Stössel, and Dr. Jeff Harlan helped me with their excellent experimental techniques. I am also thankful to Dr. Anthony Rappé for his insightful suggestion regarding the dialkyne chelating ligand. My thanks go to many past and present members of Norton group for their feedbacks on this project. Lastly and most importantly I thank my wife, Tong Hu, who supports me throughout the ups and downs in my graduate studies.

To My Family

Table of Contents

List of Figures

List of Tables

List of Abbreviations

ArF′	3,5-bis(trifluoromethyl)phenyl
en	ethylenediamine
Et	ethyl
IR	infrared
Me	methyl
NMR	nuclear magnetic resonance
Ph	phenyl
R*f*	retardation factor
UV-Vis	ultraviolet and visible

CHAPTER ONE—BACKGROUND OF THE CURRENT STUDY

I. Proton Transfer Reactions

Overview. Acid was discovered and used by ancient human beings in their food and drinks. Later, acids and bases played key roles in the development of experimental chemistry. Acid-base reactions have been extensively studied, and a lot of data have been collected regarding the strength of acids and bases.

Proton transfer reactions are ubiquitous in nature and are important in biological systems. Often they are very fast, but some are slow.

A. Acids and Bases

Definition of Acid and Base. There are two definitions of acid and base, one proposed by Brønsted and the other proposed by Lewis. In 1923, J. N. Brønsted [1] proposed that "An acid is a species having a tendency to lose a proton, and a base is a species having a tendency to add on a proton." G. N. Lewis [2] had a somewhat different definition. A Lewis acid is defined as a species that can accept an electron pair with the

[1] Brønsted, J. N. *Rec. Trav. Chim.* **1923**, *42*, 718.

formation of a covalent bond. Similarly, a Lewis base is defined as species that can donate an electron pair with the formation of a covalent bond. Proton is a Lewis acid.

A proton is unique. It has no electron outside the nucleus. Therefore it has a radius of only 10^{-5} Å, compared to other ions whose radii are about 1 Å and larger.[3] It has strong polarizing power on atoms nearby. For this reason it is always associated with other molecules in solution, sometimes solvent molecules.

Strength of Acids and Bases. The pK_a values of a vast number of inorganic, organic, and organometallic compounds have been measured and tabulated in aqueous solution and in many other organic solvents. Other ways to measure the strength of an acid include its Hammett acidity function. Superacids are defined as acid systems that are stronger than 100% sulfuric acid, as proposed by Gillespie.[4] The Hammett acidity function of pure sulfuric acid, H_0, is -11.93.[5] Fluorosulfuric acid and trifluoromethanesulfonic acid, whose Hammett acidity functions H_0 are -15.1 and -14.1 respectively, are Brønsted acids with superacid strength.[6] Trifluoromethanesulfonic acid has been extensively used as a strong acid to protonate metal complexes. It is stable, safe, easy to handle and readily available.

---

[2] Lewis G. N. *Valency and the Structure of Atoms and Molecules*; Reinhold: New York, 1923.

[3] Bell, R. P. *The Proton in Chemistry*, Cornell University Press: Ithaca, New York, 1973.

[4] (a) Gillespie, R. J.; Peel, T. E. *Adv. Phys. Org. Chem.* **1972**, *9*, 1. (b) Gillespie, R. J.; Peel, T. E *J. Am. Chem. Soc.* **1973**, *95*, 5173.

[5] O'Donnell, T. A. *Superacids and Acidic Melts as Inorganic Chemical Reaction Media*, VCH: New York, 1993.

[6] Olah, G. A.; Prakash, G. K. S.; Sommer, J. *Superacids*, John Wiley & Sons: New York, 1985.

Mechanistic Aspects of Proton Transfer Reaction. Extensive studies have been carried out to probe how this simple reaction happens. Eigen[7] proposed a three-step mechanism (Figure 1.1):

1) Hydrogen bond formation upon the diffusion of acid and base together.

2) Proton transfer through the hydrogen bond.

3) Diffusion apart of the products.

$$A{-}H + B \rightleftharpoons A{-}H^{\cdots}B \rightleftharpoons A^{-}{\cdots}H{-}B^{+} \rightleftharpoons A^{-} + H{-}B^{+}$$

Figure 1.1. Proposed scheme for a proton transfer reaction.

Brønsted Relationship. The rate of a proton transfer reaction and the thermodynamic driving force of the reaction are correlated by the Brønsted relation, also called the Brønsted catalysis law. It was first proposed by Brønsted and Pedersen[8] in 1924. It states that the log of the rate constant is a function of the equilibrium constant (usually the pK_a difference between the two acids involved). Over a narrow range of thermodynamic driving force the Brønsted relation (eq 1.1.) is obeyed (Figure 1.2). It is useful to know the value of α so that at a given driving force the rate of a proton transfer reaction can be predicted.

---

[7] Eigen, M 'Fast React. Primary Processes Chem. Kinet.', in *Proc. Nobel Symp.*, Claessen, S. Ed., Almqvist and Wisksell: Stockholm, 1967, pp. 245.

[8] Brønsted, J. N.; Pedersen, K. Z. *Phys. Chem.* **1924**, *108*, 185.

$$\log k = \alpha \log K + C \qquad C = \text{constant} \qquad \text{(eq 1.1.)}$$

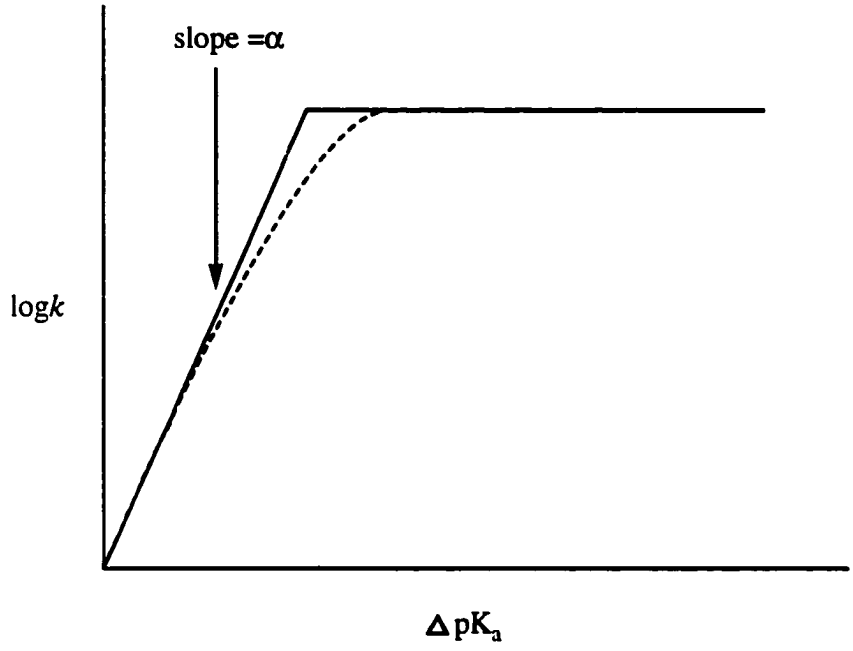

Figure 1.2. Typical Brønsted plot.

Marcus Theory Applied to Proton Transfer Reactions. Originally Marcus theory[9] was developed for electron transfer processes. It has been expanded to include atom transfer and proton transfer reactions. In Marcus theory, the activation energy of a reaction consists of two components, one from the thermodynamic driving force of the reaction, e.g. the free energy difference between the starting materials and the products;

[9] (a) Marcus, R. A. *Ann. Rev. Phys. Chem.* **1964**, *15*, 155. (b) Marcus, R. A. *J. Phys. Chem.* **1968**, *72*, 891. (c) Albery, W. J. *Ann. Rev. Phys. Chem.* **1980**, *31*, 227.

the other from the intrinsic barrier arising from the reaction if it were thermoneutral. With some assumptions, the overall activation energy of a reaction can be derived as the following (eq 1.2). The Brønsted exponent α is given by (eq 1.3.) and the variation of α is given by (eq 1.4). Extrapolation of a Brønsted plot to ΔpK_a (ΔG^0) = 0 should give the value of $\Delta G^{\ddagger}_{int}$, the intrinsic barrier. Proton transfer reactions can be compared with each other on the basis of their intrinsic barrier. The rate of the reaction could be predicted from the free energy change of the reaction.

$$\Delta G^{\ddagger} = \Delta G^{\ddagger}_{int} + \frac{1}{2}\Delta G^{0} + \frac{(\Delta G^{0})^{2}}{16\,\Delta G^{\ddagger}_{int}} \qquad \text{(eq 1.2.)}$$

$\Delta G^{\ddagger}$: overall activation energy, $\Delta G^{\ddagger}_{int}$: intrinsic barrier, ΔG^{0}: overall free energy change of the reaction.

$$\alpha = \frac{\partial \Delta G^{\ddagger}}{\partial \Delta G^{0}} = \frac{1}{2} + \frac{\Delta G^{0}}{8\Delta G^{\ddagger}_{int}} \qquad \text{(eq 1.3.)}$$

$$\frac{\partial \alpha}{\partial \Delta G^{0}} = \frac{1}{8\Delta G^{\ddagger}_{int}} \qquad \text{(eq 1.4.)}$$

B. Kinetic Issues of Proton Transfer Reactions

Fast Proton Transfer Reactions. Typically proton transfer to or from an oxygen or nitrogen atom in an organic molecule is fast. There is little reorganization of the bonding electrons and no repulsion between non-bonding electrons involved in this type

of proton transfer reaction. The second-order rate constants for such reactions are usually greater than 10^{10} $M^{-1}s^{-1}$ at room temperature in aqueous solution when the pK_a difference between the two acids involved shows that the reaction is favored by more than 4 units.[3] Even if the pK_a difference is uphill by 4 pK_a units, the rate constant will still be greater than 10^6 $M^{-1}s^{-1}$. There is a small barrier to transferring a proton onto, or removing a proton from, an oxygen or nitrogen lone pair as long as the hybridization remains sp^3 (Figure 1.3).

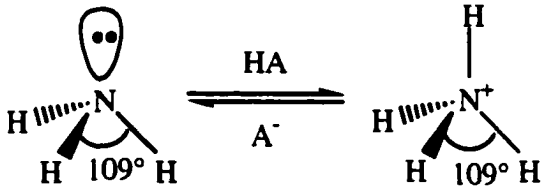

Figure 1.3. Little rearrangement associated with proton transfer to nitrogen base.

Slow Proton Transfer Reactions. Proton transfer reactions involving carbon acids can be slow.[10] There are substantial electronic and structural rearrangements in the process. A negative charge on a carbon atom, produced by the loss of a proton, is not stable. It tends to delocalize to the heteroatom in the molecule or to be stabilized by other rearrangements.

The second order rate constant of the proton transfer reaction between nitromethane and strong base (OH^-) is about 25 $M^{-1}s^{-1}$ at 25 °C (Figure 1.4).[3] Structure II is the dominant resonance structure for this molecule. There are electronic and structural

[10] Kramarz, K. W.; Norton, J. R. *Prog. Inorg. Chem.* **1994**, *42*, 1.

rearrangements involved in this reaction. The negative charge on the carbon atom upon deprotonation is delocalized to an oxygen atom eventually. The hybridization of the carbon atom must change from sp^3 to sp^2. The bond order and bond angle are also changed.

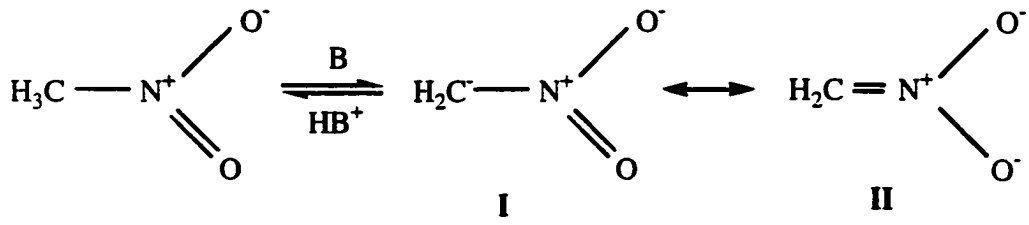

Figure 1.4. Substantial rearrangement associated with proton transfer from carbon acid.

Recently, slow protonations of $[NBu^n_4]_2[Fe_4S_4Cl_4]$ with $(NHEt_3)BPh_4$ or $[NH_2(CH_2)_3CH_2](BPh_4)$ have been observed (eq 1.5).[11] The upper limit for the protonation rate constant is estimated to be $k \leq 4.8 \times 10^2\ M^{-1}s^{-1}$ when the reaction is thermodynamically uphill for 2.8 pK_a unit. The rate constants are estimated to be in the range of $2 \times 10^5 \leq k \leq 4.8 \times 10^6\ M^{-1}s^{-1}$ when the reaction is downhill for 1 pK_a unit. The authors attributed this slower than diffusion-controlled rate constant of protonation to the structural rearrangement assumed to occur when one atom of the cluster framework is protonated.[12]

[11] Henderson, R. A.; Oglieve, K. E. *J. Chem. Soc., Dalton Trans.* **1999**, 3927.

[12] Henderson, R. A. *Angew Chem. Int. Ed. Engl.* **1996**, *35*, 946.

$$[Fe_4S_4Cl_4]^{2-} + [NHR_3]^+ \overset{k}{\rightleftharpoons} [Fe_4S_3(SH)Cl_4]^- + NR_3 \qquad \text{(eq 1.5.)}$$

In *summary*, the rate constant of proton transfer reaction is fast if there is little rearrangement involved; on the other hand, the rate constant of a proton transfer reaction is slow if there is considerable rearrangement involved.

C. Proton Transfer Reactions of Organometallic Complexes

1. Proton Transfer Reactions of Transition Metal Hydride Complexes

Electronic and Structural Rearrangement. Considerable electronic and structural rearrangements occur in the proton transfer reactions of transition metal hydrides. Therefore it is expected that the rate constants of these reactions could be significantly slower than those of diffusion-controlled processes even with a favorable thermodynamic driving force. Carbonyl stretching frequencies in IR spectra change over 100 cm^{-1} when $HCo(CO)_4$ or $HMn(CO)_5$ is deprotonated.[10] The negative charge generated upon the loss of the proton does not stay on the metal but is delocalized onto the carbonyl ligands. Structural change also occurs when $HCo(CO)_4$ is deprotonated by $(CH_3)_3N$.[13] The bond angles change around the Co but there is little change around the nitrogen atom (Figure 1.5). Hydrogen bonding between acids and bases, which is considered as an essential step prior to proton transfer (see figure 1.1), is not observed

[13] (a) Kristjánsdóttir, S. S.; Norton, J. R. in *Transition Metal Hydride: Recent Advances in Theory and Experiment*, Dedieu, A, Ed., VCH: New York, 1992; pp. 309-359. (b) Beagley, B.; Hewitt, T. G. *Trans. Faraday Soc.* **1968**, *64*, 2561. (c) McNeil, E. A.; Scholer, F. R. *J. Am. Chem. Soc.* **1977**, *99*, 6243. (d) Calderazzo, F.; Fachinetti, G.; Marchetti, F.; Zanazzi, P. F. *J. Chem. Soc. Chem. Commun.* **1981**, 181.

with $HCo(CO)_4$ and $(CH_3)_3N$ by infrared and Raman spectroscopy.[14] The rationale for this is that H-Co bond in neutral hydride, like $HCo(CO)_4$, is polarized $H^{\delta-}$-$Co^{\delta+}$; thus $HCo(CO)_4$ cannot be a hydrogen-bond donor. Therefore during proton transfer H-Co must to be repolarized so that the hydrogen atom leaves as a proton and the Co center keeps the electrons. This can lead to a significant intrinsic barrier for such reactions.

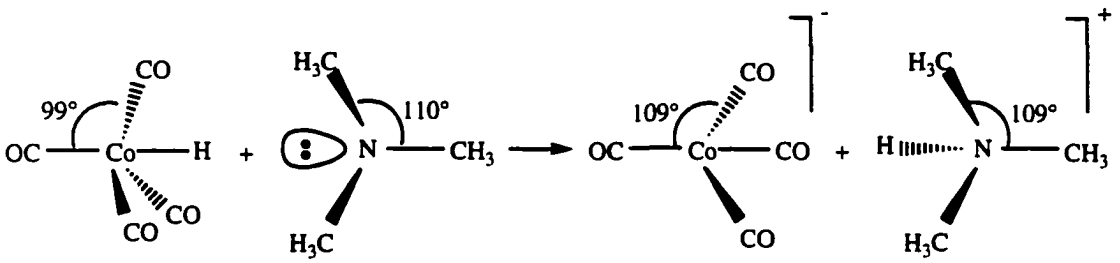

Figure 1.5. Structural rearrangement associated with proton transfer from transition metal hydride complex, $HCo(CO)_4$.

Hydrogen bonding between cationic transition metal hydrides and bases with lone pairs has been detected.[15] The formation of ionic hydrogen bonds between cationic hydrides and trifluoroacetate anion, $[MH]^+ \cdots OCOCF_3^-$ is observed in the deprotonation of $[Cp^*OsH]A$ ($A = BF_4$, PF_6, SO_2CF_3)[15b] and $[WH_5(dppe)_2]A$.[15a] IR evidence for hydrogen bonding is also observed with $[Cp^*OsH]PF_6$ and triphenylphosphine oxide.[15c]

---

[14] Kristjánsdóttir, S. S.; Norton, J. R.; Moroz, A.; Sweany, R. L.; Whittenburg, S. L. *Organometallics*, **1991**, *10*, 2357.

[15] (a) Shubina, E. S.; Krylov, A. N.; Belkova, N. V.; Epstein, L. M.; Borisov, A. P.; Makaev, V. D. *J. Organomet. Chem.* **1995**, *493*, 275. (b) Shubina, E. S.; Krylov, A. N.; Kreindlin, A. Z.; Rybinskaya, M. I.; Epstein, L. M. *J. Organomet. Chem.* **1994**, *465*, 259. (c) Epstein, L. M.; Shubina, E. S.; Krylov, A. N.; Kreindlin, A. Z.; Rybinskaya, M. I. *J. Organomet. Chem.* **1993**, *447*, 227. (d) Peris, E.; Crabtree, R. H. *J. Chem. Soc., Chem. Commun.* **1995**, 2179.

In the presence of phosphine oxide, the intensity of ν_{OsH} increases and the growth of the low frequency absorption takes place. The intensity of $\nu_{PO\text{-}free}$ decreases and the lower frequency bands belonging to bonded phosphine, $\nu_{PO\text{-}bonded}$, increase. With $(Me_2N)_3PO$ hydrogen bonding is observed along with the partial proton transfer from the hydride to $(Me_2N)_3PO$.[15c] No hydrogen bonding is observed with nitrogen bases (Et_3N, pyridine). Spectral evidence for hydrogen bonding is also observed in cationic dihydrides, $[IrH_2(PPh_3)_2L_2]BF_4$ (L = Co, Me_2CO, and $P(OMe)_3$), with Ph_3PO.[15d] Novel hydrogen bonding modes have also been detected between acids and the metal centers of transition metal complexes, XH ••• M,[16] and between acids and metal hydrides, XH ••• HM.[15b,17]

Slow Proton Transfer Rate Constants. Our group has been studying proton transfer reactions of transition metal hydrides over the years. Rate constants of proton transfer reactions between transition metal hydrides and bases have been measured. For example the rate constants of a series of reactions between transition metal hydride and aniline had been measured (eq 1.6).[14,18] The second order rate constants for $HCo(CO)_4$ and $HMn(CO)_5$ in acetonitrile at 25 °C are 1.7×10^6 $M^{-1}s^{-1}$ and 2.1×10^2 $M^{-1}s^{-1}$,

---

[16] For recent reviews: (a) Shubina, E. S.; Belkova, N. V.; Epstein, L. M. *J. Organomet. Chem.* **1997**, *536-537*, 17. (b) Epstein, L. M.; Shubina, E. S. *Ber. Bunsenges. Phys. Chem.* **1998**, *102*, 359.

[17] For recent reviews: (a) Shubina, E. S.; Belkova, N. V.; Bakhmutova, E. V.; Saitkulova, L. N.; Ionidis, A. V.; Epstein, L. M. *Russ. Chem. Bull.* **1998**, *47*, 817. (b) Crabtree, R. H. *J. Organomet. Chem.* **1998**, *557*, 111. (c) Crabtree, R. H.; Siegbahn, P. E. M.; Eisenstein, O.; Rheingold, A. L.; Koetzle, T. F. *Acc. Chem. Res.* **1996**, *29*, 348.

[18] (a) Jordan, R. F.; Norton, J. R. *J. Am. Chem. Soc.* **1982**, *104*, 1255. (b) Jordan, R. F.; Norton J. R. *ACS Symp. Ser.* **1982**, *198*, 403. (c) Edidin, R. T.; Sullivan, J. M.; Norton, J. R. *J. Am. Chem. Soc.* **1987**, *109*, 3945. (d) Weberg, R. T.; Norton, J. R. *J. Am. Chem. Soc* **1990**, *112*, 1105. (e) Kristjánsdóttir, S. S.; Norton, J. R. *J. Am. Chem. Soc* **1991**, *113*, 4366. (f) Kristjánsdóttir, S. S.; Loendorf, A. J.; Norton, J. R. *Inorganic Chemistry* **1991**, *30*, 4470. (g) Moore, E. J.; Sullivan, J. M.; Norton, J. R. *J. Am. Chem. Soc* **1986**, *108*, 2257. (h) Kristjánsdóttir, S. S.; Moody, A. E.; Weberg, R. T.; Norton, J. R. *Organometallics*, **1988**, *7*, 1983. (i) Weberg, R.; Norton, J. R. *J. Am. Chem. Soc* **1990**, *112*, 1105.

respectively. These rates are slower than those of proton transfer reactions from oxygen or nitrogen acids of comparable thermodynamic strength under similar conditions.

$$M—H + \text{aniline} \xrightarrow{k_{H+}} M^- + \text{aniline}—H^+ \qquad \text{(eq 1.6.)}$$

2. Proton Transfer Reactions of Transition Metal Complexes with Oxygen Ligand.

As mentioned above, proton transfer to or from oxygen in an organic molecule is fast if the thermodynamic driving force is sufficiently favorable. However oxo ligands in transition metal complexes are not like oxygens in organic molecules.[10] Depending on the metal involved and other conditions, the bond between the metal and a terminal oxo ligand can be a single, double, or triple bond (Figure 1.6);[19] for example the bond between Re(III) and oxo ligand in a series of $Re(O)X(RC{\equiv}CR)_2$ is believed to have triple bond character.[20] Theoretical study supports the suggestion that the bond between the metal (Mo, W, Re) and the oxo ligand in some metathesis catalysts could be a triple bond.[21] Protonation of such an oxo ligand could change the bonding situation significantly. Electronic and structural rearrangement must occur. The rate of protonation could be much slower than that of protonation of an organic oxygen under

[19] Nugent, W. A.; Mayer, J. M. *Metal-Ligand Multiple Bond*, Wiley-Interscience: New York, 1988.

[20] (a) Mayer, J. M.; Thorn, D. L.; Tulip, T. H. *J. Am. Chem. Soc.* **1985**, *107*, 7454. (b) Mayer, J. M.; Tulip, T. H.; Calabrese, J. C.; Valencia, E. *J. Am. Chem. Soc.* **1987**, *109*, 157.

[21] Rappé, A. K.; Goddard, III, W. A. *J. Am. Chem. Soc.* **1982**, *104*, 448.

similar thermodynamic driving force. Protonation of bridging oxo ligand also causes electronic rearrangement between metals and the oxo ligand involved.[22]

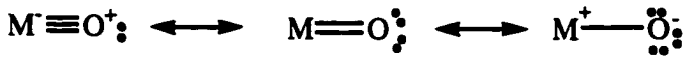

Figure 1.6. Different bonding modes between metal and an oxo ligand in a terminal oxo complex.

a. Proton Transfer Reactions of Transition Metal Complexes with Terminal Oxo Ligands.

Examples of Fast Proton Transfer in Dioxo Metal Complexes. The X-ray structures of $K_3Na[Mo(O)_2(CN)_4 \cdot 6H_2O]$,[23] $[Cr(en)_3][Mo(O)(OH)(CN_4)] \cdot H_2O$,[24] and $(PPh_4)_2[Mo(O)(OH_2)(CN)_4] \cdot 4H_2O$[25] have been reported. The Mo=O bond length shows an increase in double bond character, from 1.834 (9) Å for the oxo complex, to 1.698 (7) Å for the hydroxo complex, and to 1.668 (5) Å for the aqua complex; the Mo-O bond distance are 2.077 (7) Å for the hydroxo and 2.27-2.48 Å for the aqua complex.

---

[22] Knopp, P.; Wieghardt, K. *Inorg. Chem.* **1991**, *30*, 4061.

[23] Day, V. W.; Hoard, J. L. *J. Am. Chem. Soc.* **1968**, *90*, 3374.

[24] Robinson, P. R.; Schlemper, E. O.;Murmann, R. K. *Inorg. Chem.* **1975**, *14*, 2035.

[25] Wieghardt, K.; Backes-Dahmann, G.; Holzbach, W.; Swiridoff, W. J.; Weiss, J. Z. *Anorg. Allg. Chem.* **1983**, *499*, 44.

Proton transfer rate constants have been measured using ^{17}O NMR line broadening for $[M(O)_2(CN)_4]^{(n+2)-}$ (M = Mo(IV) and W(IV)) (eq 1.7).[26] In strongly basic media (pH > 11) for the Mo(IV) and W(IV) systems, the deprotonation rate constants (k_{-2b}) for the $[M(O)(OH)(CN)_4]^{4-}$ complexes have been determined as 2 (1) $\times 10^7$ and 4 (2) $\times 10^8$ $M^{-1}s^{-1}$, while protonation rate constants (k_{2b}) for the $[M(O)_2(CN)_4]^{3-}$ complexes have been determined to be 1.3 (2) $\times 10^9$ and 7 (2) $\times 10^8$ s^{-1}.

$$[M(O)(OH)(CN)_4]^{3-} + OH^- \underset{k_{2b}}{\overset{k_{-2b}}{\rightleftharpoons}} [M(O)_2(CN)_4]^{4-} + H_2O \qquad \text{(eq 1.7.)}$$

Proton transfer rate constants have also been measured for Re(V) and Tc(V) systems in acidic media (pH < 5) (eq 1.8, 1.9), $k_{1a} \geq 1 \times 10^8$ s^{-1} (for Tc: $\geq 1 \times 10^7$), k_{2a} = 1.1 (2) $\times 10^7$ s^{-1} (for Tc: 1.1 (5) $\times 10^7$), $k_{-2a} = 6$ (1) $\times 10^{10}$ $M^{-1}s^{-1}$ (for Tc: ~ 1×10^{11}), and $k_{-1a} \geq 2 \times 10^9$ $M^{-1}s^{-1}$ ($\geq 8 \times 10^9$). The reason why these protonations are fast is not clear.

$$[M(O)(OH_2)(CN)_4]^- \underset{k_{-1a}}{\overset{k_{1a}}{\rightleftharpoons}} [M(O)(OH)(CN)_4]^{2-} + H^+ \qquad \text{(eq 1.8.)}$$

$$[M(O)(OH)(CN)_4]^{2-} \underset{k_{-2a}}{\overset{k_{2a}}{\rightleftharpoons}} [M(O)_2(CN)_4]^{3-} + H^+ \qquad \text{(eq 1.9.)}$$

[26] Roodt, A.; Leipoldt, J. G.; Helm, L.; Merbach, A. E. *Inorg. Chem.* **1994**, *33*, 140.

Evidence for Slow Proton Transfer to Terminal Oxo Ligands. Qualitative evidence exists suggesting that proton transfer to terminal oxo ligands of transition metal complexes can be slow.

Erikson and Mayer[27] have reported the extremely slow (half-life about 11 hrs) tautomerization between the oxo and hydroxo ligands in $Re(O)(OH)(2\text{-butyne})_2$ by monitoring an ^{18}O label (eq 1.10). Addition of a catalytic amount of triflic acid dramatically accelerates the equilibration by protonation of the oxo ligand. They suggest that the slow tautomerization can be rationalized by the fact that the proton transfers to a rhenium-oxygen π-bonding orbital and not to an oxygen lone pair. Therefore, as mentioned earlier, the proton transfer is coupled to dramatic changes in the bonding and structure.

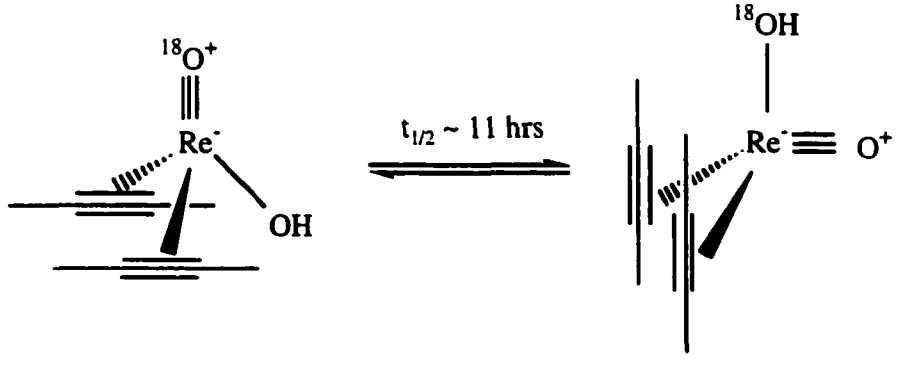

(eq 1.10.)

Dovletoglou and Meyer[28] have reported that the isomerization of trans-$[Ru^{II}(tpy)(O)(O{=}P(PPh_2)CH_2CH_2PPh_2)(H_2O)]^{2+}$ (tpy = 2, 2': 6', 2"-terpyridine) is

---

[27] Erikson, T. K. G.; Mayer, J. M. *Angew. Chem. Int. Ed. Engl.* **1988**, *27*,1527.

[28] Dovletoglou, A.; Meyer, T. J. *J. Am. Chem. Soc.* **1994**, *116*, 215.

achieved by proton transfer from an aqua to an oxo ligand (eq 1.11). In 1.75 M acetonitrile in water the rate constant has been measured as $k = (6.20 \pm 0.12) \times 10^{-2}$ s^{-1} at 20 °C.

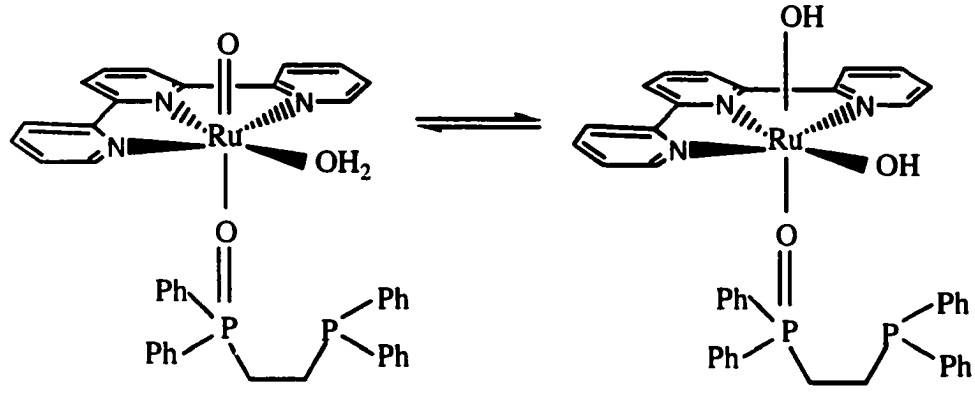

(eq 1.11.)

Terminal Oxo and Hydroxo Complexes with Metals at Same Oxidation States. Not many well-characterized pairs of terminal oxo and hydroxo complexes have been reported. Some examples include $[Re(en)_2(O)_2]^+/[Re(en)_2(O)(OH)]^{2+}$,[29] $[Re(py)_4(O)_2]^+/[Re(py)_4(O)(OH)]^{2+}$,[29a] $[Re(py)_2(Cl)_2(OH)_2]Cl/[Re(py)_2(Cl)_2(O)(OH)]$,[29a] $[Re(en)(OH)_2(Cl)_2]Cl/[Re(en)(Cl)_2(O)(OH)]$,[29a] $[Re(O)_2(cyclam)]^+/[Re(O)(OH)(cyclam)]^{2+}$,[30] *trans*-$[Mo(O)_2(dppe)_2]$/*trans*-$[Mo(O)(OH)(dppe)_2]^+$,[31] $[Re(O)_2L_4]^+/[Re(O)(OH)L_4]^{2+}$ (L = ImH (imidazole) and related

[29] (a) Beard, J. H.; Casey, J.; Murmann, R. K. *Inorg. Chem.* **1965**, *4*, 797. (b) Murmann, R. K *Inorganic Synthesis* **1966**, 8, 172.

[30] Tsang, B. W.; Reibenspies, J.; Martell, A. E. *Inorg. Chem.* **1993**, *32*, 988.

[31] Bendix, J.; Birkedal, H.; Bøgevig, A. *Inorg. Chem.* **1997**, *36*, 2702.

compounds),[32] $(\eta^5\text{-}C_5Me_5)_2Zr(O)(NC_5H_5)$ and $(\eta^5\text{-}C_5Me_5)_2Zr(OH)_2\bullet(H_2O)$,[33] and $Re(O)(Et)(MeC{\equiv}CMe)_2$/ $[Re(OH)(Et)(MeC{\equiv}CMe)_2]^+$.[34]

The IR and UV-Vis characterization of rhenium complexes of $[Re(en)_2(O)_2]^+$/$[Re(en)_2(O)(OH)]^{2+}$, $[Re(py)_4(O)_2]^+$/$[Re(py)_4(O)(OH)]^{2+}$, $[Re(py)_2(Cl)_2(OH)_2]Cl$/$[Re(py)_2(Cl)_2(O)(OH)]$, and $[Re(en)(OH)_2(Cl)_2]Cl$/$[Re(en)(Cl)_2(O)(OH)]$ has been reported.[29a]

$[Re(O)_2(cyclam)](ClO_4)$ and $[Re(O)(OH)(cyclam)](ClO_4)_2$ (cyclam = 1,4,8,11-tetraazacyclotetradecane) and related derivatives of cyclam complexes have been reported.[30] The cyclam ligand is drawn in Figure 1.7. The X-ray structure of $[Re(O)(OH)(cyclam)](ClO_4)_2$ has been determined. The complex forms weak hydrogen bonds between the axial hydroxo ligands and the oxygen atoms of adjacent molecules. The complex with the open-chain version of the ligands (1,4,8,11-tetraazaundecane and its related compounds) has also been reported.[35]

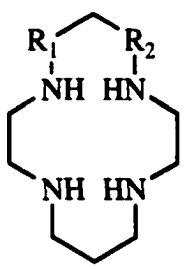

[32] Bélanger, S.; Beauchamp, A. L. *Inorg. Chem.* **1996**, *35*, 7836.

[33] (a) Howard, W. A.; Waters, M.; Parkin, G. *J. Am. Chem. Soc.* **1993**, *115*, 4917. (b) Howard, W. A.; Parkin G. *Polyhedron* **1993**, *12*, 1253.

[34] Spaltenstein, E.; Erikson, T. K. G.; Critchlow, S. C.; Mayer, J. M. *J. Am. Chem. Soc.* **1989**, *111*, 617.

cyclam: $R_1 = R_2 = CH_2$

O_1-cyclam: $R_1 = CH_2$, $R_2 = C{=}O$

O_2-cyclam: $R_1 = R_2 = C{=}O$

Figure 1.7. The cyclam ligand and the related derivatives.

The synthesis of *trans*-$[Mo(O)_2(dppe)_2]$ (dppe = $Ph_2PCH_2CH_2PPh_2$) has been reported.[31] The X-ray structure of the methanol adduct of the complex has been determined. It is insoluble in most solvents and reacts with halogenated hydrocarbon solvents. When this complex is treated with an excess of acid ($HClO_4$ or H_2SO_4), UV-Vis spectra show that *trans*-$[Mo(O)(OH)(dppe)_2]^+$ is formed. With stronger acids like CF_3SO_3H, *trans*-$[Mo(O)(OH_2)(dppe)_2]^{2+}$ is believed to be formed.

$[Re(O)_2L_4]^+$and $[Re(O)(OH)L_4]^{2+}$ complexes with L = ImH (imidazole) and its methylated derivatives 1-MeIm, 1,2-Me_2Im, 2-MeImH, and 4(5)-MeImH and different counterions (I and $B(C_6H_5)_4$) have been reported.[32] The X-ray structures of some of the dioxo and oxo-hydroxo complexes have been determined. The Re-OH bond length is 1.896 Å compared to the average of 1.76 Å for Re=O (oxo). The Re=O bond length in oxo-hydroxo complex is 1.732 Å, decreasing a little from an average of 1.77 Å for dioxo complexes.

The X-ray structures of $(\eta^5\text{-}C_5Me_5)_2Zr(O)(NC_5H_5)$ and $(\eta^5\text{-}C_5Me_5)_2Zr(OH)_2{\bullet}(H_2O)$ have been reported.[33] The Zr=O bond length in $(\eta^5\text{-}C_5Me_5)_2Zr(O)(NC_5H_5)$ is 1.804 (4) Å, shorter than the Zr-O(H) bond length in

---

[35] Parker, D.; Roy, P. S. *Inorg. Chem.* 1988, 27, 4127.

$(\eta^5\text{-}C_5Me_5)_2Zr(OH)_2\bullet(H_2O)$, 1.976 (2)-2.028 (3) Å. The Zr-O(H) bond length in $(\eta^5\text{-}C_5Me_5)_2Zr(OH)Cl$ is 1.950(2) Å.[36]

In the case where the structures of both the terminal oxo and hydroxo complexes have been determined there are significant structural differences between the two. Protonation on the terminal oxo ligand causes structural rearrangement.

Terminal Oxo and Hydroxo Complexes with Metals at Different Oxidation States. In studies of the oxidation of $CpMoH(PMe_3)_3$, two complexes, $[CpMo(O)(PMe_3)_2][BF_4]$ and $[CpMo(OH)(PMe_3)_3][BF_4]$, have been isolated and their X-ray structures have been determined.[37] The Mo-O bond length is 1.674 (13) Å in the oxo complex and 2.080 (3) Å in the hydroxo complex. The Mo-P bond length is 2.445 (4) Å for the oxo complex and an average of 2.48 Å for hydroxo complex. The Mo-CNT distances (CNT = centroid of cyclopentadienyl ring) are 2.05 (2) Å for the oxo complex and 1.980 (2) Å for the hydroxo complex. $CpMo(O)(PMe_3)_2$ is formed in solution when $CpMoH(PMe_3)_3$ is treated with water and $AgBPh_4$.

Oxo Mn^{V}TMPyP (TMPyP = tetra-(N-methylpyridyl)porphyrinato) has been formed in solution when aqua Mn^{III}TMPyP is treated with the oxidants HSO_5^-, *m*-chloroperoxybenzoic acid and ClO^-.[38] With further treatment with $NaNO_2$, oxo

---

[36] Bortolin, R.; Patel, V.; Munday, I.; Taylor, N. J.; Carty, A. J. *J. Chem. Soc., Chem. Commun.* **1985**, 456.

[37] Fettinger, J. C.; Hraatz, H.-B.; Poli, R.; Quadrelli, E. A. *J. Chem. Soc., Dalton Trans.* **1999**, 497. $[CpMo(O)(PMe_3)_2](BF_4)$ was previously synthesized by others. See reference: Brookhart, M.; Cox, K.; Cloke, F. G. N.; Green, J. C.; Green, M. L. H.; Hare, P. M.; Bashkin, J.; Derome, A. E.; Grebenik, P. D. *J. Chem. Soc., Dalton Trans.* **1985**, 423. .

[38] (a) Groves, J. T.; Lee, J.; Marla, S. S. *J. Am. Chem. Soc.* **1997**, *119*, 6269. (b) Jin, N.; Groves, J. T. *J Am. Chem. Soc.* **1999**, *121*, 2923.

Mn^{IV}TMPyP is obtained. UV-Vis spectra and ^1H NMR characterization have been reported.

$LMo^{VI}(O)_2(SPh)$ (L = hydrotris(3,5-dimethyl-1-pyrazolyl)) has been obtained from the reaction of $LMoO_2Br$, HSPh, and NEt_3 in CH_2Cl_2 and $LMo^{V}(O)(OH)(SPh)$ has been detected when Me_2SO adds to $LMo^{IV}(O)(SPh)$ in wet toluene.[39] $LMo^{V}(O)(OH_2)(SPh)$ is believed to be involved in the process.

In the studies of reduction of *trans*-$[Ru^{IV}L(O)(H_2O)]^{2+}$ to *trans*-$[Ru^{III}L(OH)(H_2O)]^{2+}$ (L = 6,7,8,9,11,17,18-octahydro-6,10-dimethyl-5*H*-dibenzo[*e*,*n*][1,4,8,12]dioxadiazacyclopentadecine) and *trans*-$[Ru^{III}L(OH)(H_2O)]^{2+}$ to *trans*-$[Ru^{II}L(H_2O)_2]^{2+}$ via proton transfer coupled with electron transfer, the hydroxo complexes of Ru(IV) and Ru(III) are believed to be intermediates.[40] The self-exchange rate constants for *trans*-$[RuL(OH)(H_2O)]^{3+/2+}$ and *trans*-$[RuL(H_2O)_2]^{3+/2+}$ have been estimated.

From the above mentioned examples it is clear that the M-O bond length changes when the terminal oxo ligand is protonated. These rearrangements could cause significant barriers for proton transfer with these complexes.

b. Proton Transfer Reactions of Transition Metal Complexes with Bridging Oxo Ligands

[39] Xiao, Z.; Young, C. G.; Enemark, J. H.; Wedd, A. G. *J. Am. Chem. Soc.* **1992**, *114*, 9194.

[40] Li, C.-K.; Che, C.-M.; Tong, W.-F.; Lai, T.-F. *J. Chem. Soc., Dalton Trans.* **1992**, 813.

Rearrangement with Proton Transfer to Bridging Oxo Ligands. There is evidence that extensive geometric rearrangement is associated with protonation of an oxo bridge ligand. The most dramatic structural change upon protonation is the significant increase of the metal-oxygen bond length[22]. Lippard and coworkers[41] reported an increase from 1.780(2) Å, 1.788(2) Å to 1.960(4) Å, 1.952(4) Å in the Fe-O distance following the protonation of oxo ligand in $[Fe_2(\mu\text{-}O)(\mu\text{-}O_2CCH_3)_2(HBpz_3)_2]$ ($HBpz_3$ = hydrotris(1-pyrazoyl)borate). In $[L_2Mo_2(\mu\text{-}O)(\mu\text{-}O_2CCH_3)_2]^{2+}$ (L=1,4,7-trimethyl-1,4,7-triazacyclononane) Wieghardt[42] found that the Mo-O distances increase from 1.945(4) Å, 1.946(4) Å to 2.098(7) Å, 2.107(7) Å following protonation. A similar effect was also observed in the protonation of $[L_2Ru_2(\mu\text{-}O)(\mu\text{-}O_2CCH_3)_2]^{2+}$ (L: same as above), with an increase of the M-O bond distance by 0.10 Å.[43]

While the M-O bond length often increases upon protonation of a μ-oxo ligand the M-O-M angles do not always show a large effect. In the Fe case above, the angle changes from 123.1° to 123.6° upon protonation. For Ru complex above, the angle changes from 119.7° to 122.5°. There is a substantial change of the M-O-M angle in the Mo complex, from 95.7 to 115.4°. Necessarily the M-M distance also increases from 2.885Å to 3.555Å. A good example of a large M-O-M angle change is shown in Figure 1.8.[44]

---

[41] Armstrong, W. H.; Lippard, S. J. *J. Am. Chem. Soc.* **1984**, *106*, 4632.

[42] Neves, A.; Bossek, U.; Wieghardt, K.; Nuber, B.; Weiss, J *Angew. Chem. Int. Ed. Engl.* **1988**, *27*, 685.

[43] Neubold, P.; Wieghardt, K.; Nuber, B.; Weiss, J. *Inorg. Chem.* **1989**, *28*, 459.

[44] (a) Lueken, H.; Buchler, J. W.; Lay, K. L. *Z. Naturforsch. B*, **1976**, *31*, 1596. (b) Scheidt, W. R.; Cheng, B.; Safo, M. K.; Cukiernik, F.; Marchon, J.-C.; Debrunner, P. G. *J Am. Chem. Soc.* **1992**, *114*, 4420.

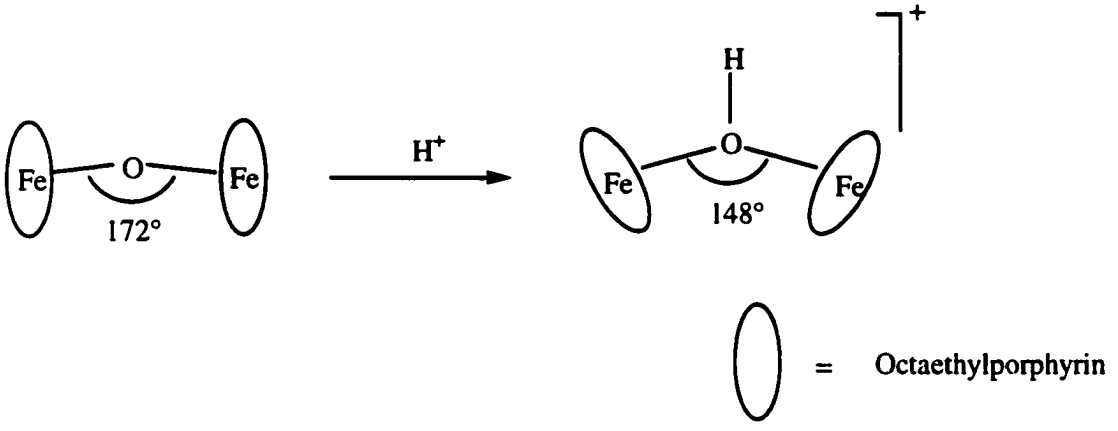

Figure 1.8. Fe-O-Fe angle changes upon proton transfer to bridge oxo ligand.

Recently, another μ-oxo iron porphyrin complex and its protonated form, [(tpp)Fe-O-Fe(tpp)] and [(tpp)Fe-OH-Fe(tpp)]Y (Y = $CB_{11}H_6X_6$ (X = Cl, Br, and I), or F_{20}-BPh_4) (tpp = tetraphenylporphyrinate), have been reported; the X-ray structures of both complexes have been determined.[45] The Fe-O-Fe is linear with an angle of 176.1 (2)° in the oxo complex, while the angles are 173.6 (5)° and 169.2 (1)° in the hydroxo complex with two different counterions. The authors suggest that the insignificant changes in this angle are due to the steric bulkiness of the tpp phenyl rings. The Fe-O bond lengths do change from 1.759 (1) Å in the oxo complex to 1.92 (3) Å and 1.821 (8) Å in the two hydroxo complexes. The iron atoms are closer to the porphyrin planes by 0.13 - 0.19 Å in the two hydroxo complexes, offsetting the increase in Fe-O bond lengths, so the separation of the porphyrin planes is little changed. The strong antiferromagnetic

[45] Evans, D. R.; Mathur, R. S.; Heerwegh, K.; Reed, C. A.; Xie, Z. *Angew. Chem. Int. Ed. Engl.* **1997**, *36*, 1335.

coupling ($J \approx -135\ cm^{-1}$) in the oxo complex is attenuated to nearly zero in the hydroxo complex due to the change of spin state and the longer Fe-O bonds, indicating that there is some electronic rearrangement upon protonation. Indeed, when the oxo and hydroxo complexes are mixed, no exchange is observed in the ^1H NMR spectrum. The authors argued that "this probably reflects the steric impossibility of the close approach of the protonated Fe-O(H)-Fe moiety to the unprotonated Fe-O-Fe moiety." It is clear that the accessibility of the base needs to be considered along with the structural and electronic rearrangement when slow proton transfer rate constants are rationalized.

The electronic and geometric rearrangement upon protonation of the oxo bridge ligand may be a possible cause for substantial kinetic barriers associated with these reactions similar to the ones observed in protonation or deprotonation at carbon and at transition metal hydrides. As a result, proton transfer involving an oxo bridge ligand could be considerably slower than those with comparable equilibrium constants involving oxygen in an organic compound.

Slow Rate Constant of Proton Transfer to Bridging Oxo Ligands. Proton transfer reactions involving an oxo bridge ligand of transition metal complexes can be slow. Qualitative evidence has been provided by Finke and co-workers[46] in their NMR studies of $(Bu_4N)_4H_3SiW_9V_3O_{40}$. The rate constant of the first protonation step of $[Mn(O)(salpn)]_2$ (salpn = 1,3-Bis(salicylideneiminato)propane) with 2,6-di-*t*-butyl-4-methyl pyridinium in acetonitrile is approximately 1500 $M^{-1}s^{-1}$ at -25 °C.[47] With chloride

[46] Finke, R. G.; Rapko, B.; Saxton, R. J.; Domaille, P. J. *J. Am. Chem. Soc.* **1986**, *108*, 2947.

[47] Kramarz, K. W.; Norton, J. R. unpublished results.

ion in the solution the rate constant of above protonation is 1.3×10^7 $M^{-1}s^{-1}$. The rate constant of the protonation of $[Mn(salpn)]_2(O)(OMe)^+$ with strong acids such as perchloric acid in acetonitrile is 5.5×10^6 $M^{-1}s^{-1}$ at -40 °C.[48] These results offer quantitative evidence that protonation of an oxo bridge ligand in transition metal complexes can be slow in some cases.

3. Methods for Determining Rate Constant

Methods that can be used to measure the rate constants of proton transfer reactions include rapid-scan stopped flow, NMR, UV-Vis and IR.

The rapid-scan stopped flow method can be used to measure the rate constant of a process that has a time scale ranging from milliseconds to seconds. If one follows the reaction over a wide range of wavelengths, unambiguous identification of the reaction that is monitored may be possible.

Several NMR techniques can be used to measure the rate constant of a reaction. Line broadening analysis measures rate constants from 3 to100 s^{-1}.[10] One advantage of this method is that it can measure the rate constant of a self-exchange process when no net reaction is happening. The line width of an isolated ^1H NMR resonance represents the lifetime of a proton in that chemical environment (eq 1.12.). Line shape analysis can be used to determine the rate constant when the reaction is faster or overlapping of

[48] Marchaj, A. L.; Norton, J. R. unpublished results.

resonances occurs. Collectively, dynamic NMR techniques can be used to measure rate constants from 10^{-1} - 10^{6} s^{-1}.[49]

$$k = \pi(\Delta\nu_{excess}) \qquad \text{(eq 1.12.)}$$

$\Delta\nu_{excess}$: the increase in line width.

Rate constants too small to affect line shape can be measured by magnetization transfer. Rate constants ranging from 0.01 to 100 s^{-1} between two sites with different frequencies can be obtained.[50]

UV-Vis and IR methods can be used to measure rate constants with lab time scales.[10]

Slow proton transfer reactions are fundamentally important. The practical concern for these reactions is that these reactions may be important in some biological systems.

D. Proton Transfer Reactions in Metalloenzyme Systems and Proteins.

Overview. Terminal oxo and bridging oxo ligands are found coordinated to the metal centers of metalloenzymes.[51] The X-ray structures of vanadium chloroperoxidase

---

[49] Sandström, J. *Dynamic NMR Spectroscopy*, Academic: London, 1982.

[50] Sanders J. K. M.; Hunter, B. K. *Modern NMR Spectroscopy*, 2nd ed., Oxford University Press: Oxford, UK, 1993, pp. 205-234.

[51] (a) Holm, R. H.; Kennepohl, P.; Solomon, E. I. *Chem. Rev.* **1996**, *96*, 2239. (b) Lippard, S.J. *Angew. Chem. Int. Ed. Engl.* **1988**, *27*, 344. (c) Kurtz, D. M., Jr. *Chem. Rev.* **1990**, *90*, 585. (d) Que, L., Jr.; True, A. E. *Prog. Inorg. Chem.* **1990**, *38*, 98. (e) Vincent, J. B.;Olivier-Lilley, G. L.; Averill, B. A.

reveal that terminal oxo ligands are coordinated to the metals.[52] Terminal oxo ligands are also found in oxotransferases, such as aldehyde oxidoreductase,[53] aldehyde ferredoxin oxidoreductase,[54] and DMSO reductase.[55] The protein X-ray structures of some more oxomolybdoenzymes and their tungsten counterparts have recently been determined and have revealed that terminal oxo and/or hydroxo ligands are bound to the metal center.[56] Other crystallographic studies show that hydrogen bonding between the oxo ligand of the metal and an adjacent amino acid side chain may be the cause for the elongation of metal-oxygen bond,[57] which is considered to be essential for oxygen transfer processes.[51a]

Oxo-bridged polynuclear complexes are common in metalloenzymes.[51] Examples include ribonucleotide reductase (R2 subunit),[58] methane monooxygenase (MMO),[59]

Chem. Rev. **1990**, *90*, 1447. (f) Wilkins, R. G. *Chem. Soc. Revs.* **1992**, *21*, 171. (g) Wieghardt, K. *Angew. Chem. Int. Ed. Engl.* **1989**, *28*, 1153. (h) Karlin, K. D. *Science* **1993**, *261*, 701.

[52] Messerschmidt, A.; Wever, R. *Proc. Natl. Acad. Sci. U.S.A.* **1996**, *93*, 392.

[53] Romão, M. J.; Archer, M.; Moura, I.; Moura, J. J.; LeGall, J.; Engh, R.; Schneider, M.; Hof, P.; Huber, R. *Science* **1995**, *270*, 1170.

[54] Chan, M. K.; Mukund, S.; Kletzin, A.; Adams, M. W. W.; Rees, D. C. *Science* **1995**, *267*, 1463.

[55] Schindelin, H.; Kisker, C.; Hilton, J.; Rajagopalan, K.; Rees, D. C. *Science* **1996**, *272*, 1615.

[56] (a) Schindelin, H.; Kisker, C.; Rees; D. C. *J. Biol. Inorg. Chem.* **1997**, *2*, 773. (b) Romão, M. J.; Rösch, N.; Huber, R. *J. Biol. Inorg. Chem.* **1997**, *2*, 782. (c) Schindelin, H.; Kisker, C.; Hilton, J.; Rajagopalan, K. V.; Rees, D. C. *Science*, **1996**, *272*, 1615.

[57] Bailey, S.; McAlpine, A. S.; McEwan, A. G.; Shaw, A. L. *J. Biol. Inorg. Chem.* **1997**, *2*, 690. (b) Bailey, S.; McAlpine, A. S.; Duke, E. M. H.; Benson, N.; McEwan, A. G. *Acta Cryst.* **1996**, *D52*, 194.

[58] (a) Mulliez, E.; Fontecave, M. *Coord. Chem. Rev.* **1999**, *185-186*, 775. (b) Fontecave, M.; Ménage, S.; Duboc-Toia, C. *Coord. Chem. Rev.* **1998**, *178-180*, 1555. (c) Sjöberg, B.-M. *Struct. Bonding* **1997**, *88*, 139. (d) Wallar, B. J.; Lipscomb, J. D. *Chem. Rev.* **1996**, *96*, 2625. (e) Feig, A. L.; Lippard, S. J. *Chem. Rev.* **1994**, *94*, 759. (f)Goldberg, D. P.; Lippard, S. J. *Adv. Chem. Ser.* **1995**, *246*, 61. (g) Stassinopoulos, A.; Mukerjee, S.; Caradonna, J. P. *Adv. Chem. Ser.* **1995**, *246*, 83. (h) Rova, U.; Adrait, A.; Potsch, S.; Graslund, A.; Thelander, L. *J. Biol. Chem.* **1999**, *274*, 23746. (i) Ekberg, M.; Potsch, S.; Sandin, E.; Thunnissen, M.; Nordlund, P.; Sahlin, M.; Sjöberg, B.-M. *J. Biol. Chem.* **1998**, *273*, 21003. (j) Burdi, D.; Aveline, B. M.; Wood, P. D.; Stubbe, JoAnne, Redmond, R. W. *J. Am. Chem. Soc.* **1997**, *119*, 6457.

catalase,[60] the oxygen-evolving complex (OEC) in photosystem II (PS II),[61] hemerythrin (Hr),[62] and purple acid phosphatase (PAP).[63]

Terminal Oxo Ligands and Proton Transfer in Metalloenzymes and Related Complexes. Xanthine oxidases, sulfite oxidase and the assimilatory nitrate reductases, and DMSO reductase are all mononuclear molybdenum enzymes.[51a] Many mononuclear molybdenum enzymes, which are often referred to as oxotransferases, are involved in catalytical transfer of an oxygen atom to or from a physiological acceptor/donor

---

[59] (a) Valentine, A. M.; Lippard, S. J. *J. Chem. Soc., Dalton Trans.* **1997**, 3925. (b) Lee, S.-K.; Lipscomb, J. D. *Biochemistry*, **1999**, *38*, 4423. (c) Fontecave, M.; Ménage, S.; Duboc-Toia, C. *Coord. Chem. Rev.* **1998**, *178-180*, 1555. (d) Wallar, B. J.; Lipscomb, J. D. *Chem. Rev.* **1996**, *96*, 2625. (e) Feig, A. L.; Lippard, S. J. *Chem. Rev.* **1994**, *94*, 759. (f) Lipscomb, J. D. *Annu. Rev. Microbiol.* **1994**, *48*, 371. (g) Liu, K. E.; Lippard, S. J. *Adv. Inorg. Chem.* **1995**, *42*, 263. (h) Stassinopoulos, A.; Mukerjee, S.; Caradonna, J. P. *Adv. Chem. Ser.* **1995**, *246*, 83.

[60] Barynin, V. V.; Hempstead, P. D.; Vagin, A. A.; Antonyuk, S. V.; Melik-Adamyn, W. R.; Lamzin, V. S.; Harrison, P. M.; Artymiuk, P. J. *J. Inorg. Biochem.* **1997**, *67*, 196.

[61] (a) Pecoraro, V. L.; Baldwin, M. J.; Caudle, M. T.; Hsieh, W.-Y.; Law, N. A. *Pure Appl. Chem.* **1998**, *70*, 925. (b) Tommos, C.; Babcock, G. T. *Acc. Chem. Res.* **1998**, *31*, 18. (c) Witt, H.T. *Ber. Bunsen-Ges. Phys. Chem.* **1996**, *100*, 1923. (d) Kilman, L.; LoBrtto, R.; Allen, J. P.; Williams, J. C. *Nature (London)* **1999**, *402 (6762)* 696. (e) Hays, A.-M. A.; Vassiliev, I. R.; Golbeck, J. H.; Debus, R. J. *Biochemistry*, **1998**, *37*, 11352. (f) Ahlbrink, R.; Haumann, M.; Cherepanov, D.; Bögershausen, O.; Mulkidjanian, A.; Junge, W. *Biochemistry*, **1998**, *37*, 1131. (g)Thorp, H. H.; Brudvig, G. W. *New J. Chem.* **1991**, *15*,479. And reference 52.

[62] (a) Stenkamp, R. E. *Chem. Rev.* **1994**, *94*, 715. (b) Wilkins, R. G. *Chem. Soc. Rev.* **1992**, *171*. (c) Howard, J. B.; Rees, D. C. *Adv. Protein Chem.* **1991**, *42*, 199. (d) Shiemke, A. K.; Loehr, T. M.; Sanders-Loehr, J. *J. Am. Chem. Soc.* **1986**, *108*, 2437. (e) Reem, R. C.; McCormick, J. M.; Richardson, D. E.; Devlin, F. J.; Stephens, P. J.; Musselman, R. L.; Solomon, E. I.; *J. Am. Chem. Soc.* **1989**, *111*, 4688. (f) Armstrong, G.; Skyes, A. *Inorg. Chem.* **1986**, 25, 3135.

[63] (a) Twitchett, M. B.; Sykes, A. G. *Eur. J. Inorg. Chem.* **1999**, 2105. (b) Than, R.; Feldmann, A. A.; Krebs, B. *Coord. Chem. Rev.* **1999**, *182*, 211. (c)) Fontecave, M.; Ménage, S.; Duboc-Toia, C. *Coord. Chem. Rev.* **1998**, *178-180*, 1555. (d) Krebs, B.; Ahlers, F.; Bremer, B.; Eulering, B.; Klabunde, T.; Schepers, K.; Schmit, M.; Strater, N.; Than, R.; Witzel, H. *Bioinorg, Chem.* **1997**, 2, 412.

molecule. Many of them possess Mo=O in their active sites; thus they are called oxomolybdenum enzymes.[64]

Metalloenzymes with terminal oxo ligands have important biologic functions. Xanthine oxidases catalyze the hydroxylation of RH with water as the ultimate source of the oxygen atom.[65] Sulfite oxidase and the assimilatory nitrate reductases catalyze net oxygen atom transfer to or from a lone pair of electrons on a heteroatom.[65] In the case of sulfite oxidase, the sulfites are oxidized to sulfate.[66] DMSO reductase catalyzes the reductive deoxygenation of dimethyl sulfoxide to dimethyl sulfide.[65] Vanadium chloroperoxidases are capable of oxidizing chloride, bromide, and iodide.[65]

The X-ray structure of the aldehyde oxidoreductase from *Desulfovibrio gigas*, which is a member of the xanthine oxidase family, has been determined.[53] One Mo=O and one pterin cofactor have been found in the active site. A general reaction scheme is as follows (Figure 1.9).[67]

---

[64] (a) Mcmaster, J.; Enemark, J. H. *Curr. Opin. Chem. Biol.* **1998**, 2, 201. (b) Enemark, J. H.; Garner, C. D. *J. Biol. Inorg. Chem.* **1997**, 2, 817.

[65] Hille, R. *Chem. Rev.* **1996**, *96*, 2757.

[66] Hille, R. *Biochim. Biophys. Acta* **1994**, *1184*, 143.

[67] (a) Hille, R.; Sprecher, H. *J. Biol. Chem.* **1987**, *262*, 10914. (b) Holm, R. H. *Coord. Chem. Rev.* **1990**, *100*, 183.

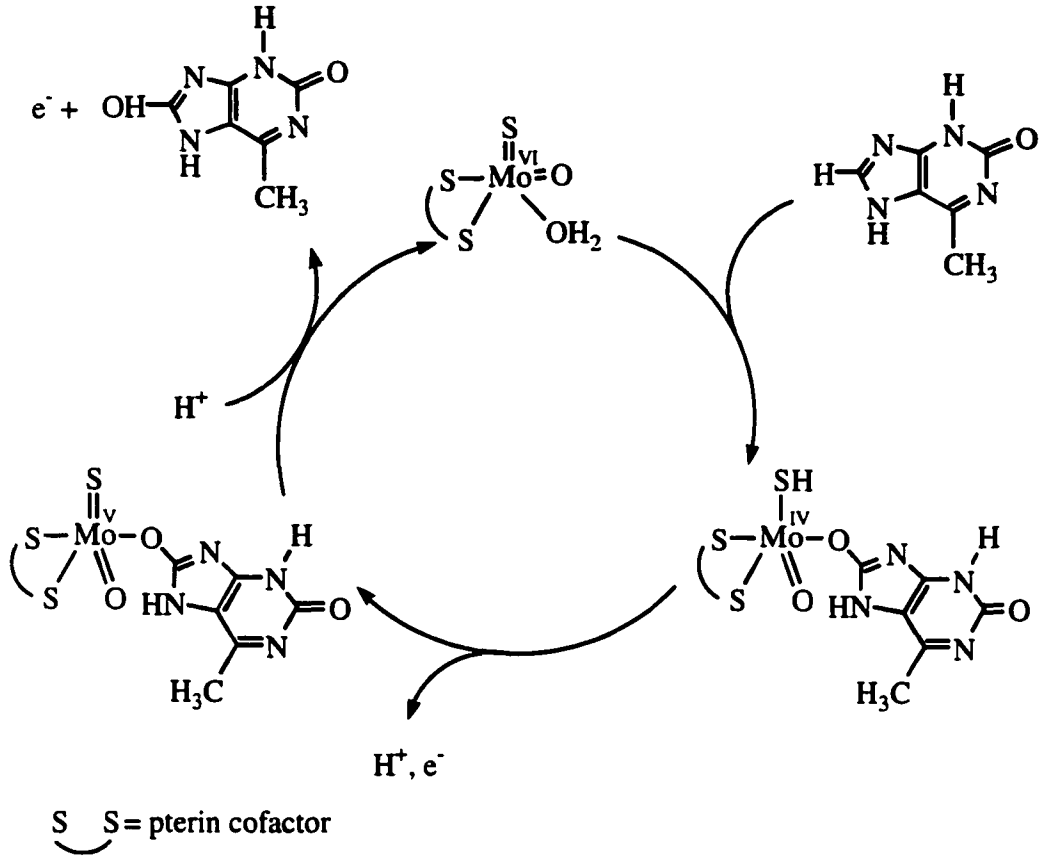

Figure 1.9. Reaction scheme for xanthine oxidases.

The X-ray structures of DMSO reductase from *Rhodobacter sphaeroides* in two different oxidation states have been determined.[55] Two pterin cofactors and one Mo=O have been found in the active site. The double oxo transfer experiment has been carried out with DMSO reductase using ^{18}O labeling (Figure 1.10).[68]

[68] Schultz, B. E.; Hille, R.; Holm, R. H. *J. Am. Chem. Soc.* **1995**, *117*, 827.

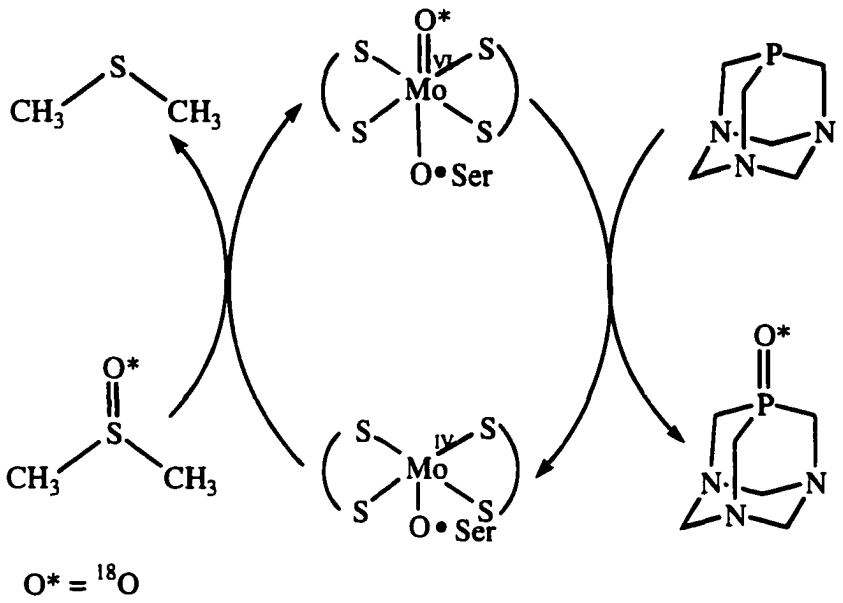

Figure 1.10. The double oxo transfer for DMSO reductase.

X-ray absorption spectra have been obtained for sulfite oxidase to collect the structural information.[69] One pterin cofactor and two Mo=O have been indicated from these studies. A reaction mechanism has been proposed for the sulfite oxidase (Figure 1.11).[70]

[69] (a) Cramer, S. P.; Wahl, R.; Rjagopalan, K. V. *J. Am. Chem. Soc.* **1981**, *103*, 7721. (b) Cramer, S. P.; Gray, H. B.; Rajagopalan, K. V. *J. Am. Chem. Soc.* **1979**, *101*, 2772. (c) Berg, J. M.; Hodgson, K. O.; Cramer, S. P.; Corbin, J. L.; Elsberry, A.; Periyadath, N.; Stiefel, E. I. *J. Am. Chem. Soc.* **1979**, *101*, 2774. (d) George, G. N.; Kipke, C. A.; Prince, R. C.; Sunde, R. A.; Enemark, J. H.; Cramer, S. P. *Biochemistry*, **1989**, *28*, 5075.

[70] Hille, R. *Biochim. Biophys. Acta* **1994**, *1184*, 143.

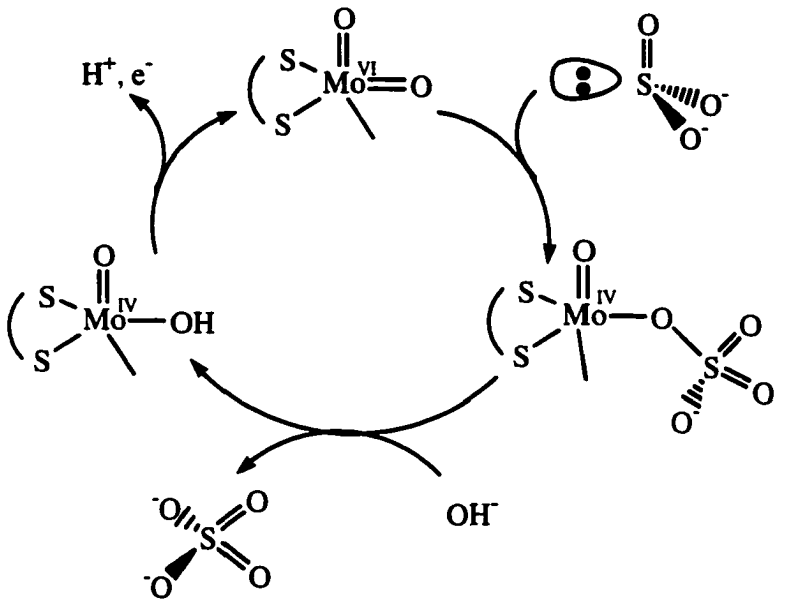

Figure 1.11. Reaction mechanism for sulfite oxidase.

The X-ray structure of a vanadium chloroperoxidase from the fungus *Curvularia inaequalis* has been reported.[52] The vanadium center has trigonal bipyramidal geometry with three oxo ligands in the equatorial plane, and one hydroxo and one His•N which is covalently linked to the protein at the axial positions. Hydrogen bonding has been found between the three oxo ligands and the protein moiety. The vanadium chloroperoxidase is not redox-active during the catalytic cycle. The peroxide is bound to V(V), replacing the hydroxo ligand, and the vanadium(V) center acts as a strong Lewis acid to activate the bound peroxide.[71] Halide ions attack the bound peroxide and ultimately produce the

[71] De Boer, E.; Boon, K.; Wever, R. *Biochemistry* **1988**, *27*, 1629.

corresponding hypohalous acid, which can halogenate organic substrates.[72] In the absence of suitable substrates, a second molecule of hydrogen peroxide reacts with hypohalous acid to produce dioxygen and water.

Proton transfer as well as electron transfer must be involved in the catalytic cycles of some of above the mentioned metalloenzymes.

Bridging Oxo Ligand and Proton Transfer in Some Metalloenzymes. The metalloenzymes with oxo bridge ligands have critical roles. Methane monooxygenase[73] oxidizes methane in methanotrophic bacteria. Ribonucleotide reductase[74] reduces ribonucleotides to deoxyribonucleotides in most living cells. The oxygen-evolving complex (OEC) in photosystem II[75] provides oxygen from oxidation of water driven by the energy from visible light in the thylakoid membrane of chloroplasts of green plants.

The best-characterized forms of soluble methane monooxygenase (sMMO) contain a hydroxylase (MMOH), a reductase (MMOR), and component B (MMOB).[59] The hydroxylase subunits in MMO have binuclear iron clusters bridged by hydroxyl

---

[72] (a) van Schijndel, J. W. P. M.; Barnett, P.; Roelse, J.; Vollenbroek, E. G. M.; Wever, R. *Eur. J. Biochem.* **1994**, *225*, 151. (b) Soedjak, H. S.; Walker, J. V.; Butler, A. *Biochemistry* **1995**, *34*, 12689. (c) Everett, R. R.; Butler, A. *Inorg. Chem.* **1989**, *28*, 393.

[73] a) Dalton, H. Adv. *Appl. Microbiol.* **1980**, *26*, 71. b) Lund, J.; Woodland, M. P.; Dalton, H Eur. *J. Biochem.* **1985**, *147*, 297. c) Woodland, M.P.;Dalton, H. *J. BiolChem.* **1984**, *259*, 53.

[74] a) Lammers, M.; Follmann, H. *Struct. Bonding* **1983**, *5*, 87. b) Sjöberg, B. M.; Gräslund, a. *Adv. Inorg. Biochem.* **1983**, *5*, 87.

[75] Sivaraja, M.; Philo, J. S.; Lary, J.; Dismukes, G. C. *J. Am. Chem. Soc.* **1989**, *111*, 3221.

ligands.[76] Both oxygen activation and substrate hydroxylation occur in the diiron site in MMOH. One proposed catalytic cycle is as follow (Figure 1.12).[59a]

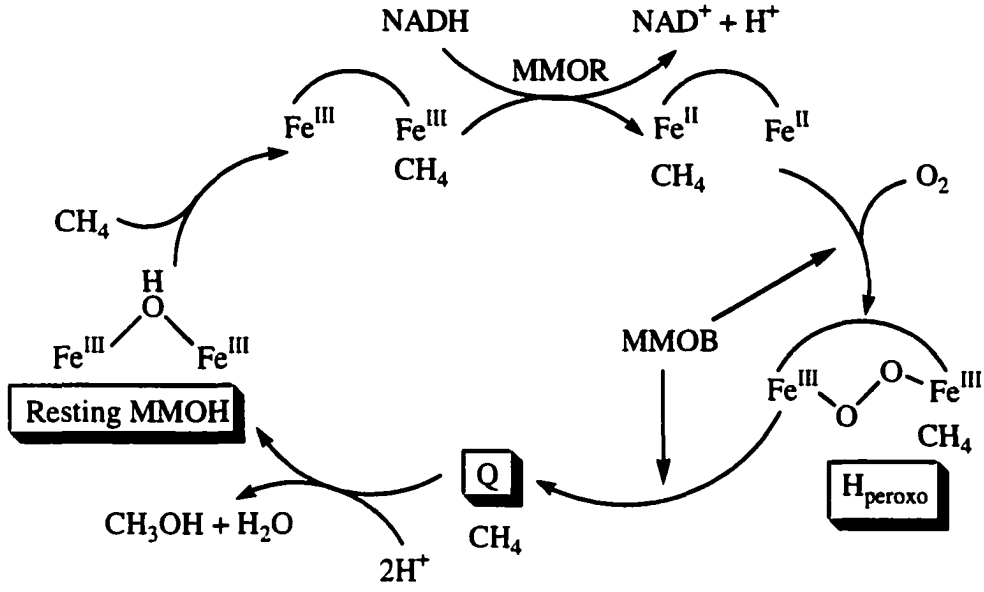

Figure 1.12. Catalytic cycles for sMMO from *M. capsulatus* (Bath) including all observed intermediates. The exact nature of intermediate Q is not tocompletely clear.

The mammalian ribonucleotide reductase consists of two non-identical subunits, R1 and R2, each inactive alone.[58] The R1 subunit contains the active site, whereas R2 contains a binuclear iron cluster and a tyrosyl free radical essential for catalysis. The X-ray structure of the protein (R2) of ribonucleotide reductase in *Escherichia coli* has been determined.[77] It contains a stable tyrosyl free radical and two iron centers, which are bridged by a glutamic acid residue at position115 and an oxo ligand, to stabilize the

[76] Fox, B. G.; Hendrich, M. P.; Suerus, K. K.; Anderson, K. K.; Froland, W. A.; Lipscomb, J. D.; Münck, E. *J. Am. Chem. Soc.* **1993**, *115*, 3688.

[77] Nordlund, P.; Sjöberg, B.-M.; Eklund, H. *Nature* **1990**, *345*, 593.

radical.[78] Proton transfer as well as electron transfer are involved in the formation of tyrosyl radical. One proposed mechanism is shown below (Figure 1.13).[58a]

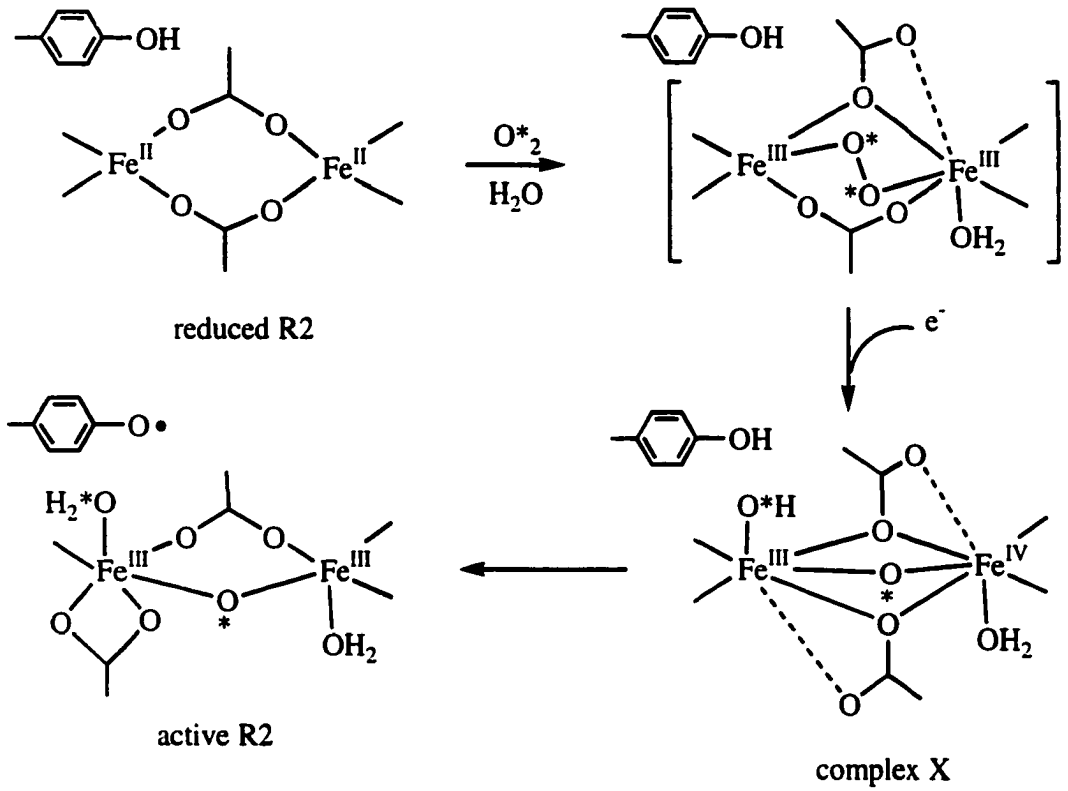

Figure 1.13. The proposed mechanism for the formation of the tyrosyl radical in R2 subunit in ribonucleotide reductase.

Photosystem II (PS II) occurs as a multi-subunit, membrane-spanning complex in the thylakoid membrane. In oxygen-evolving complex (OEC) of the PS II during water oxidation, four oxidizing equivalents are sequentially generated by the photoexcited state of a chlorophyll dimer, P_{680}.[61] These oxidizing equivalents are believed to be stored in a

[78] Barlow, T.; Eliasson, R.; Platz, A.; Reichard, P.; Sjöberg, B.-M. *Natl. Acad. Sci. USA* **1983**, *80*, 1492.

multinuclear manganese complex that proceeds through five distinct oxidation states to release oxygen and regenerates the reduced catalyst. Different catalytic cycles have been proposed. One proposed catalytic cycle is shown below (Figure 1.14).

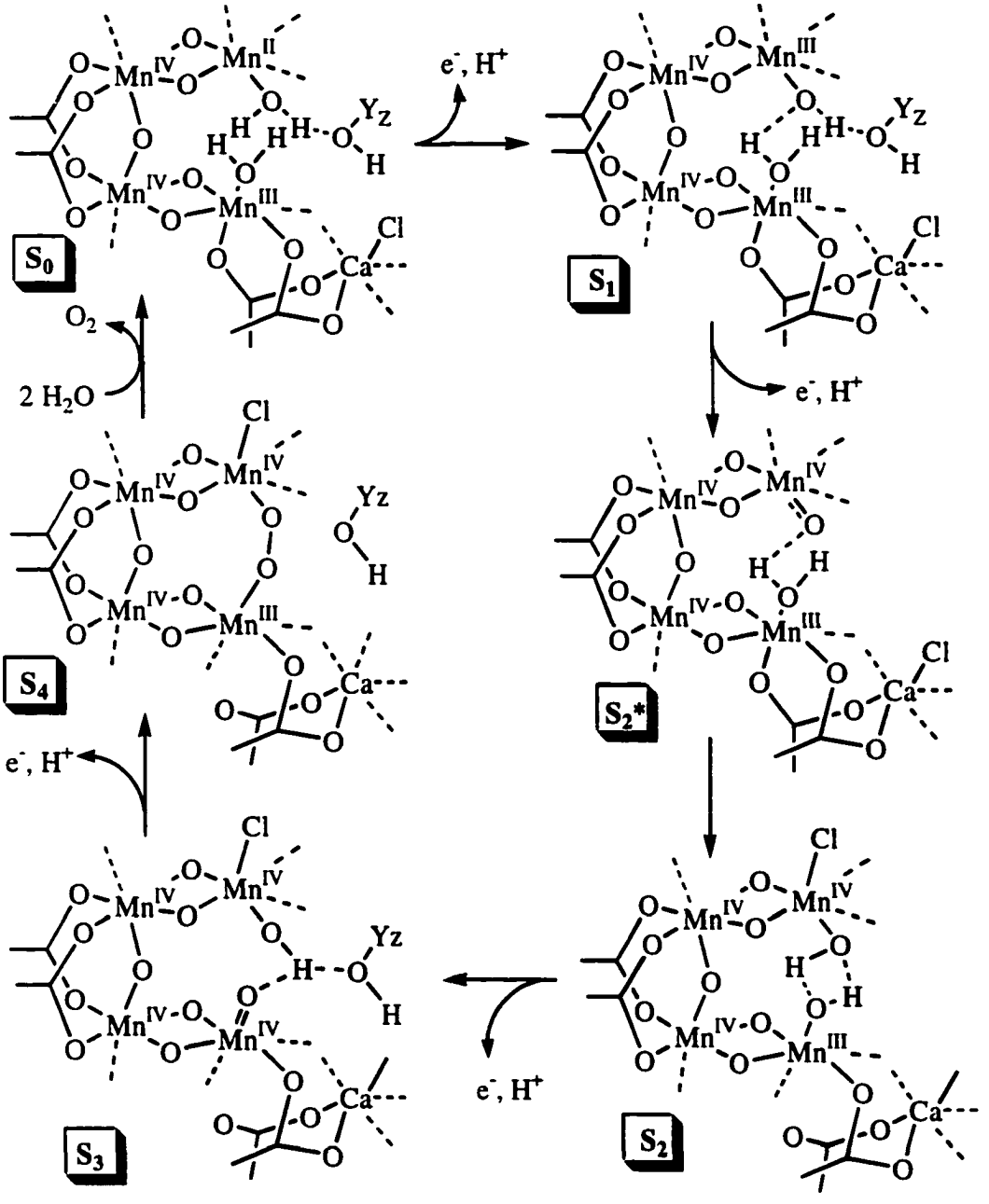

Figure 1.14. Proposed catalytic cycle for PS II. The S_2* state occurs only transiently, and S_4 is unstable to O_2/S_0 production.

Slow Proton Transfer in Metalloenzyme. In glyoxalase I the rate-limiting proton transfer rates are calculated to be approximately 300-1500 s^{-1} with Zn^{2+}, Mg^{2+}, or Ca^{2+} bound to the active site.[79] Slow proton transfer from a surface base to the buried cluster has been observed in the $\{Fe_3S_4\}$ cluster of ferredoxin I from *Azotobacter vinelandii*.[80] In the mutant form the proton transfer rate constant is measured to be 3×10^7 $M^{-1}s^{-1}$, slightly slower than the diffusion-controlled rate constant. Proton transfer has been proposed to be involved in the rate-limiting step of some enzymatic systems.[81]

II. Rhenium Oxo Complexes

A. Organorhenium Oxides

Overview. Rhenium was discovered in 1925 as the last non-radioactive element.[82] It is a relatively rare element, only 0.7 ppb in earth's crust.[83] It is isolated as a by-product from refining molybdenum ore, most commonly as $KReO_4$.[84] Re has some

---

[79] Feierberg, I.; Cameron, A. D.; Aqvist, J. *FEBS Lett.* **1999**, *453*, 90.

[80] Hirst, J.; Duff, J. L. C.; Jameson, G. N. L.; Kemper, M. A.; Burgess, B. K.; Armstrong, F. A. *J. Am. Chem. Soc.* **1998**, *120*, 7985.

[81] (a) Javid-Majd, F.; Blanchard, J. S. *Biochemistry*, **2000**, *39*, 1285. (b) (c) Briganti, F.; Mangani, S.; Orioli, P.; Scozzafava, A.; Vernaglione, G.; Supuran, C. T. *Biochemistry* **1997**, *36*, 10384. (d) Lindskog, S. *Pharmacol. Ther.* **1997**, *74*, 1.

[82] Emsley, J *The Elements* Oxford University Press: New York, 1990.

[83] Casey, C. P. *Science* **1993**, *259*, 1552.

[84] Cotton, F. A.; Wilkinson, G *Advanced Inorganic Chemistry*, 4th Eds., Wiley-Interscience: New York, 1980, p 886.

unique features.[83,85] Re has the widest range of available oxidation state among the transition metals, from -III in $Re(CO)_4^{3-}$ to +VII in $RReO_3$ (R = alkyl). Re forms strong bonds with other elements, stabilizing ordinarily reactive species. Thus, its compounds are used as models for the intermediates in the reactions of other transition metal compounds. Re is unusually reluctant to form coordinatively unsaturated complexes.

Organorhenium chemistry was little explored until twenty years ago.[85] Much of the early work was with carbonyl ligand; metallocene derivatives or arene complexes were hard to prepare. Re complexes tend to aggregate and clusters of Re complexes with intermediate oxidation states are formed.[83] Since then there has been an explosive growth in organorhenium chemistry. Organorhenium complexes are useful in C-H bond activations and catalytic oxidations of alkenes.

Methyltrioxo Rhenium. Organorhenium oxides, especially methyltrioxo rhenium, are versatile catalysts in many of the important organic transformations. Methyltrioxo rhenium (abbreviated as MTO) has become one of the best-studied organometallic complexes.[86] It was first detected in trace amount in the reaction of $(CH_3)_4Re(O)$ with air in 1979 by I. R. Beattie and P. J. Jones.[87] Herrmann and his

---

[85] Romão, C. C. in *Encyclopedia of Inorganic Chemistry* King R. B. Ed., John Wiley & Sons: New York, 1994, Vol. 6 p 3437.

[86] (a) Espenson, J. H.; Abu-Omar, M. M. *Adv. Chem. Ser.* **1997**, *253*, 99. (b) Espenson J. H. *Chem. Commun.* , **1999**, 479. (c) Herrmann, W. A.; Kühn, F. E. *Acc. Chem. Res.* **1997**, *30*, 169. (d) Gable, K. P *Advances in Organometallic Chemistry* **1997**, *41*, 127. (e) Romão, C. C.; Kühn, F. E.; Herrmann, W. A. *Chem. Rev.* **1997**, *97*, 3197. (f) Herrmann, W. A. *J. Organomet. Chem.* **1995**, *500*, 149.

[87] Beattie, I. R.; Jones, P. J. *J. Inorg. Chem.* **1979**, *18*, 2318.

coworkers[88] reported the direct synthesis of MTO in 1988. It is an air- and water- stable, high-valent organometallic complex, easy to handle. It dissolves in water and in most of the organic solvents. It works well in water, a solvent that reacts with many organometallic complexes and is kept away from them rigorously. This makes MTO an environment-friendly system. It is a mild oxidant, not explosive like Mn_2O_7. In catalytic reactions, the Re in MTO usually does not change its oxidation state.[89]

Oxidation. MTO transfers oxygen atoms to and from different species. Hydrogen peroxide is often the ultimate oxygen source. Herrmann and coworkers[90] reported the first example of organic oxidations catalyzed by MTO, using H_2O_2 as the stoichiometric oxidant in 1991. The substrates successfully oxidized by this system include alkenes, alkynes, aromatic compounds, sulfur compounds, phosphines, arsines and stibines, amines, halide ions, and alcohols and many others.[91] All the oxidations of alkenes are selective without overoxidation. The yields of these reactions are good to excellent.

---

[88] Herrmann, W. A.; Kuchler, J. G.; Felixberger, J. K.; Herdtweck, E.; Wagner, W. *Angew. Chem., Int. Ed. Engl.* **1988**, *27*, 394.

[89] Espenson J. H. *Chem. Commun.* , **1999**, 479.

[90] Herrmann, W. A.; Fischer, R. W.; Marz, D. W *Angew. Chem., Int. Ed. Engl.* **1991**, *30*, 1638.

[91] (a) Herrmann, W. A.; Fischer, R. W.; Rauch, M. U.; Scherer, W. *J. Mol. Catal.* **1994**, *86*, 243. (b) Herrmann, W. A.; Fischer, R. W.; Marz, D. W. *Angew. Chem., Int. Ed. Engl.***1991**, *30*, 1638. (c) Al-Ailoun, A.; Espenson, J. H. *J. Am. Chem. Soc.* **1995**, *117*, 9243. (d) Herrmann, W. A. In *Organic Peroxygen Chemistry*; Herrmann, W. A., Ed.; Springer Verlage: Berlin, 1993; Vol. 164, p 130. (e) Boehlow, T. R.; Spilling, C. D. *Tetrahedron Lett.* **1996**, *37*, 2717. (f) Murray, R. W.; Singh, M.; Williams, B. L.; Moncrieff, H. M. *Tetrahedron Lett.* **1995**, *36*, 2437. (g) Al-Ajlouni, A. M.; Espenson, J. H. *J. Org. Chem.* **1996**, *61*, 3969. (h) Adam, W.; Mitchell, C. M. *Angew. Chem., Int. Ed. Engl.* **1996**, *35*, 533.

Active Species in the Oxidations by MTO/H_2O_2. The chemistry of MTO with H_2O_2 has been extensively studied by the Herrmann group in München, Germany and the Espenson group at Iowa State University in US. Espenson and coworkers[89] have proposed the following reaction (eq 1.13). MTO reacts with H_2O_2 to produce two η_2-peroxo complexes, **A** and **B**, in equilibrium. UV-Vis spectra of the mixture of all three complexes under various conditions allowed them to determine the equilibrium constants using the following equation (eq 1.14).[92] The rate constants for each individual step and the activation parameters are determined by kinetic measurements.[93] With knowledge of the equilibrium constants, each of the two peroxo complexes can be formed selectively by choosing the right conditions. At low concentrations of H_2O_2, complex **A** dominates, while complex **B** dominates when $[H_2O_2] > 0.5$ M and $[MTO]_T = (3.2 - 8.0) \times 10^{-4}$ M.[86d] Both peroxo complexes are active in catalytic reactions with about equal activity.

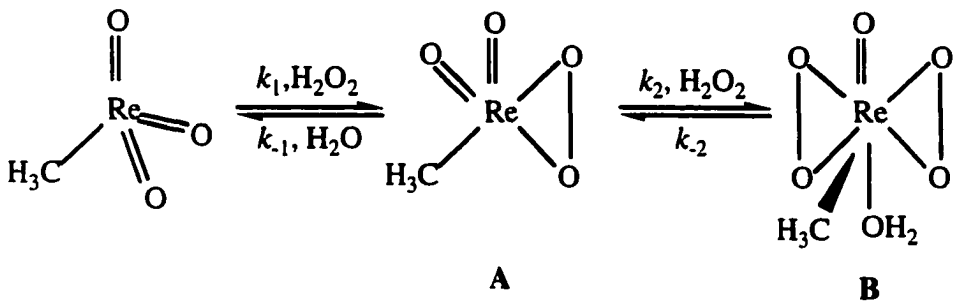

A B (eq 1.13.)

[92] (a) Hansen, P. J.; Espenson, J. H *Inorg. Chem.* **1995**, *34*, 5839. (b) Wang, W.-D.; Espenson, J. H *Inorg. Chem.* **1997**, *36*, 5069.

[93] Pestovsky, O.; Van Eldik, R.; Huston P.; Espenson, J. H. *J. Chem. Soc., Dalton Trans.*, **1995**, 133.

$$\bar{\varepsilon} = \frac{Absorbance}{b[\mathrm{Re}]_T} = \frac{\varepsilon_{MTO} + \varepsilon_A K_1[H_2O_2] + \varepsilon_B K_1 K_2 [H_2O_2]^2}{1 + K_1[H_2O_2] + K_1 K_2 [H_2O_2]^2} \qquad \text{(eq 1.14.)}$$

Exchanges of oxygen between oxo and peroxo ligands in peroxo rhenium complexes are very slow,[89] like the slow exchange of oxygen between water and hydrogen peroxide.[94] Oxygen exchanges rapidly between MTO and water (eq 1.15).[89]

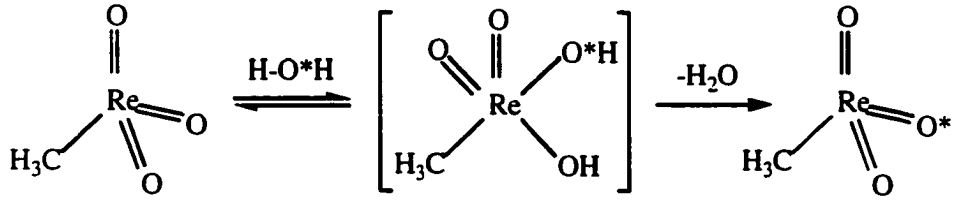

(eq 1. 15.)

Herrmann group[95] reported the X-ray structure of the adduct of complex **B** with ligand L (L = H_2O or $O{=}P(N(CH_3)_2)_3$), with a pentagonal bipyramidal structure around Re and axial oxo and aqua ligands.

Other Catalytic Reactions with MTO. Aldehydes or strained cyclic ketones react with aliphatic diazoalkanes to afford olefinic coupling products in the presence of MTO, with tertiary phosphine as oxygen acceptor.[96] MTO/Al_2O_3-SiO_2 with tetraalkyl tin

---

[94] Taube, H. *Rec. Chem. Prog.* **1956** *17*, 277.

[95] (a) Herrmann, W. A.; Fischer, R. W.; Scherer, W.; Rauch, M. U.; *Angew. Chem., Int. Ed. Engl.* **1993**, *32*, 1157. (b) Herrmann, W. A.; Correia, J. D. G.; Artus, G. R. J.; Fischer, R. W.; Romão, C. C *J. Organomet. Chem.* **1996**, *520*, 139.

[96] Herrmann, W. A.; Wang, M. *Angew. Chem., Int. Ed. Engl.* **1991**, *30*, 1641.

complexes can catalyze the metathesis of functionalized olefins.[97] MTO, acting as a Lewis acid, increases the rate of Diels-Alder reaction and can subsequently epoxidize the products.[98] The alkoxylation of cyclohexene oxide with secondary and tertiary alcohols is catalyzed by MTO.[99] MTO also causes the disproportionation of epoxides, producing olefins and diols. Aromatic imines are converted to aziridines by MTO with ethyl diazoacetate.[100] Ketones and aldehydes also react with epoxides in the presence of MTO .[101] Cyclotrimerization of aldehydes to 1, 3, 5 - trioxanes is catalyzed by MTO.[102] The direct formation of ethers from alcohols has also been carried out in the presence of MTO[103] — the first example that a transition metal complex catalyzes such reaction. Finally MTO catalyzes the 1, 3 - transposition of allylic alcohols.[104]

B. Application of Rhenium Oxo Complexes as Radiopharmaceuticals

---

[97] (a) Mol, J.C.; Woerlee, E. F. G. *J. Chem. Soc., Chem. Commun.* **1979**, 330. (b) Verkuijlen, E.; Kapsteijn, F.; Mol, J. C.; Boelhouwer, C. *J. Chem. Soc., Chem. Commun.* **1977**, 198. (c) Mol, J. C. *J. Mol.Catal.* **1982**, *15*, 35.

[98] Correia, J. D. G.; Ph. D. Thesis, Technical University of Munich, 1996.

[99] Kholopov, A. B.; Nikitin, A. V.; Rubailo, V. L. *Kinet. Catal.* **1995**, *36*, 101; *Kinetika i Kataliz* **1995**, *36*, 111.

[100] Zhu, Z; Espenson, J. H. *J. Org. Chem.* **1995**, *60*, 7090.

[101] Zhu, Z.; Espenson, J. H. *Organometallics*, **1997**, *16*, 3658.

[102] Zhu, Z.; Espenson, J. H. *Synthesis* **1998**, 417.

[103] Zhu, Z; Espenson, J. H. *J. Org. Chem.* **1996**, *61*, 324.

[104] Jacob, J.; Espenson, J. H.; Jensen, J, H.; Gordon, M. S. *Organometallics*, **1998**, *17*, 1835.

Overview. Radioactive Re isotope (^{186}Re, ^{188}Re) complexes can be used as radiopharmaceuticals for therapeutic purpose.[105] Researchers in the pharmaceutical industry, as well as academic researchers have put a lot of effort into trying to synthesize the most selective Re complexes targeting specific organs. The metabolism of these complexes in the human body needs to be understood so that no serious side effects would occur. The chemistry of Re complexes has become important in practical use.

Rhenium Isotopes. Rhenium isotope ^{186}Re has been determined as one of the best therapy radiolabels due to its unique half-life, particulate and γ emissions, and the chelation properties.[106] ^{186}Re has a reasonably long half-life of 90 hours, long enough for therapeutic purposes, but not too long so that the rhenium complex may move away from the target and give undesirable radiation to other tissues. It has a strong β emission (1.07 MeV), essentially singular 137 keV imaging γ emissions (9%), and it decays into a stable daughter product. It can be conveniently monitored by the same γ camera instrument employed for ^{99m}Tc agents. Its penetration range in tissue is about 5mm making it suitable for the treatment of small tumors. ^{188}Re has a shorter half-life of 17 hours.[107] It also has a strong β emission (2.1 MeV), 155 keV γ emissions (15%). Its penetration range in tissue is longer, about 11mm, making it more appropriate for large masses.

---

[105] (a) Alberto, R.; Schubiger, P. A. *Recent Res. Dev. Inorg. Chem.* **1998**, *1*, 73. (b) Hashimoto, K.; Yoshihara, K. *Top. Curr. Chem.* **1996**, *176*, 275. (c) Fritzberg, A. R. *Rhenium Rhenium Alloys, Proc. Int. Symp.* 1997, 479. (d) Dilworth, J. R.; Parrott, S. J. *Dev. Nucl. Med.* **1996**, *30*, 1. (e) Griffiths, G. L.; Goldenberg, D. M.; Sharkey, R. M.; Knapp, F. F. Jr.; Callahan, A. P.; Tejada, G.; Hansen, H. J. *Radioact. Radiochem.* **1992**, *3*, 33, 36.

[106] Quadri, S. M.; Wessels B. W. *Nucl. Med. Biol.* **1986**, *13*, 447.

[107] Dilworth, J. R.; Parrott, S. J. *Chem. Soc. Rev.* **1998**, *27*. 43.

What makes rhenium isotopes really stand out among all the available radiolabel isotopes is that it has very similar physical properties to those of ^{99m}Tc.[108]

Radiolabel ^{99m}Tc Complexes. ^{99m}Tc has been widely used as an imaging agent for diagnostic purposes[107]. Over 90% of all diagnostic nuclear medicine imaging studies carried out worldwide use ^{99m}Tc. About 160 tons of technetium will be produced by the year 2000. Different technetium complexes have been shown to be able to target specific organs in human body. For example, oxo Technetium complexes, **1** and **2**, are selective for brain imaging;[109,110] **3** is for heart imaging;[111] and **4** is for liver imaging (Figure 1.15).[112] There are also complexes selective for kidney and bone.[113,114] There are second-generation agents now[115] and third generation are on the way.[105a]

---

[108] Deutsch, E.; Libson, K.; Vanderheyden, J.-L.; Ketring, A. R.; Maxon, H. R. *Nul. Med. Biol.* **1986**, *13*, 465.

[109] Leonard, J. P.; Novotnik, D. P.; Neirinckx, R. D. *J. Nucl. Med.* **1986**, *27*, 1819.

[110] Cheesman, E. H.; Blanchette, M. A.; Ganey, M. V.; Maheu, L. J.; Miller, S. J.; Watson, A. D. *J. Nucl. Med.* **1986**, *29*, 288.

[111] Linder, K. E.; Malley, M. F.; Gongoutas, J. Z.; Unger, S. E.; Nunn, A. D. *Inorg. Chem.* **1990**, *29*, 2428.

[112] Fritzberg, A. R.; Kasina, S.; Eshima, D.; Johnson, D. L. *J. Nucl. Med.* **1986**, *27*, 111.

[113] For kidney: (a) DeRosch, M. A.; Brodack, J. W.; Grummon, M. E.; Marmian, M. E.; Nosco, D. L.; Deutsch, K. F.; Deutsch, E. A. *J. Nucl. Med.* **1992**, *33*, 850. (b) Costello, C. E.; Brodack, J. W.; Jones, A. G.; Davison, A.; Johnson, D. L.; Kasina S.; Fritzberg, A. R. *J. Nucl. Med.* **1983**, *24*, 353. (c) Ponto, J. A.; Chilton, H. M.; Watson, H.M. *Pharmaceuticals in Medical Imaging* Swanson, D. P.; Chilton, H. M.; Thrall, J. H. Eds., MacMillan: New York, 1990, p 501.

[114] For bone: (a) Singh, J.; Powell, A. K.; Clark, S. E. M.; Blower, P. J. J. Chem. Soc., Chem. Commun. 1991, 15. (b) Libson, K.; Deutsch, E. A.; Barnett, B. J. Am. Chem. Soc. 1980, 102, 2476.

[115] (a) Welch, M. J.; Downer, J. B.; Katzenellenbogen, J. A. *Current Directions in Radiopharmaceutical Research and Development* Mather, S. J. Ed., Kluwer Academic Press: Netherlands, 1996, p 137. (b) Spies, H.; Fietz, T.; Blacer, M.; Pietsch H.-J.; Johanssen, B. in *Technetium and Rhenium Chemistry and Nuclear Medicine* Nicolini, M.; Bandoli G.; Mazzi, U.; Editorali, S. G. Eds., Padova, Italy, 1995, Vol. 4, p 243. (c) Fritzberg, A. R.; Wilbur, D. S. in *Handbook of Targeted Delivery of Imaging*

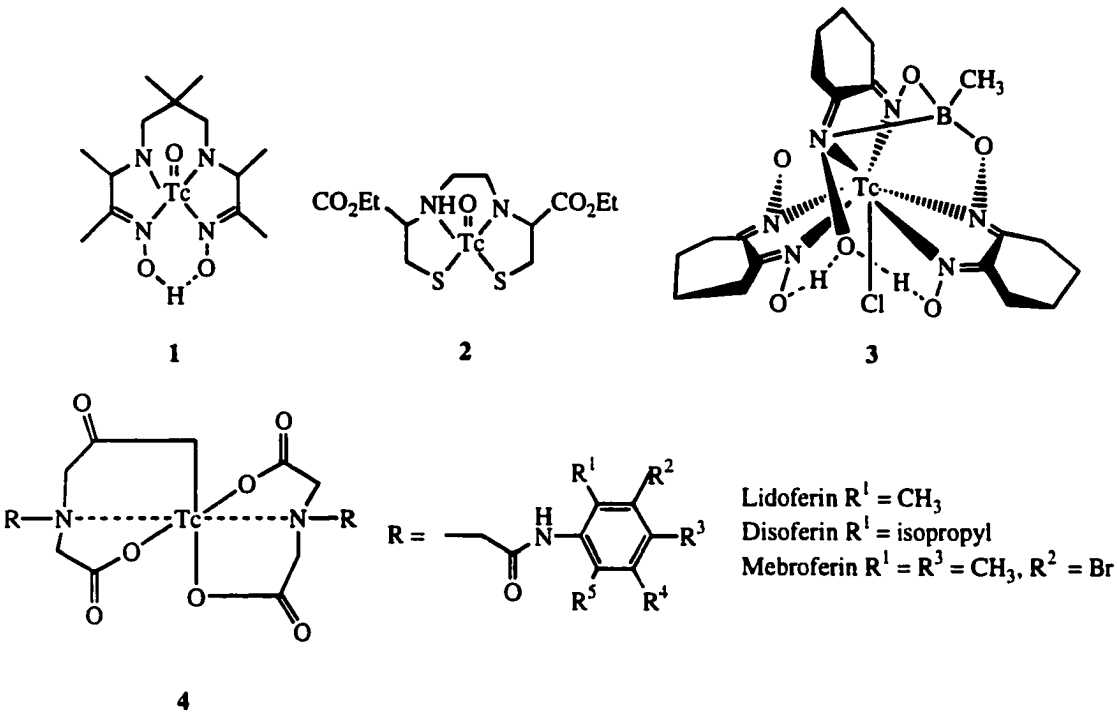

Figure 1.15. Radiolabel ^{99m}Tc imaging agents.

Rhenium Radiopharmaceuticals. Re complexes have been used to treat bone cancer and other cancers.[116] ^{186}Re-HEDP complexes (HEDP: (1-hydroxyethylidene) diphosphonic acid) demonstrate effective palliation of bone pain due to metastases of

---

Agents Torchilin, V. P. Ed., CRC: New York, 1995, p 83. (d) George A. J. T.; Jamar, F.; Tai, M.-S.; Heelan, B. T.; Adams, G. P.; McCartney, J. E.; Houston, L. L.; Weiner, L. M. Opperman, H.; Peters, A. M.; Huston, J. S. *Proc. Natl. Acad. Sci.* **1995**, *92*, 8538. (e) Archer, C. M.; Edwards, B.; Powell, N. A. in *Current Directions in Radiopharmaceutical Research and Development* Mather, S. J. Ed., Kluwer Academic Press: Netherlands, 1996, p 81.

[116] (a) Knapp, F. F. Jr.; Beets, A. L.; Guhlke, S.; Zamora, P. O.; Bender, H.; Palmedo, H.; Biersack, H.-J. *Anticancer Res.* **1997**, *17*, 1783. (b) Knapp, F. F. Jr. *Cancer Biother. Radiopharm.* **1998**, *13*, 337. (c) Iznaga-Escobar, N. *Nucl. Med. Biol.* **1998**, *25*, 441. (d) Lewington, V. J. *Phys. Med. Biol.* **1996**, *41*, 2027. (e) Kopf-Maier, P.; Kopf, H. *Met. Compd. Cancer Ther.* **1994**, 109. (f) Visser, G. W. M.; Gerretsen, M.; Herscheid, J. D. M.; Snow, G. B.; van Dongen, G. *J. Nucl. Med.* **1993**, *34*, 1953. (g) John, E.; Thakur, M. L.; DeFulvio, J.; McDevitt, M. R.; Damjanov. I. *J. Nucl. Med.* **1993**, *34*, 260.

primary carcinomas.[117] ^{188}Re-HEDP complexes have been used for treatment of osseous metastases.[118] ^{186}Re-DMSA complex (DMSA = *meso*-1,2-dimercaptosuccinic acid) is possibly suitable for tumor therapy.[119] The complex is identified as $[Re^{V}(O)(DMSA)_2]^-$, *a rhenium oxo complex* (Figure 1.16). One way to prepare this complex is shown in eq 1.16.[120]

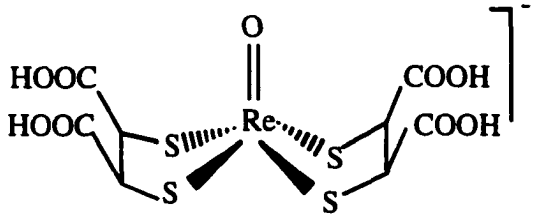

Figure 1.16. *syn-endo* isomer of $[Re^{V}(O)(DMSA)_2]^-$

$$ReO_4^- \xrightarrow[CH_2Cl_2 \text{ extraction}]{1.\ PPh_3,\ 2.\ HCl} \underset{\text{Re(V) intermediate}}{Re(O)(Cl)_3(PPh_3)_2} \xrightarrow[\text{aqueous extraction}]{\text{DMSA}} \underset{\text{Re(V)}}{[Re(O)(DMSA)_2]^-} \quad \text{(eq 1.16.)}$$

III. Statement of Problem.

---

[117] Eisenhut, M. *Int. J. Appl. Radiat. Isot.* **1982**, *33*, 99.

[118] Maxon, H. R. III; Schroder, L. E.; Washburn, L. C.; Thomas, S. R.; Samaratunga, R. C.; Biniakiewicz, D.; Moulton, J. S.; Cummings, D.; Ehrhardt, G. J.; Morris, V. *J. Nul. Med.* **1998**, *39*, 659.

[119] (a) Ohta, H, Yamamoto, K, Endo, K.; Mori, T.; Hamanaka, D.; Shimazu, A.; Ikekubo, K.; Makimoto, K.; Iieda, Y.; Konishi, J.; Morita R.; Hata, N., Horiuchi K.; Yokoyama, A.; Torizuka, K.; Kuma K. *J. Nucl. Med.* **1984**, *25*, 323. (b) Clarke, S. E. M.; Lazarus, C. R.; Wraight, P.; Sampson, C.; Maisey M. N. *J. Nucl. Med.* **1988**, *29*, 33.

We have searched for cases where protonation of the terminal oxo ligands in transition metal complexes is slow enough to be directly observed, and have tried to measure the rate constant for the proton transfer process. We wanted to determine the rate constants of such proton transfers, k_H, over a range of acids of different strengths in order to construct Brønsted plots, and to determine the intrinsic barriers of slow proton transfer processes involving terminal oxo ligands. We hoped to develop the ability to predict intrinsic barriers for other terminal oxo protonation reactions.

---

[120] Lisic E. C.; Mirzadeh, S.; Knapp Jr.,F. F. *J. Labeled Compd. Radiopharm.* **1993**, XXXIII, 65.

CHAPTER TWO—KINETIC STUDIES OF PROTONATION OF TERMINAL OXO RHENIUM(III) COMPLEXES

I. Introduction.

In order to test the hypothesis that slow proton transfer could occur when there is substantial structural and electronic rearrangement involved in the process we need to find terminal oxo complexes whose unprotonated and protonated forms are well characterized and stable. They need to have some spectral differences so that changes in their concentrations could be monitored. It would be nice if they were soluble in many different solvent systems.

Rhenium (III) Alkyl Oxo Bis(acetylene) Complexes and their Protonated Forms.[34] These complexes are reported by Mayer and coworkers, and meet our criteria. The synthesis is straightforward for $Re(O)(Et)(MeC{\equiv}CMe)_2$ (eq 2.1). The complex has been well characterized. The X-ray structure of the complex has been determined. It is stable even at elevated temperature. No β-hydrogen elimination is observed.

$$KReO_4 + HI + PPh_3 \longrightarrow Re(O)(I)(PPh_3)_2 \xrightarrow{EtC\equiv CEt} Re(O)(I)(EtC\equiv CEt)_2$$
$$\xrightarrow{Et_2Zn} Re(O)(Et)(EtC\equiv CEt)_2 \qquad \text{(eq 2.1.)}$$

Treatment of $Re(O)(Et)(MeC\equiv CMe)_2$ with acids such as CF_3SO_3H, $MeC_6H_4SO_4$, HBF_4, and CF_3COOH produces the protonated derivative of the complex.[34] The addition of pyridine regenerates the oxo complex (eq 2.2). The triflate salt of the protonated complex is reported to be an extremely air-sensitive complex. It is characterized by ^1H and ^{13}C NMR at -15 and 0 °C. Its IR spectrum showed a strong peak at 628 cm^{-1}, which was assigned to the Re-OH stretching mode (ν(Re-OH)). The assignment was confirmed by isotopic labeling with ^{18}O ((ν(Re-^{18}OH) = 595 cm^{-1}). This is lower than the Re-O stretching frequency, 975 cm^{-1}, in $Re(O)(Et)(MeC\equiv CMe)_2$, indicating that there is electronic rearrangement upon protonation and suggesting that the protonation occurs on the oxo ligand. That conclusion has been further confirmed by the ^1H NMR and ^{13}C NMR spectra.

$$Re(O)(Et)(EtC\equiv CEt)_2 \underset{\text{Pyridine}}{\overset{HX}{\rightleftharpoons}} [Re(OH)(Et)(EtC\equiv CEt)_2]X \qquad \text{(eq 2.2.)}$$

$[Re(OH)(Et)(MeC\equiv CMe)_2]^+$ is reported to be fluxional on the NMR time scale.[34] The peaks for the methyl groups on the acetylene ligand broaden in the ^1H NMR spectra and eventually coalesce when the temperature is raised. The peaks for the ethyl and hydroxo ligands are unchanged. The fluxional behavior is attributed to the rotation of the acetylene ligands around the metal-ligand axis.

Addition of more than one equivalent of CF_3SO_3H to $Re(O)(Et)(MeC{\equiv}CMe)_2$ is reported to result in the formation of another complex in addition to the hydroxo complex.[34] It has NMR spectra similar to those of the hydroxo complex. The ratio of the two complexes depends on temperature, with the hydroxo complex favored at low temperature. The exact nature of this second complex is unclear, although it has been suggested that it could be a diprotonated aqua complex, or different ion pairs in chloroform solution. This second complex is not observed when the parent complex is treated with weaker acids, CF_3COOH or $MeC_6H_4SO_3H$.

A series of rhenium analogs of $Re(O)(Et)(MeC{\equiv}CMe)_2$, the methyl, isopropyl, allyl, and hydride complexes with 2-butyne and 3-hexyne ligands, have been synthesized.[34] The ^1H NMR chemical shift of the hydride is at 6.18 ppm. Protonation of the isopropyl derivatives results in the formation of hydride complexes, indicating that β-hydrogen elimination can occur at room temperature from the hydroxo complexes . This contrasts with the fact that β-hydrogen elimination is not observed for $Re(O)(Et)(MeC{\equiv}CMe)_2$ and for $[Re(OH)(Et)(MeC{\equiv}CMe)_2]^+$.

II. Results and Discussion.

The Reaction of $Re(O)(Et)(MeC{\equiv}CMe)_2$ with Different Acids.

$[Re(OH)(Et)(MeC{\equiv}CMe)_2]^+$ was reportedly formed when $Re(O)(Et)(MeC{\equiv}CMe)_2$ was treated with acid, and the reaction could be reversed by the addition of pyridine, indicating that this reaction was indeed a protonation.[34] However, we were unable to isolate the pure protonated product, $[Re(OH)(Et)(MeC{\equiv}CMe)_2](X)$ ($X^- = CF_3SO_3^-$), as a

solid under the reported conditions. Many other conditions, including the change of solvents, the use of different acids, and different work up processes were tried. From our experience the protonated complex was not thermally stable enough to be isolated cleanly, and decomposed rapidly at room temperature in the solid state under a nitrogen atmosphere.

Slow Proton Transfer Process Observed between $Re(O)(Et)(MeC{\equiv}CMe)_2$ and its Conjugate Acid in the Variable Temperature ^1H NMR Studies. Low temperature ^1H NMR spectra were recorded after $Re(O)(Et)(MeC{\equiv}CMe)_2$ had been treated with a half equivalent of CF_3SO_3H in CD_2Cl_2. Half of the $Re(O)(Et)(MeC{\equiv}CMe)_2$ was converted to the protonated product. At low temperature (-15 °C) the ^1H NMR peaks of the two complexes were separated and not broadened very much, indicating that the exchange of the proton between the protonated and unprotonated complexes was fairly slow on the NMR time scale (Figure 2.1). This was the first qualitative evidence we obtained suggesting that *the proton transfer to or from our terminal oxo ligand was slow.*

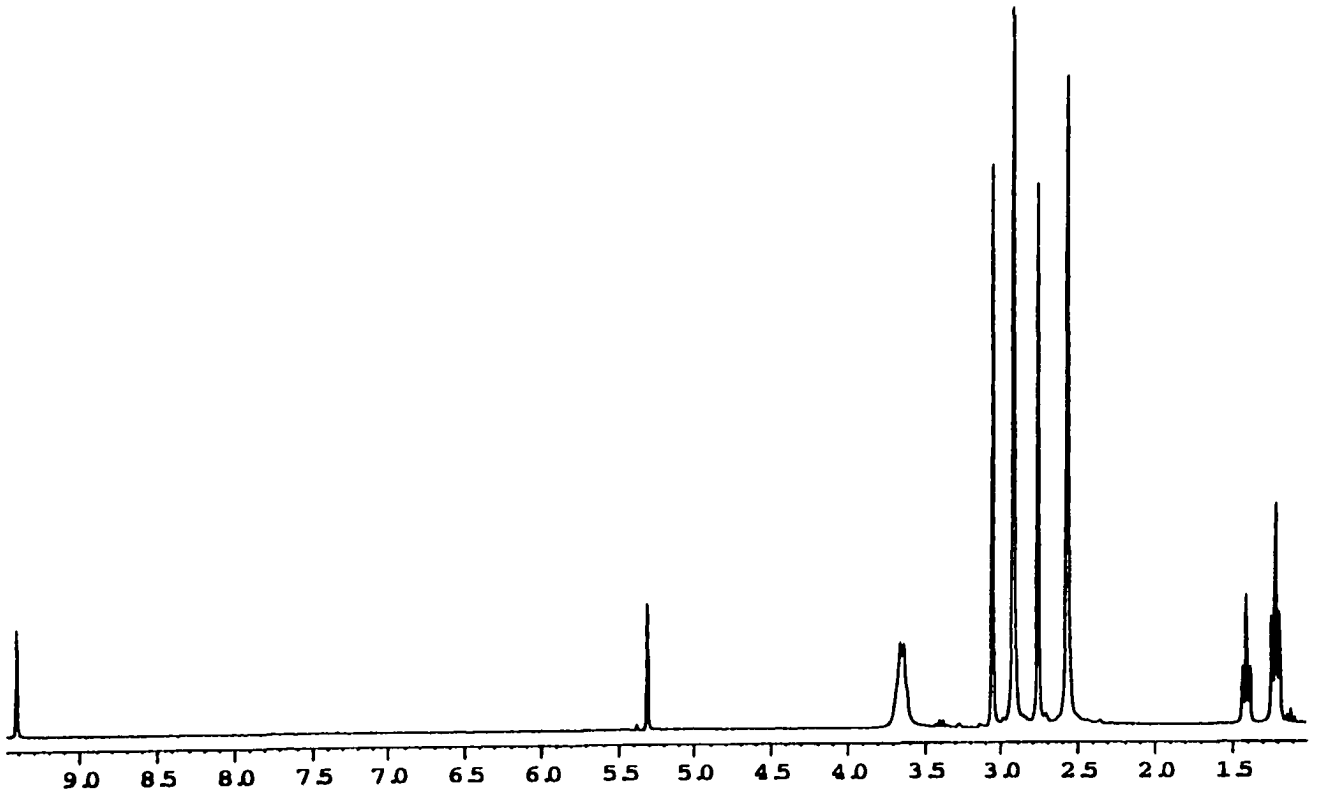

Figure 2.1. ^{1}H NMR spectrum of the proton exchange process between Re(O)(Et)(MeC≡CMe)$_2$ and its conjugate acid at -15 °C in CD_2Cl_2.

Attempts to Obtain Rate Constants of the Proton Exchange Process between $Re(O)(Et)(MeC{\equiv}CMe)_2$ with its Conjugate Acid by Line Shape Analysis. The peaks of the methyl groups of the 2-butyne ligands in the ^1H NMR spectrum would be obvious choices for the study since they are all singlets. However, the methyl groups of the 2-butyne ligands in the protonated product were reported to be fluxional (see introduction of this chapter),[34] indicating that the 2-butyne ligand rotates around the midpoint of the triple bond. This would complicate the situation and make it difficult to derive the rate constant of the proton transfer process using the methyl peaks of 2-butyne. Indeed a 2D EXSY NMR spectrum[121] at -15 °C showed that all four peaks for the methyl groups of 2-butyne ligand of both the unprotonated and protonated complexes were exchanging with each other (Figure 2.2). This implied that the broadening of these peaks could come either from the proton transfer process or from the ligand rotation process or both.

[121] Derome, A. E. *Modern NMR Techniques for Chemistry Research* Pergamon: New York, 1987.

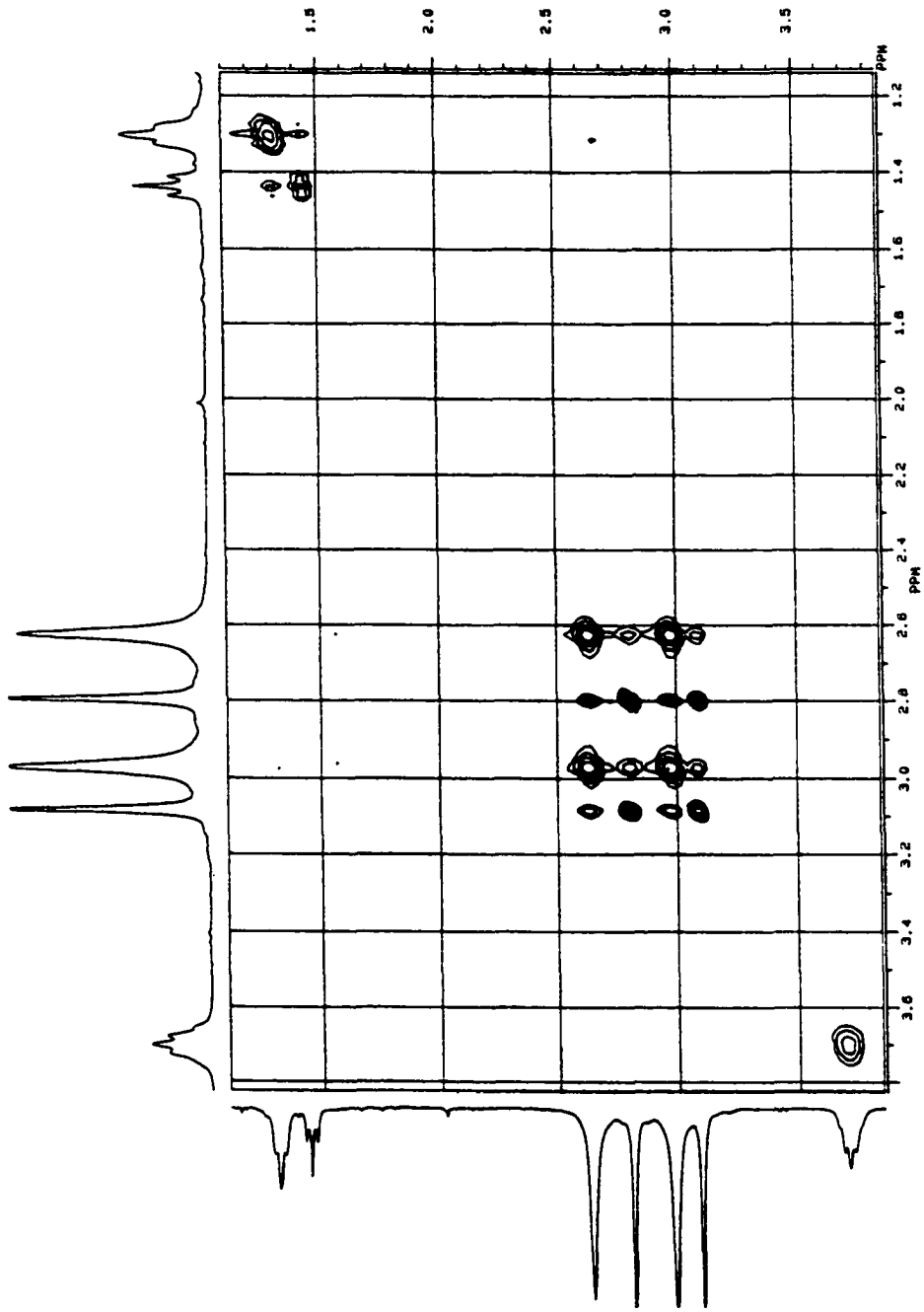

Figure 2.2. 2D EXSY spectrum of $Re(O)(Et)(MeC{\equiv}CMe)_2$ with its conjugate acid at -15 °C in CD_2Cl_2.

In theory, the ^{1}H NMR peaks of the ethyl ligand could be used in a full line shape analysis by the program gNMR, as the broadening of these peaks should be due exclusively to proton transfer between the unprotonated and protonated complexes. The spectrum of the complex without exchange was first simulated. The exchange rate constants could be obtained by iterating on the experimental spectrum while varying these rate constants. However the calculated spectrum didn't fit the experimental spectrum very well. It could be that the exchange process is more complicated than the model we assumed.

Estimation of the Upper Limit of the Rate Constants of Proton Transfer Between Re(O)(Et)(MeC≡CMe)$_2$ and its Conjugate Acid. The fact that the widths of the peaks of Re(O)(Et)(MeC≡CMe)$_2$ in the ^{1}H NMR spectra did not change much in the presence of its conjugate acid allowed us to estimate (eq 2.3, 2.4) an upper limit of the rate constants for all the processes contributing to line broadening, including proton transfer.

$$k_{obs} = \pi \cdot \Delta\nu_{1/2} \qquad \text{(eq 2.3.)}$$

$$k_{obs} = k_{ex} \cdot [\text{ReOH}]$$

$$\therefore k_{ex} = \frac{k_{obs}}{[\text{ReOH}]} \qquad \text{(eq 2.4.)}$$

$\Delta\nu_{1/2}$: line width difference at half height between peaks without exchange and peaks with exchange. k_{ex}: the second-order rate constant for exchange process.

In this case the broadening of the methyl signals of the 2-butyne ligand of $Re(O)(Et)(MeC{\equiv}CMe)_2$ was used. Less than 1 Hz broadening was observed in those peaks at -15 °C, implying that k_{obs} was less than 3.14 s^{-1} when [ReOH] was 0.026 M. So k_{ex} was less than 120 $M^{-1}s^{-1}$ at that temperature. The sum of the rate constants of all the processes that contributed to line broadening, including proton transfer, was thus < 120 $M^{-1}s^{-1}$.

These proton transfer processes were slow because significant electronic rearrangements were involved. The IR stretching frequency of the Re-O(H) in the protonated complex was reported to be 587 cm^{-1} (see introduction part of this chapter), smaller than the stretching frequency of Re-O, 975 cm^{-1} in $Re(O)(Et)(MeC{\equiv}CMe)_2$[34]. This suggested that upon protonation, the bond strength of Re-O bond was weakened because some of the electron density between rhenium and oxygen was removed. The bond order probably changed to single bond and the bond could also be elongated. This certainly fits our hypothesis that substantial electronic and structural rearrangements could result in slow proton transfer process.

Protonation of $Re(O)Me(MeC{\equiv}CMe)_2$ with Different Acids. No detail about the protonation of $Re(O)Me(MeC{\equiv}CMe)_2$ has been reported by Mayer and coworkers,[34] although the ^1H NMR spectrum of $[Re(OH)Me(MeC{\equiv}CMe)_2]^+$ at -20 °C has been reported. The protonation of $Re(O)Me(MeC{\equiv}CMe)_2$ was studied by us at some length. It was hoped that the change of ethyl group to methyl group would stabilize the protonation product by eliminating the decomposition pathway of β hydride elimination. (Indeed,

Mayer and coworkers[34] had observed the formation of propene after Re(O)(isopropyl)(MeC≡CMe)$_2$ was treated with CF_3SO_3H for ten minutes or more.) The ^{1}H NMR spectra of the reactions of Re(O)Me(MeC≡CMe)$_2$ with CF_3SO_3H and CF_3COOH we obtained were broad and complex in CD_2Cl_2, not like the reported spectrum. No products could be clearly identified. The addition of pyridine cleanly reversed the reaction, indicating that the broad peaks observed were protonation products. We were unable to obtain kinetic information from these spectra.

Three sets of broad peaks were observed when Re(O)Me(MeC≡CMe)$_2$ solution was treated with $MeC_6H_4SO_3H$ in CD_2Cl_2 (Figure 2.3). ^{1}H NMR spectrum indicated that all three complexes had a plane of symmetry. The reaction again could be reversed by the addition of pyridine. One set of peaks was identified as Re(O)Me(MeC≡CMe)$_2$. They were broad. The spectrum of the reaction of Re(O)Me(MeC≡CMe)$_2$ with more acid (2.5 eq) contained two sets of peaks, "$[Re(OH)]^+$" and "$[Re(OH_2)]^{2+}$". With even more acid (7.5 eq) "$[Re(OH_2)]^{2+}$" dominated. We did not have other evidence for the identification of "$[Re(OH)]^+$" and "$[Re(OH_2)]^{2+}$" (Figure 2.4). From analogy to the protonation product of Re(O)Et(MeC≡CMe)$_2$, in which the protonation occurred at the oxo ligand, it was reasonable to assume that the protonation of Re(O)Me(MeC≡CMe)$_2$ also occurred at the oxo ligand. The fact that more acid added changed the ratio of different complexes in the solution (Figure 2.4.) indicated that these complexes were the products of consecutive protonation.

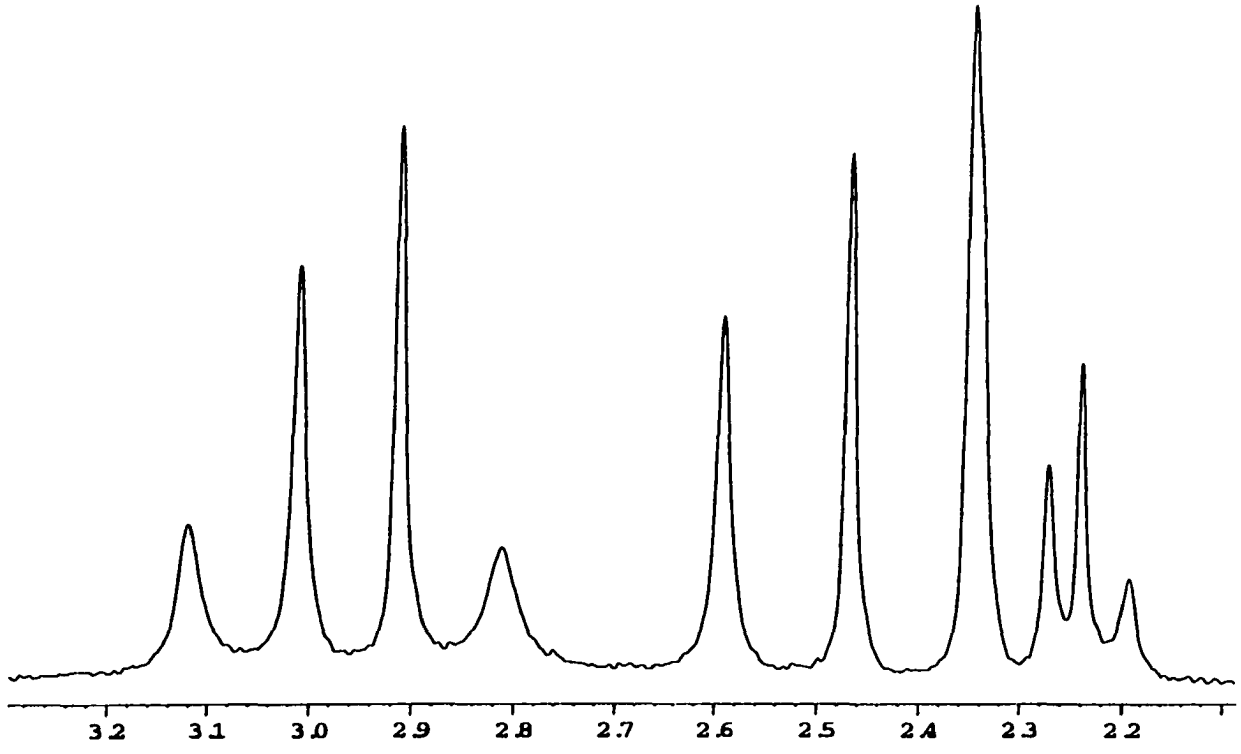

Figure 2.3. Re complex part of the ^{1}H NMR spectrum of the protonation of $Re(O)Me(MeC{\equiv}CMe)_2$ with 1.45 eq of MeC_6H4SO_3H in CD_2Cl_2 at -15 °C.

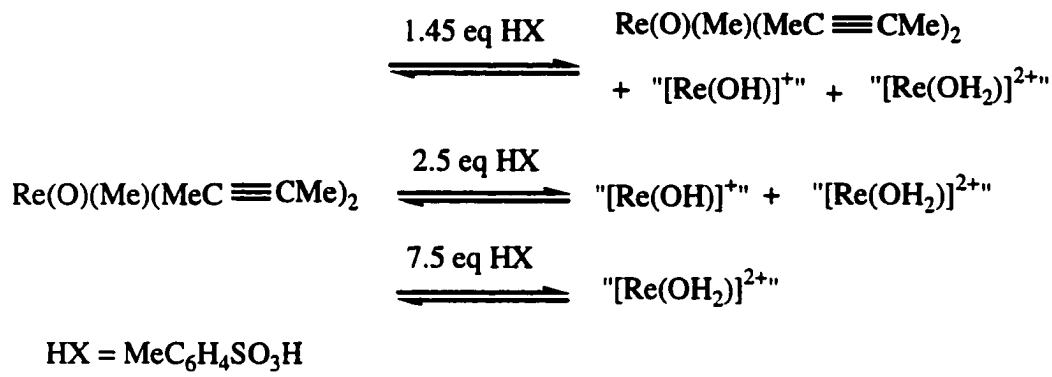

Figure 2.4 Different product distributions obtained with different amounts of HX.

The fact that addition of 2.5 and 7.5 equivalents of acid changed the distribution of the products indicated that the pK_a values for "$[Re(OH)]^+$" and "$[Re(OH_2)]^{2+}$" were close (estimated to be less than 1.2 pK_a unit different). According to Pauling's rule the difference between pK_{a1} and pK_{a2}, for consecutive HA^{n+} and $H_2A^{(n+1)+}$, is usually greater than 5 pK_a unit on adjacent oxygen; the effect should be larger with protonation on the same oxygen.[122] It is not clear why the difference between the two consecutive pK_a values in our case was so small.

The broadened but separated ^1H NMR peaks in the reaction of $Re(O)Me(MeC{\equiv}CMe)_2$ with $MeC_6H_4SO_3H$ indicated that proton transfer among $Re(O)Me(MeC{\equiv}CMe)_2$, "$[Re(OH)]^+$", and "$[Re(OH_2)]^{2+}$" was slow on the NMR time scale. The 2D EXSY spectrum obtained again suggested that the broadening of methyl peaks of the 2-butyne ligands of all three complexes came from proton transfer or rotation around the triple bond or both. Again the rate constants of the proton transfer

[122] Shriver, D. F.; Atkins, P.; Langford, C. H. *Inorganic Chemistry* 2nd Ed.; Freeman: New York, 1994.

process could in theory be obtained from the broadening of the methyl group coordinated to the rhenium. However, because the products of this protonation could not be isolated and well characterized, the natural line width of their methyl signals was not available.

Protonation of Some Dioxo Rhenium Complexes. We examined the rate constants of protonation for the terminal oxo ligand in other rhenium complexes. The complexes synthesized included $[Re(en)_2O_2]Cl$,[29] $[Re(O)_2(cyclam)](ClO_4)$[30], $[Re(O)_2(O_1cyclam)](ClO_4)$, $[Re(O)_2(H_{-1}O_1cyclam)]$[30] (see Figure 1.7.), and $[Re(O)_2L_2]Cl$ (L = *trans*-1,2-$C_6H_{10}(NH_2)_2$). These complexes were only dissolved in water.

The structures of $[Re(O)_2(cyclam)]Cl(BP_3)\cdot H_2O$,[123] $[Re(O)(OH)(cyclam)](ClO_4)_2$,[30] and $Re(O)(OH)(H_{-1}O_1cyclam)ReO_4$[30] have been reported. The Re=O bond length in the dioxo complex is 1.756 (3) Å. In $Re(O)(OH)(H_{-1}O_1cyclam)ReO_4$, the Re=O bond length is 1.685 (8) Å and the Re-O(H) one is 1.970 (8) Å. In $[Re(O)(OH)(cyclam)](ClO_4)_2$, no distinction between the bond lengths of two Re-O (oxo and hydroxo) has been observed due to disorder of the oxo and hydroxo groups. The Re-O bond length was 1.766 (5) Å.

The UV-Visible spectra for $[Re(O)_2(cyclam)]^+$ and $[Re(O)(OH)(cyclam)]^{2+}$ were reported to have peaks at 440 nm and 482 nm respectively.[30] The authors also said that "attempts to achieve this second protonation for $[Re(O)(OH)(cyclam)]^{2+}$ were unsuccessful due to the rapid disproportionation of the complex." Another report gave λ_{max} of $[Re(O)_2(cyclam)]^+$ as 423 nm.[124]

---

[123] Blake, A. J.; Greig, J. A.; Schroder, M. *J. Chem. Soc., Dalton Trans.* **1988**, 2645.

[124] Wang, Y. P.; Che, C. M.; Wong, K. Y.; Peng, S. M. *Inorg. Chem.* **1993**, *32*, 5827.

We monitored the titration of $[Re(O)_2(cyclam)](ClO_4)$ with $HClO_4$ by its UV-Vis spectrum. We observed that the broad peak at 445 nm increased when the first equivalent of $HClO_4$ was added. The peaks were shifted when the second equivalent of acid was added (Figure 2.5). The appearance of the isosbestic point during the addition of the second equivalent of $HClO_4$ indicated that the second protonation was a single step process.

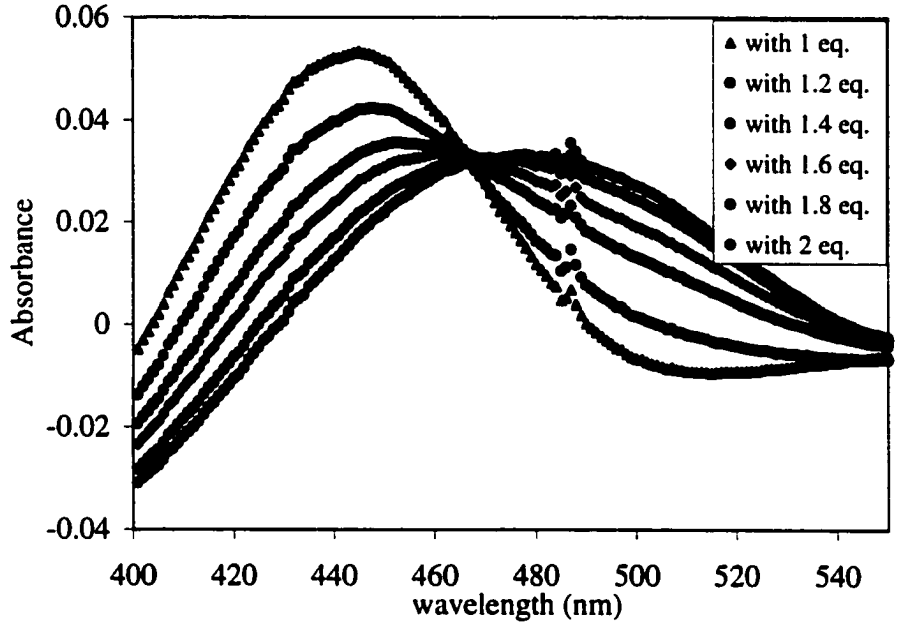

Figure 2.5. Titration of $[Re(O)_2(cyclam)](ClO_4)$ with $HClO_4$ in water. Because of an error in referencing the absorbance appears to become < 0 on the left of the spectrum; in fact the absolute absorbance values are not significant.

Kinetic studies of the protonation of $[Re(O)_2(cyclam)](ClO_4)$ with $HClO_4$ were carried out on the stopped-flow apparatus. The reaction was completed once the reagents were mixed. If we consider that the mixing time is 0.002 second in the stopped-flow

apparatus the second order rate constant can be estimated as greater than 10^5 $M^{-1}s^{-1}$. Thus the protonation of dioxo metal complexes tends to be fast. In the study of $[M(O)_2(CN)_4]^{n-}$ (M = Mo(IV), W(IV), Re(V), Tc(V)) the proton transfer rates are reported to be close to the rate of diffusion (see chapter one). Other literature examples include $[Cr(OH)(OH_2)_5]^{2+}$ [125] and $[VO(OD)_3(D_2O)_2]^-$ [126]. The forward rate constant for the reaction in eq 2.5. has been reported to be 1.7×10^6 s^{-1}; the rate of the reverse reaction is diffusion-controlled. The rate constant for proton transfer reaction (eq 2.6.) has been reported to be 8.4×10^6 $M^{-1}s^{-1}$ at 25 °C

$$Cr(H_2O)_6^{3+} + H_2O \underset{k_{-1}}{\overset{k_1}{\rightleftharpoons}} Cr(H_2O)_5(OH)^{2+} + H_3O^+ \qquad \text{(eq 2.5.)}$$

$$VO(OD)_3(D_2O)_2^- + OH^- \underset{k_{-1}}{\overset{k_1}{\rightleftharpoons}} VO(OD)_4(D_2O)^{2+} + HOD \qquad \text{(eq 2.6.)}$$

III. Conclusions and Future Work.

We found two cases where the protonation was slow enough to be directly observed. The peaks in the ^1H NMR spectra were separated and only a little broadened when $Re(O)Et(MeC{\equiv}CMe)_2$ and $Re(O)Me(MeC{\equiv}CMe)_2$ were treated with acids, indicating that proton transfer to the terminal oxo ligands was slow on the NMR time

[125] Melton, B. F.; Pollack, V. L. *J. Phys. Chem.* **1969**, *73*, 3669.

[126] Copenhafer, W. C.; Rieger, P. H. *Inorg. Chem.* **1977**, *16*, 2431.

scale. Kinetic studies with line broadening analysis obtained the upper limit for the rate constants for the proton self-exchange reaction of $Re(O)Et(MeC{\equiv}CMe)_2$ and its conjugate acid. This upper limit of the rate constants, 120 $M^{-1}s^{-1}$, was much slower than the diffusion-controlled rate constant. In summary we accomplished our preliminary goal of this project. We were unable to determine the exact rate constants for these two proton transfer processes due to the fact that the rotation of the 2-butyne ligands in these two cases complicated the situation.

The search for other slow proton transfer reactions with terminal oxo ligand was not successful. There are not many well-characterized terminal oxo/hydroxyl complexes in the literature. The proton transfer rate for one of complexes that we tried proved to be too fast to be measured by our stopped-flow apparatus.

IV. Experimental Section.

Materials. Reactions and manipulations were performed under an atmosphere of nitrogen purified by passing through BTS catalyst (BASF) and molecular sieves (3Å Linde), either using standard Schlenk techniques or in an inert atmosphere box. $Re(O)(I)_3(PPh_3)_2$[127], $NaBArF'_4$[128], $H(Et_2O)_2BArF'_4$, K_2ReCl_6[129], $[Re(en)_2O_2]Cl$[130],

---

[127] Manion, A. B.; Erikson, T. K. G.; Spaltenstein, E.; Mayer, J. M. *Organometallics*, **1989**, *8*, 1871.

[128] Brookhart, M.; Grant, B.; Volpe, Jr., A. F. *Organometallics*, **1992**, *11*, 3920.

[129] Watt, G. W.; Thompson, R. J. *Inorganic Synthesis* **1963**, *7*, 189.

[130] Murmann, R. K *Inorganic Synthesis* **1966**, 8, 172.

$[Re(O)_2(cyclam)](ClO_4)$,[30] O_1-cyclam[131], $[Re(O)_2(O_1cyclam)](ClO_4)$, $[Re(O)_2(H_1O_1cyclam)]$, $Re(O)(I)(MeC{\equiv}CMe)_2$, $Re(O)(Et)(MeC{\equiv}CMe)_2$, and $Re(O)(Me)(MeC{\equiv}CMe)_2$[34] were prepared according to published procedures.

Benzene, tetrahydrofuran (THF), hexane, pentane and pyridine were distilled from sodium-benzophenone ketyl in the presence of tetraglyme. Dichloromethane was distilled from P_4O_{10}. Acetonitrile[132] was stirred with $CuSO_4$. The solid was filtered. It was then distilled from P_4O_{10} and CaH_2. Trifluoromethanesulfonic acid and trifluoromethanesulfonic acid-*d* were stored in vacuum bulbs in the inert atmosphere box upon receiving. They were purified by three freeze/pump/thaw cycles at -196 °C and transferred into flame-dried vacuum bulbs when they turned dark after stored for some time.

Dichloromethane-d_2, benzene-d_6, chloroform-*d*, and acetonitrile-d_3 were purchased from Cambridge Isotopes Laboratories. Dichloromethane-d_2, chloroform-*d* and acetonitrile-d_3 were stirred with P_4O_{10}, degassed by three freeze/pump/thaw cycles at -196 °C and transferred into flame-dried vacuum bulbs. They were stored in the inert atmosphere box. Benzene-d_6 was distilled from sodium-benzophenone ketyl and stored in the inert atmosphere box.

$CH_3C_6H_4SO_3H$ was dried by heating it up to 50 °C under vacuum. Alternatively, benzene was distilled from a solution of the acid using a Dean-Stark trap until the distillate became clear; addition of hexane to the solution caused the precipitation of fine powder. The mixture was transferred to another pre-dried flask via cannula; the solvent was evaporated.

---

[131] Machida, R.; Kimura, E.; Kodama, M. *Inorg. Chem.* **1983**, *22*, 2055.

All other reagents employed were used without further purification.

Instruments. ^{1}H NMR spectra were recorded at 300 MHz on a Bruker AC-300P spectrometer unless otherwise noted; ^{13}C NMR spectra were recorded at 75 MHz. HMQC, COSY, NOESY, and EXSY experiments were performed on a 500 MHz Bruker spectrometer. NMR spectra were obtained at room temperature unless otherwise noted. Residual ^{1}H shifts in the deuterated solvents were used as internal standards in the ^{1}H NMR spectra. ^{13}C shifts in the solvents were used as internal standards in the ^{13}C NMR spectra.

Infrared spectra were recorded on a Perkin-Elmer 983 spectrophotometer and reported in cm^{-1}. UV-Vis spectra were recorded on a Hewlett Packard HP8453 diode array spectrophotometer. Chromatography with less than 1 g material was performed on a Chromatotron (Harrison Research Inc.) with silica gel (Merck, TLC grade 7749) as the adsorbent. Otherwise flash chromatographies were performed on silica gel 60 (Merck, 230-400 mesh).

The rapid scan stopped-flow system used was a Hi-Tech Canterbury SF-41 with OLIS RSM-1000 rapid scanning device (On-Line Instrument Systems) with temperature control of ±0.1 °C. It could obtain one thousand spectra per second with each spectrum up to 300 nm wide. The noise level of the RSM-1000 was about 0.001 au. The software used to control the apparatus and to analyze the data was OLIS System Version 6.2.4. Parameter settings for the RSM were as follows: scans were collected in dual beam mode, 1000 scan/second, with a stopped-flow delay of 20 ms and sampling time of 4 μs.

---

[132] Moore E. J.; Sullivan, J. M.; Norton, J. R. *J. Am. Chem. Soc.* **1986**, *108*, 2257.

The monochromater grating was 400 lines with a blaze wavelength of 500 nm. The speed of the 16-slit scanning disk was 62.50 Hz with the step motor set at 4.0 steps/nm.

The gNMR 4.1. program (Cherwell Scientific) was used to analyze the temperature-dependent ^{1}H NMR kinetic data. ^{1}H NMR spectra were converted to gNMR readable files via the gSPG converter in the software package. After simulating the spectra of the starting material and product, the exchange rate constants were obtained by iteration on the experimental variable temperature ^{1}H NMR spectra with variation of the rate constants.

VT ^{1}H NMR Studies of the Protonation of Re(O)(Et)(MeC≡CMe)$_2$ with CF_3COOH. A 5 mm NMR tube was charged with Re(O)(Et)(MeC≡CMe)$_2$ (0.0253 g, 0.075 mmol). CD_2Cl_2 and CF_3COOH (56.8 μL, 0.74 mmol) were transferred to the NMR tube on a high-vacuum line at -78 °C. VT ^{1}H NMR spectra were taken from -80 to 0 °C.

Protonation Product of Re(O)(Et)(MeC≡CMe)$_2$ with CF_3COOH. Modified from the reported procedure with CF_3SO_3H.[34] Re(O)(Et)(MeC≡CMe)$_2$ (0.0509 g, 0.15 mmol) in benzene (7.5 mL) was treated with CF_3COOH (15 μL, 0.2 mmol). CH_2Cl_2 (3 mL) and hexane (30 mL) were added. The solution was kept at -78 °C overnight. Some solid formed. Solvent was removed via cannula. The solid was washed with hexane (2 × 25 mL) and dried under vacuum. Ether was also tried as solvent with similar results.

VT ^{1}H NMR Studies of the Self-exchange of Re(O)(Et)(MeC≡CMe)$_2$ with its Conjugate Acid. (a) A NMR tube was charged with Re(O)(Et)(MeC≡CMe)$_2$ (0.0212 g,

0.062 mmol). CD_2Cl_2 and CF_3SO_3H (3 μL, 0.034 mmol) were transferred to the NMR tube on a high-vacuum line at -78 °C. VT ^1H NMR spectra were recorded from -70 to 0 °C. (b) A NMR tube was charged with $Re(O)(Et)(MeC{\equiv}CMe)_2$ (0.0101 g, 0.03 mmol) $[Re(OH)(Et)(MeC{\equiv}CMe)_2](CF_3SO_3)$ (0.0144 g, 0.029 mmol) in CD_2Cl_2. VT ^1H NMR spectra were recorded from -15 to 20 °C.

$[Re(OH)(Et)(MeC{\equiv}CMe)_2](CF_3SO_3)$.[34] A variation on the published procedure: $Re(O)(Et)(MeC{\equiv}CMe)_2$ (0.1 g, 0.29 mmol) in CH_2Cl_2 (1 mL) was treated with CF_3SO_3H (26 μL, 0.29 mmol) at -70 °C. CH_2Cl_2 (3.5 mL) was added to dissolve some solid formed in the solution. The solution was kept at -78 °C overnight. Some solid formed. The liquid was decanted. The solid was washed with hexane (3 × 10 mL) and dried under vacuum for two and a half hours at 0 °C. Ether was also tried as solvent in this reaction with similar result. Yield: 0.118 g (82%). ^1H NMR (CD_2Cl_2): same as the reported spectrum.

$[Re(OH)(Et)(MeC{\equiv}CMe)_2](BArF'_4)$. CH_2Cl_2 (1 mL) was added to $Re(O)(Et)(MeC{\equiv}CMe)_2$ (0.1 g, 0.29 mmol) and $H(Et_2O)_2(BArF'4)$ (0.3 g, 0.3 mmol) at -20 °C. The temperature of the solution was lowered slowly, yielding some crystals. The solution was kept at -78 °C overnight. Some solid formed. The liquid was decanted. The solid was washed with pentane (3 × 5 mL), and dried under vacuum. Ether was also tried with similar results. VT ^1H NMR spectra were taken. Yield: 0.15 g (43%). ^1H

NMR (CD_2Cl_2): similar to $[Re(OH)(Et)(MeC{\equiv}CMe)_2](CF_3SO_3)$ but broad even at low temperature.

Reversibility of the Protonation of $Re(O)Me(MeC{\equiv}CMe)_2$ with Acids. $Re(O)Me(MeC{\equiv}CMe)_2$ (0.012 g, 0.037 mmol) in $CDCl_3$ (0.6 mL) was treated with a stock solution of CF_3SO_3H (0.37 M) in $CDCl_3$ (0.1 mL). A ^1H NMR spectrum of the reaction solution was obtained. The solution was then treated with a solution of pyridine (0.19 M) in $CDCl_3$ (0.2 ml), and a ^1H NMR spectrum showed $Re(O)Me(MeC{\equiv}CMe)_2$ formed again. Other acids used were CF_3COOH and $MeC_6H_4SO_3H$. Solvents used were $CDCl_3$ and CD_3CN.

VT ^1H NMR Studies of the Protonation of $Re(O)Me(MeC{\equiv}CMe)_2$ with Acids. An NMR tube was charged with $Re(O)Me(MeC{\equiv}CMe)_2$ (0.012 g , 0.037 mmol) and $MeC_6H_4SO_3H$ (0.0112 g, 0.060 mmol). CD_3CN (0.6 mL) was added at -20 °C. Acids including $MeC_6H_4SO_3H$, CF_3SO_3H, and CF_3COOH were used. The amounts of acids were also varied. Solvents used were CD_3CN and $CDCl_3$.

$[Re(O)_2L_2]Cl$ (L = *trans*-1,2-$C_6H_{10}(NH_2)_2$). Followed the similar procedure for $[Re(O)_2(en)_2]Cl$.[29] Fine powder of K_2ReCl_6 (2.5 g, 5.24 mmol) was stirred with neat *trans*-1,2-$C_6H_{10}(NH_2)_2$ (25 mL); air was bubbled through the reaction mixture overnight. The solution was then treated with cold acetone (25 mL) and poured into more cold acetone (250 mL). The product was filtered and washed with acetone (3 × 50 mL). The solid was dissolved in water (40 mL) and treated with methanol (40 mL). The solvent

was slowly evaporated. Yield: 1.43 g (57%). IR: 817 [ν (ReO)]. UV-Vis: λ_{max} = 436 nm. These results were similar to $[Re(O)_2(en)_2]Cl$.

Titration of $[Re(O)_2(cyclam)](ClO_4)$ with $HClO_4$. $[Re(O)_2(cyclam)](ClO_4)$ (2 mL, 5.55mM) was treated with $HClO_4$ (0.2 mL, 11.1 mM). A UV-Vis spectrum was obtained. The process was repeated 12 times with $HClO_4$ (0.2 mL, 11.1 mM).

Rapid Scan Stopped-flow Studies of the Protonation of $[Re(O)_2(cyclam)](ClO_4)$ with $HClO_4$. One solution contained $[Re(O)_2(cyclam)](ClO_4)$ (0.0798 g, 0.154 mmol) in water (10 mL); the other contained $HClO_4$ (0.154 M) in water (10 mL). These solutions were placed in the two reservoirs in the stopped-flow apparatus. Most of the reaction finished during mixing. The protonation was too fast to follow using the stopped-flow apparatus.

CHAPTER THREE-THE KINETIC STUDIES OF THE PROTONATION OF OXO COMPLEXES OF (2,7-NONADIYNE) RHENIUM(III)

I. Introduction.

In order to obtain more stable protonated products of the rhenium(III) complexes and to eliminate the rotation of the 2-butyne ligand a new ligand system was needed. Dr. Anthony Rappé in Chemistry Department suggested that a dialkyne chelating system with three CH_2 units between the two triple bonds would be a potential target; it would form a pseudo six-membered chelating ring with rhenium. Later we discovered that Mayer and his coworkers[20a] had synthesized a chelating dialkyne with four CH_2 units between the triple bond, and had made rhenium iodide derivative; no details were given. The yield of that complex was low.

We synthesized the dialkyne ligand and obtained the rhenium complexes with this new ligand. $Re(O)(I)(H_3CC{\equiv}C(CH_2)_3C{\equiv}CCH_3)$ (**1**) stands out as an ideal candidate for the study of the protonation of a terminal oxo ligand. Detailed kinetic studies have been carried out of the protonation of this complex.

II. Results and Discussion.

A. Synthesis of the Dialkyne Ligand and the Rhenium Complexes with This Ligand.

Synthesis of the Dialkyne Ligand. The new chelating dialkyne ligand, 2,7-nonadiyne, was synthesized by lithiating the 1,6-heptadiyne with *n*-BuLi and quenching the intermediate with MeI (eq 3.1).

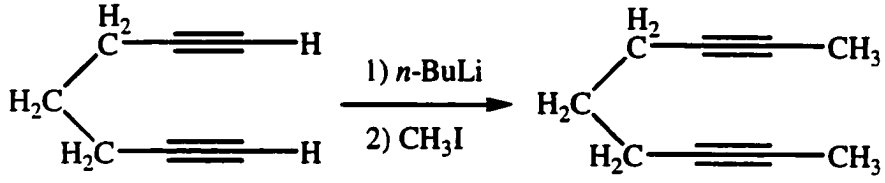

(eq 3.1)

Re(O)(I)($H_3CC{\equiv}C(CH_2)_3C{\equiv}CCH_3$) (1). Complex **1** was synthesized by following a modified form of the procedure for Re(O)(I)($MeC{\equiv}CMe)_2$,[20a] and isolated as a crystalline, air- and water- stable solid. It is soluble in typical organic solvents. The ^1H NMR spectrum of **1** contains five different C-H resonances, indicating that it has C_s symmetry (Figure 3.1). The relative intensities of the peaks were not determined due to the overlapping of the peaks. The hydrogens of the CH_2 unit in the center, and the two equivalent pairs of CH_2 units attached to the triple bond are all diastereotopic, and show an AB pattern. The complete assignment was confirmed by an HMQC spectrum.

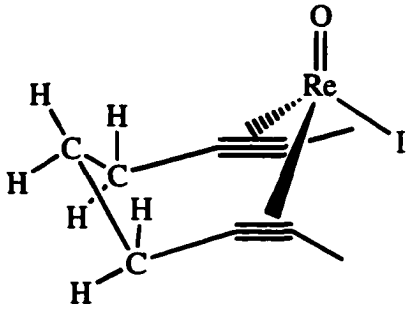

Figure 3.1. Solution structure of **1** based on NMR experiment.

The ^{13}C chemical shifts of the dialkyne ligand, 138.5 and 143.4, suggest that the chelating dialkyne ligand as a whole acts as a six-electron donor to the rhenium through σ as well as π donation. Templeton and coworkers[133] have suggested that there is a correlation between the ^{13}C chemical shifts of acetylene ligands and the number of the electrons that they donate to the metal center. Mayer and coworkers[134] applied this suggestion to their rhenium(III) complexes and concluded that the acetylene ligands were three-electron donors in their complexes. Complex **1** is an 18-electron complex if one considers the suggestion that there is significant π bonding from the terminal oxo ligand to the rhenium, making it a six-electron donor (see chapter one).

The X-ray structure of **1** (determined by Dr. Brian Bridgewater) (Figure 3.2.) is very close to that of $Re(O)(I)(MeC{\equiv}CMe)_2$ [20a]. The C_s symmetry of the complex is clearly displayed in the solid state. The geometry around the rhenium is pseudo tetrahedral with the midpoints of the two triple bonds occupying two vertices. An

[133] (a) Templeton, J. L.; Ward, B. C. *J. Am. Chem. Soc.* **1980**, *102*, 3288. (b) Templeton, J. L.; Ward, B. C.; Chen, G., J.-J.; McDonald, J. W.; Newton, W. E. *Inorg. Chem.* **1981**, *20*, 1248.

approxiate mirror plane contains rhenium, oxygen, iodine, and the central CH_2 unit of the dialkyne ligand. For example the Re-C (2) distance, 2.064 (6) Å, is the same as Re-C (8), 2.062 (6) Å, while the Re-C (3) distance, 2.019 (6) Å, is the same as Re-C (7), 2.016 (6) Å. The I-Re-O angle is 110.64 (16)°. The Re-O bond length is 1.692 (4) Å, the same as the Re-O bond length in $Re(O)(I)(MeC{\equiv}CMe)_2$ of 1.697 (3) Å.[20a] The Re-I bond length is 2.6809 (5) Å, close to the Re-O bond length in $Re(O)(I)(MeC{\equiv}CMe)_2$ of 2.691 (1) Å.[20a] The Re-C (2) distance is a little longer than Re-C (3). The C≡C bond are approximately perpendicular to the Re-O bond. The C≡C bond distances (1.293 (9), 1.279 (9) Å) are close to those reported for $Re(O)(I)(MeC{\equiv}CMe)_2$ (1.288 (7), 1.278 (7), Å).

---

[134] Mayer, J. M.; Thorn, D. L.; Tulip, T. H. *J. Am. Chem. Soc.* **1985**, *107*, 7454.

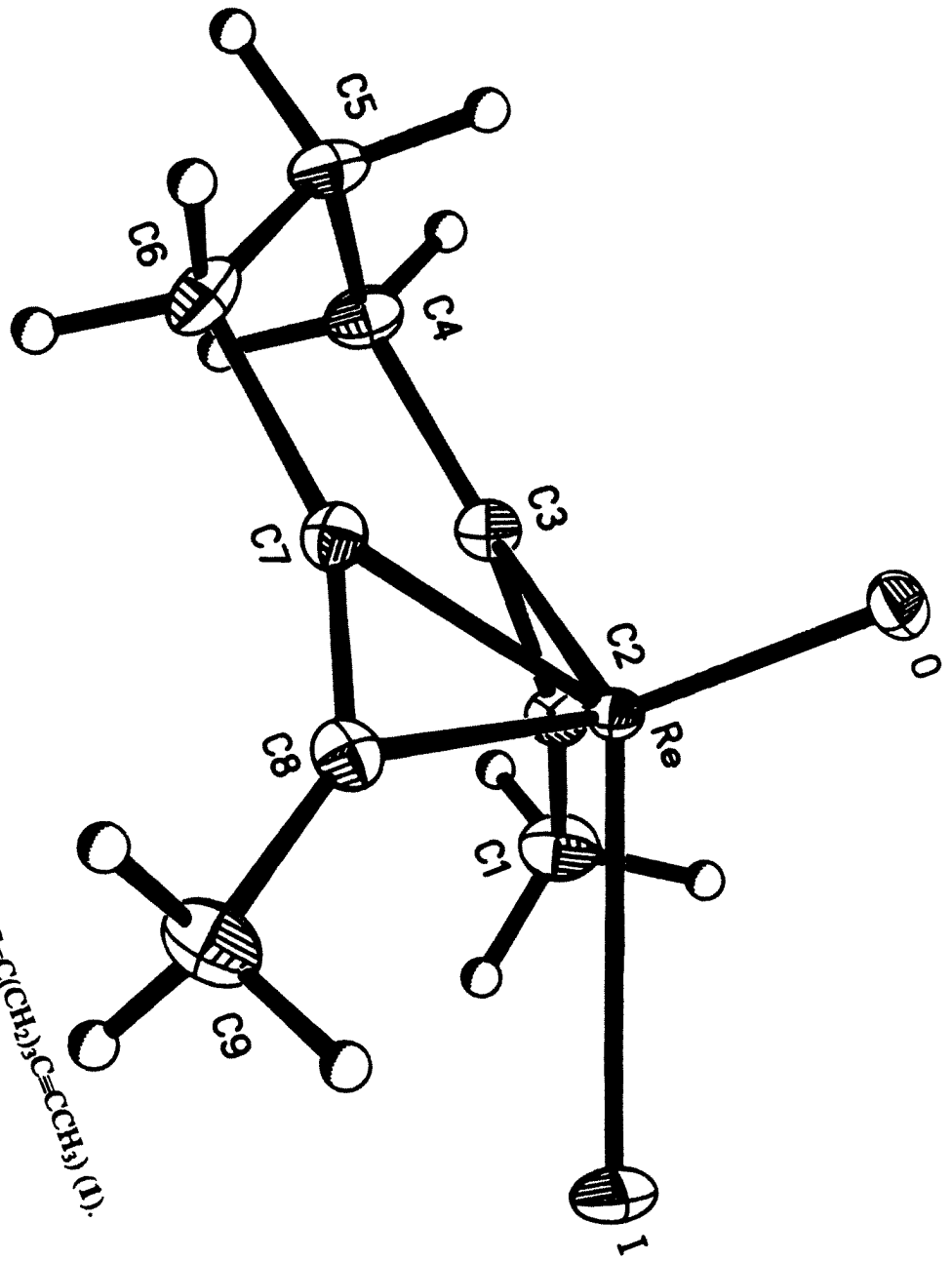

Figure 3.2. Molecular structure of $Re(O)(I)(H_3CC{\equiv}C(CH_2)_3C{\equiv}CCH_3)$ (1).

Re(O)Me($H_3CC{\equiv}C(CH_2)_3C{\equiv}CCH_3$) (2). Complex **2** was synthesized by methylation of complex **1** (eq 3.2). It was fully characterized by ^1H and ^{13}C NMR and HMQC. It had C_s symmetry in solution as complex **1** did. The X ray structure was determined by Ms. Susie Miller (Figure 3.3).

$$Re(O)(I)(H_3CCC(CH_2)_3CCCH_3 + CH_3Li \longrightarrow Re(O)(CH_3)(H_3CCC(CH_2)_3CCCH_3 + LiI \quad \text{(eq 3.2)}$$

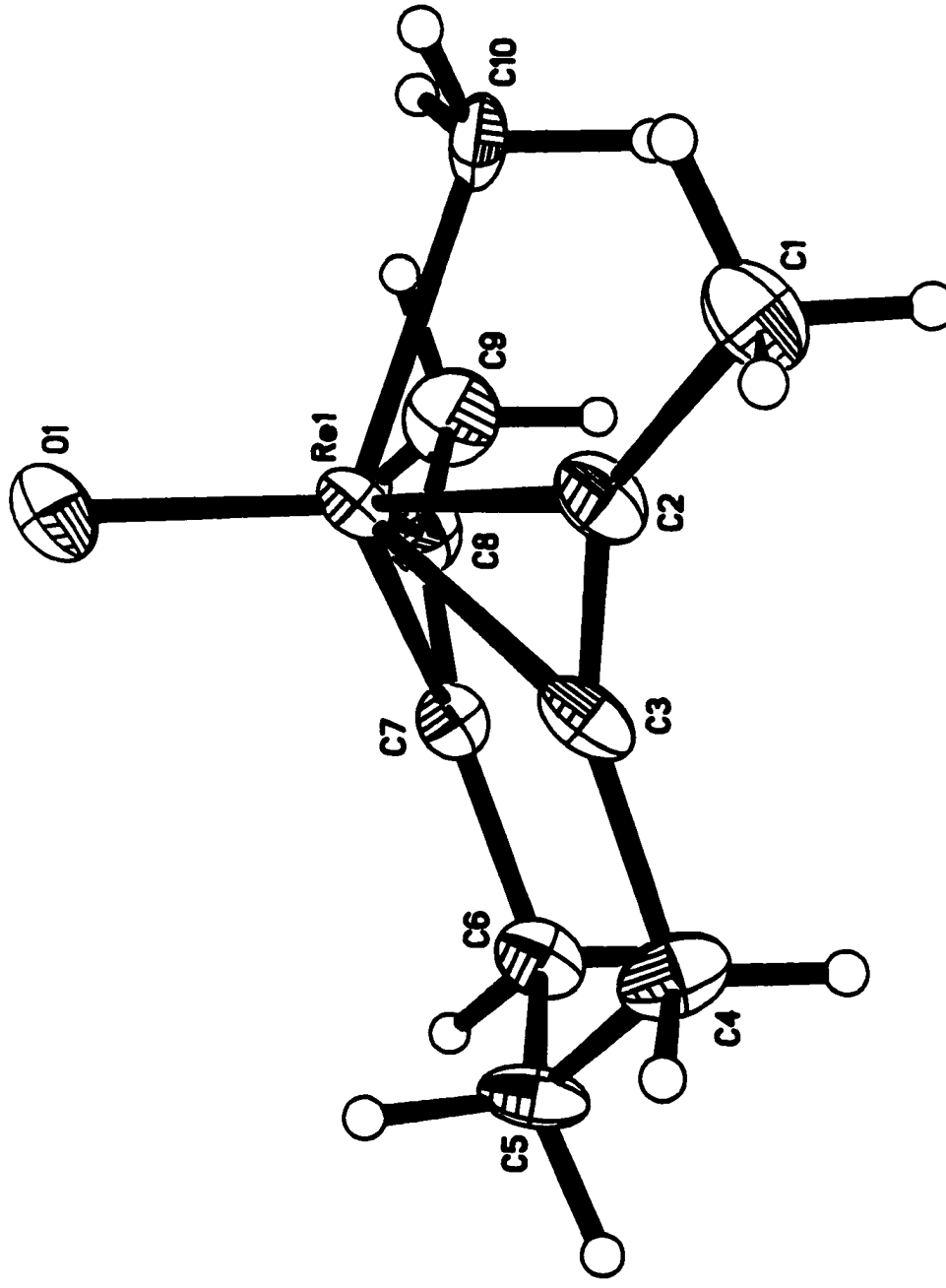

Figure 3.3. Molecular structure of $Re(O)Me(H_3CC{\equiv}C(CH_2)_3C{\equiv}CCH_3)$ (2).

The overall structure of complex **2** is close to that of complex **1**. The rhenium center adopts pseudo-tetrahedral geometry; the O-Re-C (10) angle is 111.6 (4)°. The Re-O bond length is 1.716 (8) Å, longer than that of complex **1**. The Re-C (10) bond length is 2.210 (10) Å. The Re-C (2) and Re-C (8) bond distances are 2.066 (9) Å and 2.062 (10) Å respectively. The Re-C (3) and Re-C (7) bond distances are 2.032 (11) and 2.008 (10) Å respectively. The C (2)-C (3) and C (7)-C (8) bond distances are 1.290 (14) Å and 1.287 (14) Å. These numbers are close to those in complex **1**.

The reaction of complex **2** with acid was studied. There were changes in the ^1H NMR when the solution of complex **2** was treated with *p*-$MeC_6H_4SO_3H$. The peaks were broad and not assignable. The protonation reaction was fully reversed when excess pyridine was added to the protonation solution.

B. Reaction of Re(O)(I)($H_3CC{\equiv}C(CH_2)_3C{\equiv}CCH_3$) (1) with Acids and Related Reactions.

The Reaction of Re(O)(I)($H_3CC{\equiv}C(CH_2)_3C{\equiv}CCH_3$) (1) with CF_3SO_3H. A clean product was produced when a solution of **1** was treated with excess CF_3SO_3H in acetonitrile (eq 3.3). The product, **3**, was stable at room temperature under N_2 for eight hours but eventually it decomposed.

$$Re(O)(I)(H_3CC{\equiv}C(CH_2)_3C{\equiv}CCH_3) + CF_3SO_3H \xrightarrow{CH_3CN} \mathbf{3} \qquad \text{(eq 3.3)}$$

The complete assignment of chemical shifts in the ^{1}H and ^{13}C NMR spectra of **3** was confirmed by an HMQC spectrum (Figure 3.4). The ^{1}H NMR spectrum of **3** contains five chemical shifts with the relative intensities of 6:2:2:1:1. The two CH_3 groups are equivalent like those in the complex **1**, indicating that the product also has *Cs* symmetry in solution. The two chemical shifts corresponding to CH_2 units attached to the triple bonds (6.00, 5.05 ppm) are far downfield from those in the parent complex **1** (3.50, 2.59 ppm). The chemical shift corresponding to one of the protons in the central CH_2 unit (0.64 ppm) is far upfield compared to that in complex **1** (2.05, 2.46 ppm). The possibility that the C-H bond is coordinated to the metal can be ruled out from the coupling constant argument and later from the structure of the complex. It is not clear why the upfield shift happens. The chemical shifts of the acetylene carbons in the ^{13}C NMR spectrum are 175 and 188 ppm, further downfield than those in complex **1**. All these changes in the NMR spectra indicate changes in the coordination sphere of the rhenium after the reaction. The coordinated triple bonds appear to have remained unchanged.

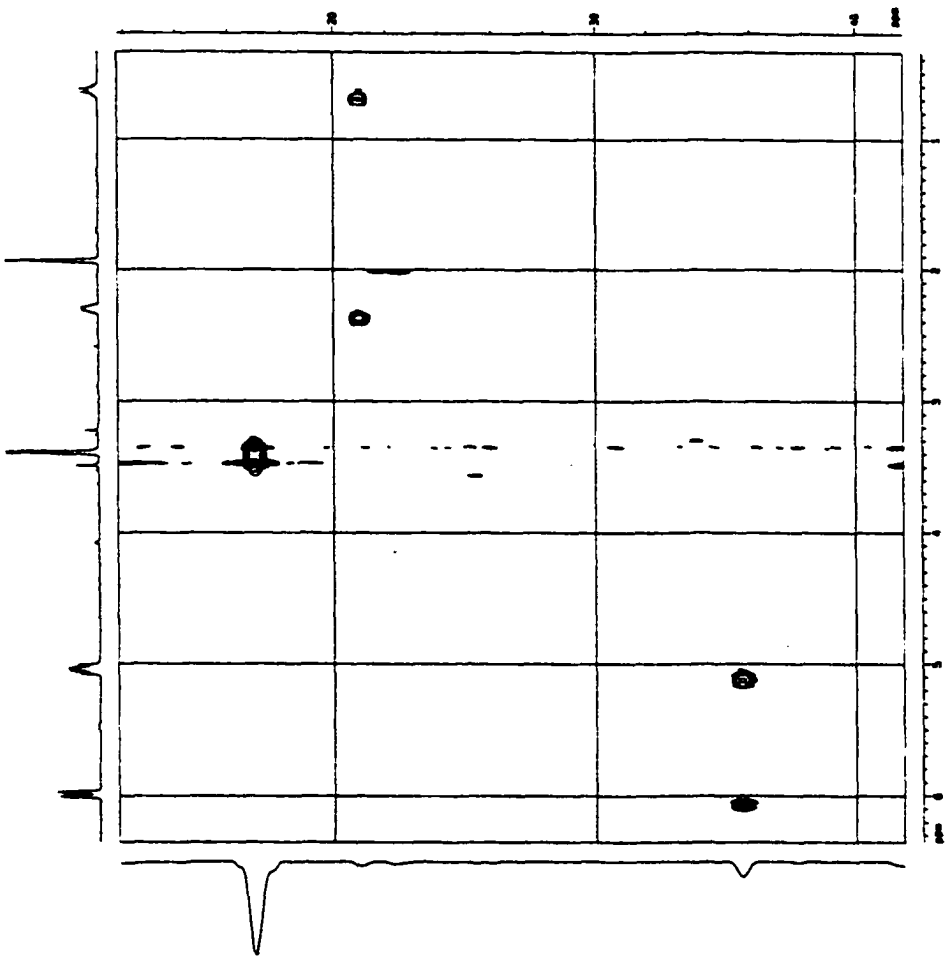

Figure 3.4. HMQC spectrum of the product of complex 1 with excess CF_3SO_3H in CD_3CN at -10 °C

Reversal by Pyridine of the Reaction of $Re(O)(I)(H_3CC{\equiv}C(CH_2)_3C{\equiv}CCH_3)$ (1) with CF_3SO_3H. The reaction in eq 3.3 was completely reversed when a solution of complex **1** with CF_3SO_3H in acetonitrile was treated with a slight excess of pyridine. The ^1H NMR spectrum confirmed the clean re-formation of complex **1** without any decomposition. This suggests that *protonation* reactions are indeed involved in the reaction of complex **1** with CF_3SO_3H. There are three possible protonation sites: the terminal oxo ligand, the iodine ligand, and the metal itself. The chelating dialkyne ligand is not protonated; if it were, the Cs symmetry of the whole complex would be disrupted.

Titration of $Re(O)(I)(H_3CC{\equiv}C(CH_2)_3C{\equiv}CCH_3)$ (1) with CF_3SO_3H. A series of titrations of $Re(O)(I)(H_3CC{\equiv}C(CH_2)_3C{\equiv}CCH_3)$ (**1**) with CF_3SO_3H in acetonitrile were performed to investigate the thermodynamic aspects of this protonation reaction (Figure 3.5). Three equivalents of CF_3SO_3H were needed to convert complex **1** to the final product completely. Thus either the product is a fairly strong acid or more than one protonation step has occurred.

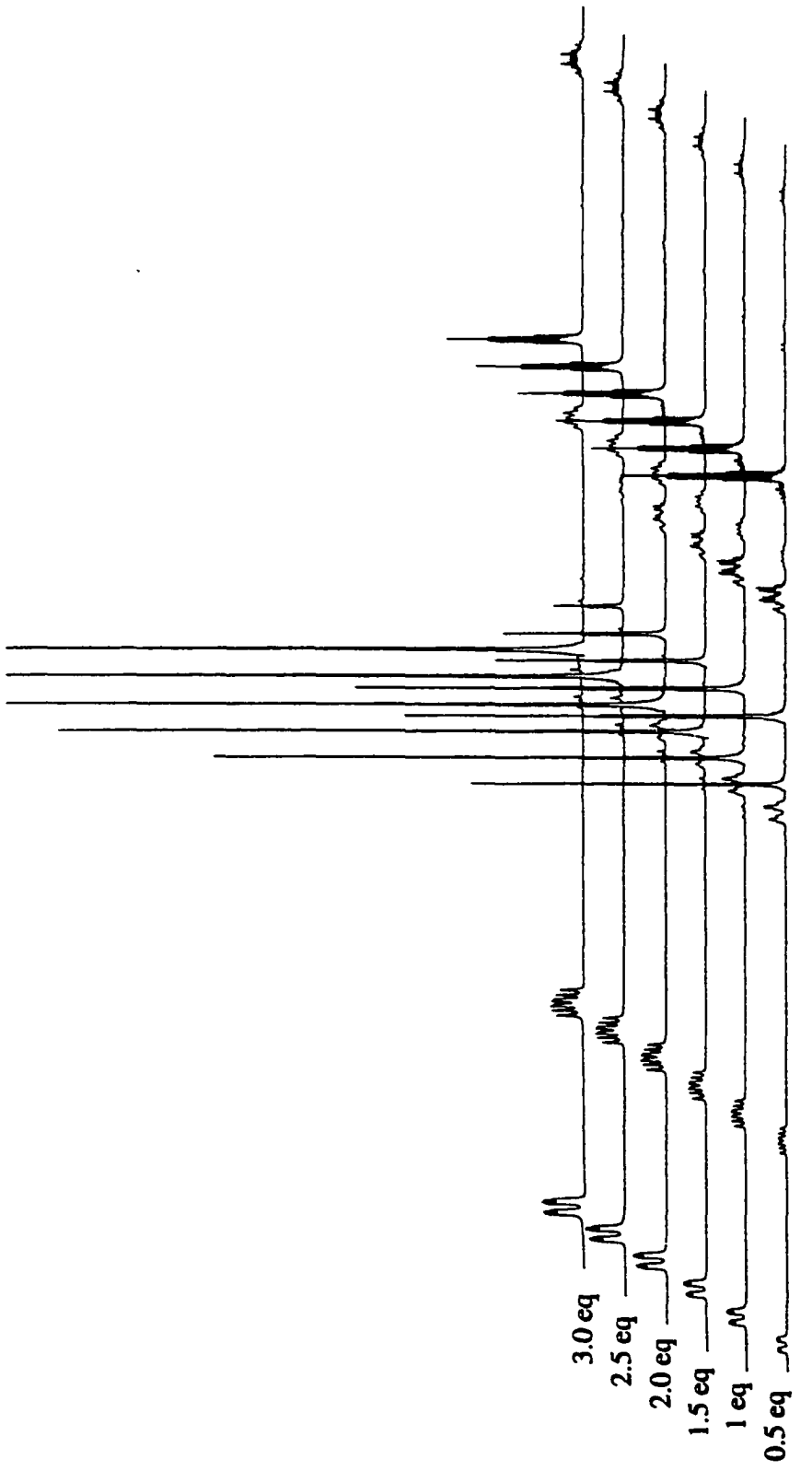

Figure 3.5. ^{1}H NMR spectra of complex **1** with 0.5, 1.0, 1.5, 2.0,2.5, and 3 eq. of CF_3SO_3H in CD_3CN at -10 °C.

Protonation of Re(O)(I)($H_3CC{\equiv}C(CH_2)_3C{\equiv}CCH_3$) (1) with Other Acids.

Different reaction conditions were examined in order to further understand the protonation reaction and to isolate the crystal of the final product. Very strong acids were needed to protonate complex **1**; there was no reaction between complex **1** and $H_3CC_6H_4SO_3H$ (pK_a = 8.7 in CH_3CN)[135] in acetonitrile. The pK_a of the protonated complex can be estimated to be less than 6.1 in CH_3CN. Both $HBF_4{\bullet}(CH_3)_2O$ and $(C_6Me_3H_4)B(C_6F_5)_4$[136] reacted with complex **1** to produce the final product. Solvent proved crucial in this reaction. Acetonitrile was needed in the reaction; otherwise no clean product could be obtained. No solid product could be isolated from the reaction of complex **1** with CF_3SO_3H. Changes of counterion, of solvent, of acid, and of the amount of acid used were investigated. No crystal of the product was isolated until $HBF_4{\bullet}(CH_3)_2O$ in CH_2Cl_2/CH_3CN was tested.

[Re(I)(CH_3CN)$_3$($H_3CC{\equiv}C(CH_2)_3C{\equiv}CCH_3$)][$BF_4$]$_2$ (3), the Product of Eq 3.3.

Crystals of complex **3**, the product of eq 3.3, suitable for X-ray diffraction study, were finally obtained from the reaction of complex **1** with excess $HBF_4{\bullet}(CH_3)_2O$ in CH_2Cl_2/CH_3CN. The ^1H and ^{13}C NMR spectra of complex **3** were identical to those obtained from solutions from the reaction of complex **1** with CF_3SO_3H. No Re-O stretching frequency was found in the IR spectrum of complex **3**, confirming the loss of the terminal oxo ligand.

---

[135] Jasinski, T.; El-Harakany, A. A.; Halaka, F. G.; Sadek, H. *Croat. Chem. Acta* **1978**, *51*, 1.

[136] Reed, C. A.; Fackler, N. L. P.; Kim, K.-C.; Stasko, D.; Evans, D. R.; Boyd, P. D.; Rickard, C. E. F. *J. Am. Chem. Soc.* **1999**, *121*, 6314.

The most noteworthy feature of the X-ray structure of complex **3** (determined by Dr. Brian Bridgewater) (Figure 3.6.) is the absence of any kind of oxygen ligand, as expected from the IR spectrum. It also confirms that the C_s symmetry is maintained in solid state as in the solution. There is a crystallographically imposed mirror plane in the structure of complex **3**. Three acetonitrile molecules are coordinated to the rhenium in a linear fashion. Re-N distances are 2.085 (11) Å for one CH_3CN and 2.185 (8) Å for the other two CH_3CN. These distances are typical for the Re-N distances reported for acetonitrile linearly coordinated to rhenium.[137] The Re-I distance is 2.7540 (11) Å, longer than that in complex **1**. The Re-C (2) and Re-C (3) distances are 2.023 (10) and 2.030 (10) Å, close to the shorter ones in complex **1**. The C≡C distance in complex **3** is 1.277 (13) Å, the same as in complex **1**. All these suggest that the chelating dialkyne ligand in complex **3** still acts as a six-electron donor and that complex **3** is overall an 18-electron complex.

[137] (a) Bernstein, S. N.; Dunba, K. R.; *Angew Chem. Int. Ed. Engl.* **1992**, *31*, 1360. (b) Storhoff, B. N.; Lewis, Jr. H. C. *Coord. Chem. Rev.* **1977**, *23*, 1. (c) Wadepohl, H.; Arnold, U.; Pritzkow, H.; Calhorda, M. J.; Veiros, L. F. *J. Organomet. Chem.* **1999**, *587*, 233.

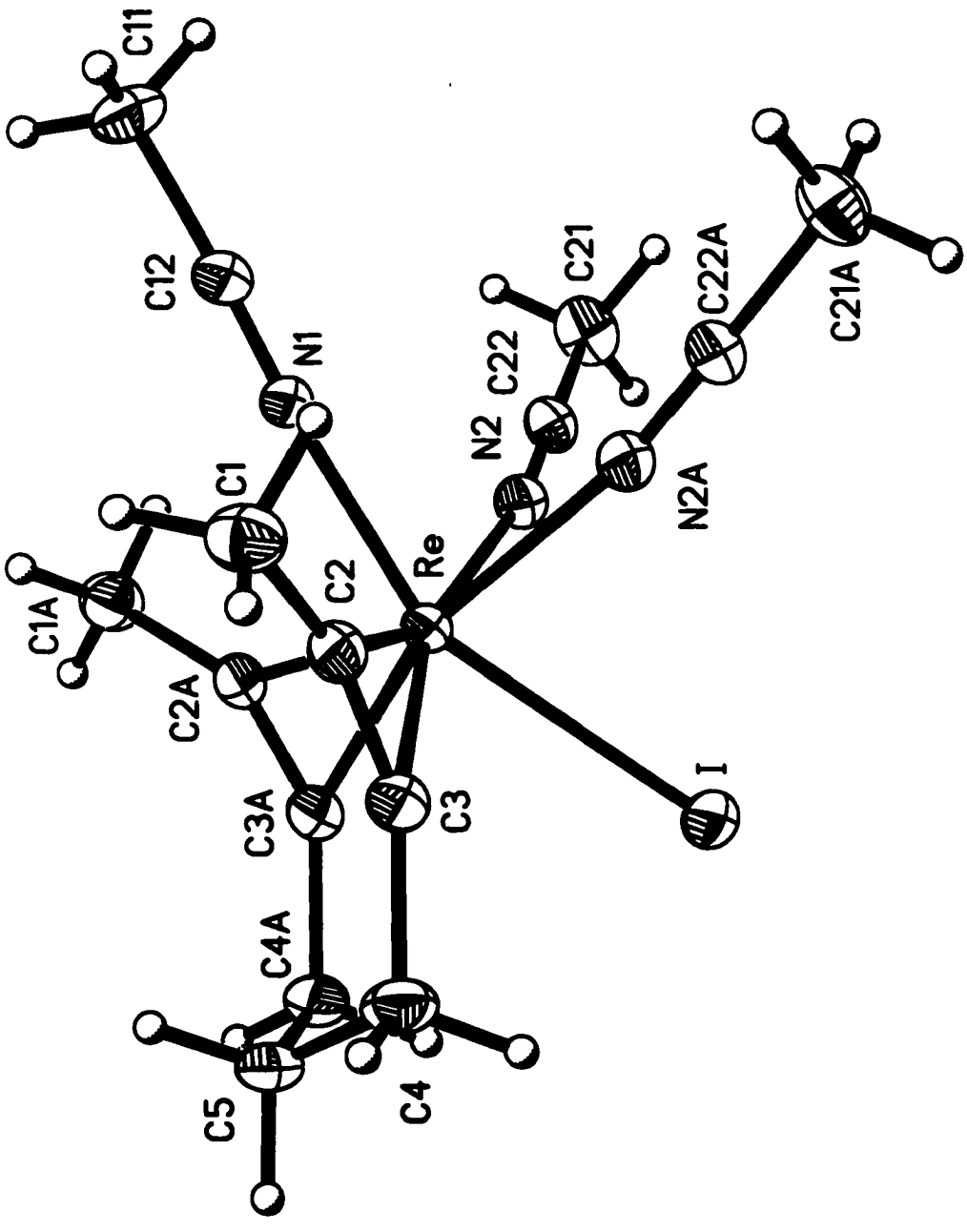

Figure 3.6. Molecular structure of cation of $[Re(I)(CH_3CN)_3(H_3CC{\equiv}C(CH_2)_3C{\equiv}CCH_3)][BF_4]_2$ **(3).**

The Reaction of $[Re(I)(CH_3CN)_3(H_3CC{\equiv}C(CH_2)_3C{\equiv}CCH_3)][BF_4]_2$ (3) with $H_2{}^{18}O$. Complex **1** was reformed when a solution of complex **3** was treated with excess $H_2{}^{18}O$, as confirmed by a ^1H NMR spectrum. A solution IR spectrum showed a strong peak at 916 cm^{-1}, agreeing well with the expected maximum isotopic shift in the Re-O stretching frequency, 918 cm^{-1}, according to eq. 3.4.[138] There is only one strong peak in the IR spectrum of ^{18}O-labeled **1**. There are two strong peaks (974 and 956 cm^{-1}) in the IR spectrum of unlabeled complex **1**; both disappeared after protonation. This could be due to Fermi resonance between the stretching frequency and an overtone or combination bond.

$$\prod\left(\frac{\nu^*}{\nu}\right) = \prod\left(\frac{m}{m^*}\right)^{1/2} \qquad \text{(eq 3.4)}$$

where ν : the frequency of normal modes, m: mass of atom with isotope change, * indicates isotope change.

As the final product **3** from the reaction of **1** with acids does not contain a terminal oxo ligand, and the addition of water to the final product **3** regenerates **1**, the protonation of **1** is likely to involve two consecutive protonations on the terminal oxo ligand, and the replacement of an aqua ligand by acetonitrile.

---

[138] From Dr. Jack Norton's course note, modified from Wilson, Jr. E. B.; Decius, J. C.; Cross, P. C. *Molecular Vibrations The Theory of Infrared and Raman Vibrational Spectra* McGraw-Hill: New York, 1955, p182-186.

The Reaction of $Re(O)(I)(H_3CC{\equiv}C(CH_2)_3C{\equiv}CCH_3)$ (1) with other Electrophiles. In order to further probe the reactivity of the terminal oxo ligand of **1** it was treated with other electrophiles.

$Re(O)(I)(H_3CC{\equiv}C(CH_2)_3C{\equiv}CCH_3){\bullet}B(C_6F_5)_3$ (**4**) was formed when a solution of complex **1** was treated with a $B(C_6F_5)_3$ solution. The ^1H NMR spectrum of complex **4** shows that the complex has C_s symmetry in solution, so the Lewis acid has not disturbed the dialkyne ligand structure. The ^{13}C NMR spectrum of complex **4** is close to that of complex **1**.

The X ray structure of complex **4** (determined by Dr. Brian Bridgewater) is similar to that of complex **1** (Figure 3.7). It has an approximate mirror plane across the Re, oxygen, iodine and the carbon of the center CH_2 unit.

$B(C_6F_5)_3$ is attached to the terminal oxo ligand along the Re-O axis. The Re-O-B angle is 169.1 (3)°, keeping the symmetry of the complex unchanged. The Re-O bond length is longer, 1.742 (3) Å, compared to 1.692 (4) Å in complex **1**. Coordination of a Lewis acid to the terminal oxo ligand causes electronic rearrangement of the Re-O bond. Less π back donation from the oxo ligand to rhenium causes electron density to move from the Re-O bond to oxygen; the bond order could decrease and the bond length increase. A covalent bond between the oxo ligand and a proton would certainly cause more dramatic changes in the bond order and bond length, because more electronic rearrangement would be involved; protonation of the oxo ligand (to produce a hydroxo ligand) would eliminate the π donation from the oxygen to the rhenium and make the Re-OH bond into a single bond.

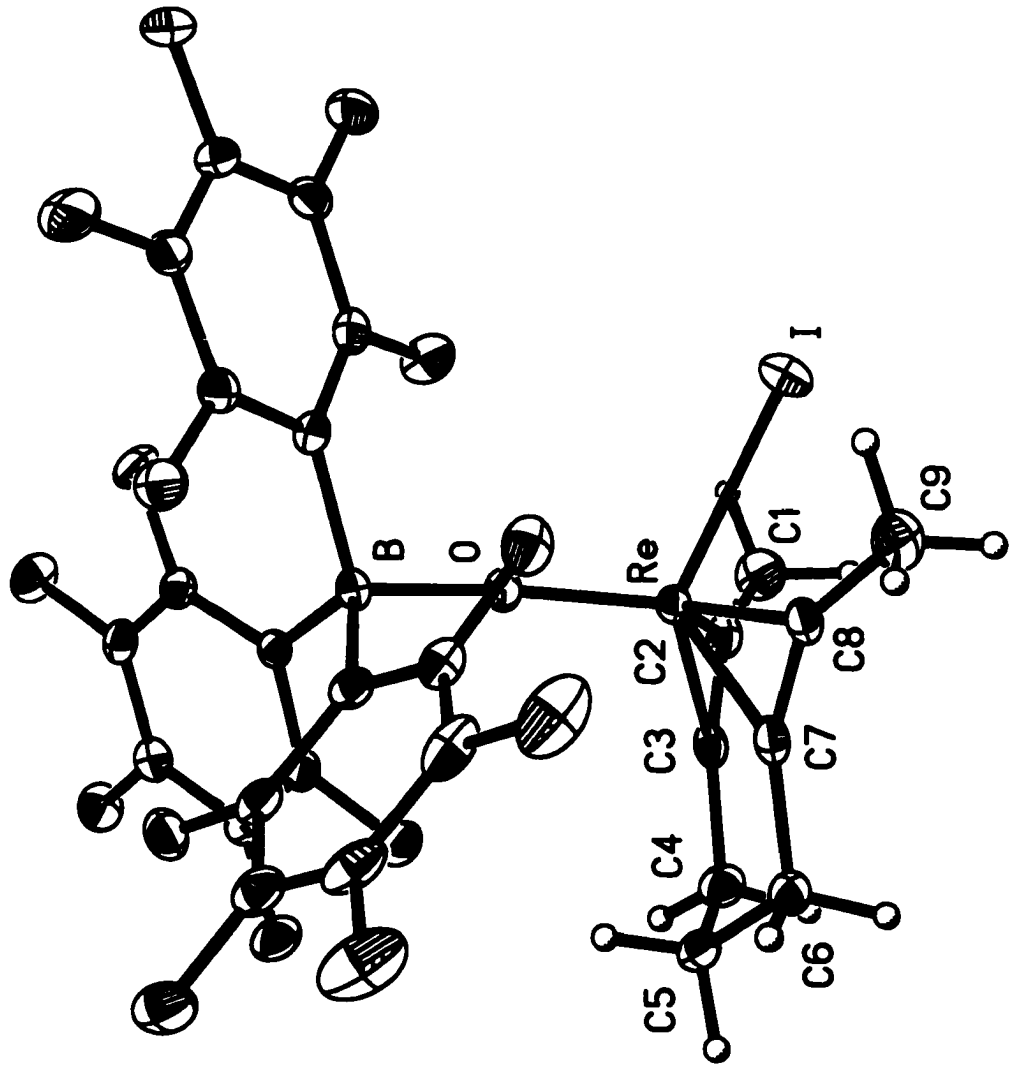

Figure 3.7. Molecular structure of $Re(O)(I)(H_3CC{=}C(CH_2)_3C{=}CCH_3)\cdot B(C_6F_5)_3$ (**4**).

Other structural changes also occurred upon the addition of $B(C_6F_5)_3$. There are changes in the distances between the rhenium and the acetylene carbons. The Re-C (2) and Re-C (8) bond lengths in complex **4** are 2.038 (5) and 2.043 (5) Å, slightly shorter than those in complex **1**. The Re-C (3) and Re-C (7) bond lengths in complex **4** are 2.010 (5) and 1.993 (5) Å, slightly shorter than those in complex **1**. The Re-I bond in complex **4** is 2.6388 (5) Å, a little shorter than that in complex **1**, 2.6809 (5) Å. Upon coordination of $B(C_6F_5)_3$ to the oxo ligand, the other ligands move closer to the rhenium center and donate more electron density to that center in order to compensate for the loss of electron density donated from the oxo ligand. Protonation on the oxo ligand would cause more dramatic changes in these bond lengths; substantial structural and electronic rearrangement should occur. The rate constant of such a protonation will be much slower than the diffusion-controlled rate constant under favorable thermodynamic driving force.

Many other electrophiles were examined. Most of them, including $Et_3SiB(C_6F_5)_4$, $CF_3SO_3CH_3$, CH_3I, and $CF_3SO_3Si(CH(CH_3)_2)_3$, failed to produce clean products,. The reaction of complex **1** with $CF_3SO_3SiEt_3$ did produce a clean product, $Re(OSiEt_3)(I)(H_3CC{\equiv}C(CH_2)_3C{\equiv}CCH_3)(CF_3SO_3)$, which was characterized by its ^1H, ^{13}C, COSY, and HMQC NMR spectra. It would be interesting to obtain the X-ray structure of that complex to see if the structure of it differs more from complex **1** than did complex **4**.

The Reaction of $Re(O)(I)(H_3CC{\equiv}C(CH_2)_3C{\equiv}CCH_3)$ (1) with $P(CH_3)_3$. Mayer and coworkers[139] reported the reactions of $Re(X)(I)(EtC{\equiv}CEt)_2$ (X = O or S) with

[139] Tahmassebi, S. K.; Mayer, J. M. *Organometallics* **1995**, *14*, 1039.

phosphines. Both complexes, acting as oxygen or sulfur donor, reacted cleanly with $PMePh_2$ in the presence of added alkyne to produce $Re(I)(EtC{\equiv}CEt)_3$ and the corresponding phosphine chalcogenide. No reaction was observed for both complexes with PPh_3 and a number of uncharacterized species were found when both complexes reacted with PMe_3.

Different reactivity was found when complex **1** was treated with PMe_3. Instead of attacking oxygen, PMe_3 replaced the iodide ligand, forming $[Re(O)(PMe_3)(H_3CC{\equiv}C(CH_2)_3C{\equiv}CCH_3)]I$ (**5**). Crystals of **5** were obtained and the X-ray structure was determined (determined by Dr. Brian Bridgewater) (Figure 3.8).

The structure of **5** is close to that of complex **1**. The approximate C_s symmetry remains in **5**. The Re-C (2) and Re-C (8) bond distances are 2.078 (4) and 2.074 (4) Å and the Re-C (3) and Re-C (7) distances are 2.016 (4) and 2.019 (4) Å. The Re-O bond distance is 1.702 (2) Å. The Re-P bond distance is 2.4148 (10) Å. The C (2)-C (3) and C (7)-C (8) bond distances are 1.285 (5) and 1.278 (5) Å. The dialkyne ligand acts as a six-electron donor. The O-Re-P angle is 108.41 (10)°. Iodide is found in the crystal lattice as the counterion. A summary of the structural features of the five complexes, characterized by X-ray, is presented in table 3.1.

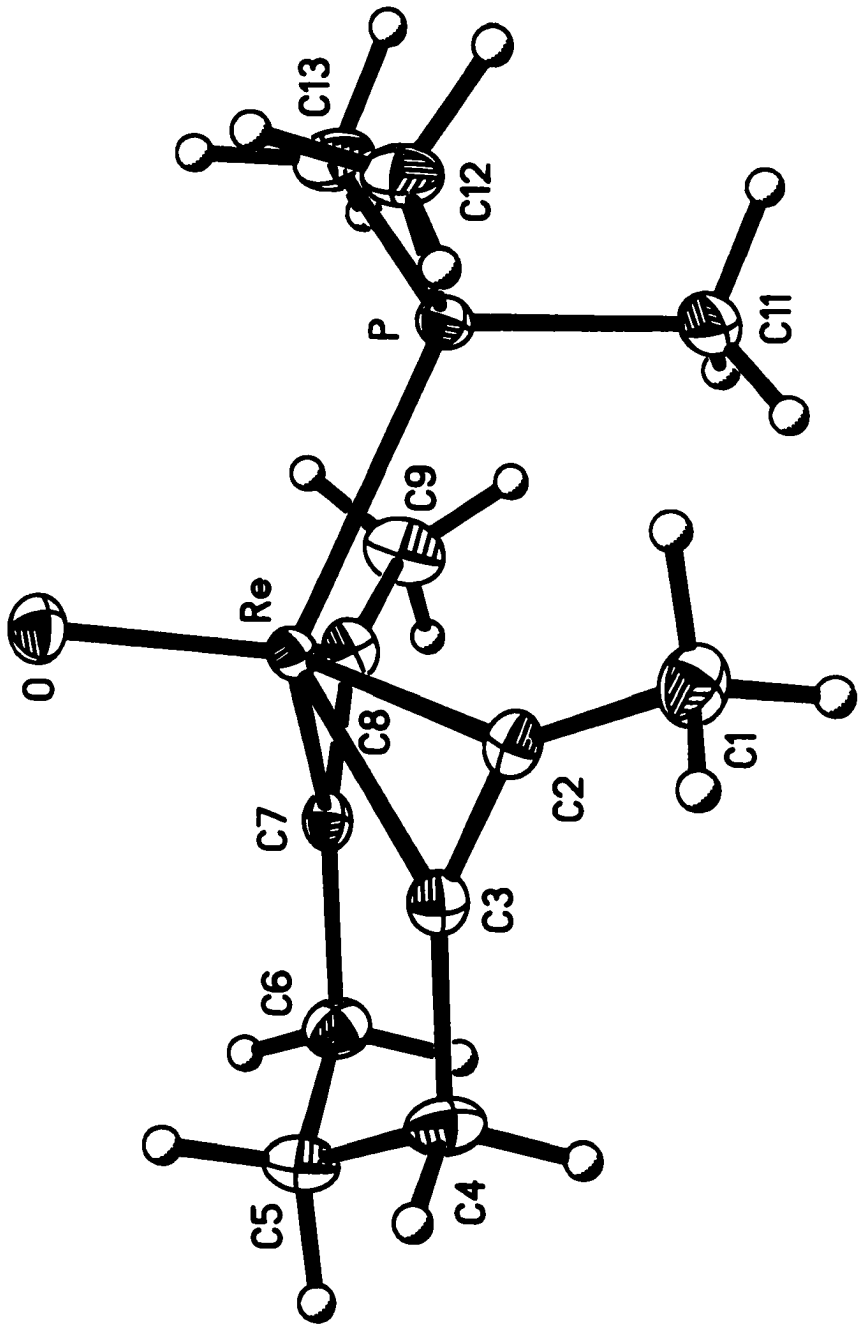

Figure 3.8. Molecular structure of the cation of $[Re(O)(P(CH_3)_3)(H_3CC{\equiv}C(CH_2)_3C{\equiv}CCH_3)]I$ **(5).**

Table 3.1. Summary of Major Structural Features of Five Rhenium Complexes.

Complexes	Complex **1**	Complex **2**	Complex **3**	Complex **4**	Complex **5**
Re-O distance (Å)	1.692 (4)	1.716 (8)	—	1.742 (3)	1.702 (2)
Re-I distance (Å)	2.6809 (5)	2.210 (10) (Re-C (10))	2.7540 (11)	2.6388 (5)	2.4148 (10) (Re-P)
Re-C (2) distance (Å)	2.064 (6)	2.066 (9)	2.030 (10)	2.038 (5)	2.078 (4)
Re-C (3) distance (Å)	2.019 (6)	2.032 (11)	2.023 (10)	2.010 (5)	2.016 (4)
Re-C (7) distance (Å)	2.016 (6)	2.008 (10)	2.023 (10)	1.993 (5)	2.019 (4)
Re-C (8) distance (Å)	2.062 (6)	2.062 (10)	2.030 (10)	2.043 (5)	2.074 (4)
O-Re-I bond angle (°)	111.64 (16)	116.6 (4) (O-Re-C (10))	—	112.29 (11)	108.41 (10) (O-Re-P)
C (2)-C (3) distance (Å)	1.293 (9)	1.290 (14)	1.277 (13)	1.284 (7)	1.285 (5)
C (7)-C (8) distance (Å)	1.279 (9)	1.287 (14)	1.277 (13)	1.275 (7)	1.278 (5)

Conductivity Measurement of $Re(O)(I)(H_3CC{\equiv}C(CH_2)_3C{\equiv}CCH_3)$ (1). In order to understand the solution behavior of **1**, and particularly to see whether the iodo ligand dissociates from the metal, a conductivity measurement was carried out for **1**. The molar conductivity of **1** in acetonitrile was 0.45 $cm^2ohm^{-1}mol^{-1}$; much lower than the value for an acetonitrile solution of 1:1 electrolyte under similar conditions, 10^2 $cm^2ohm^{-1}mol^{-1}$.[140] This shows that the iodo ligand is not dissociated appreciably in solution. However, the mechanism of the reaction of replacement of the iodo ligand with PMe_3 is unclear.

C. Kinetic Studies of $Re(O)(I)(H_3CC{\equiv}C(CH_2)_3C{\equiv}CCH_3)$ (1) with CF_3SO_3H in Acetonitrile.

1. Kinetic Studies of $Re(O)(I)(H_3CC{\equiv}C(CH_2)_3C{\equiv}CCH_3)$ (1) with CF_3SO_3H in Acetonitrile by Rapid Scan Stopped-flow Apparatus.

The Extinction Coefficients of $Re(O)(I)(H_3CC{\equiv}C(CH_2)_3C{\equiv}CCH_3)$ (1) and $[Re(I)(CH_3CN)_3(H_3CC{\equiv}C(CH_2)_3C{\equiv}CCH_3)][BF_4]_2$ (3) in CH_3CN. It is very important to obtain the UV-Vis spectra of the starting material (s) and product (s) before performing the actual stopped-flow experiments so that it is clear what reaction is followed in the stopped-flow experiments. The UV-Vis spectra of complexes **1** and **3** were recorded in

[140] (a) Geary, W. J. *Coord. Chem. Rev.* **1971**, *7*, 81. (b) Coetzee, J. F.; Cunningham, G. P. *J. Am. Chem. Soc.* **1965**, *87*, 2529.

CH_3CN (Figure 3.9). The extinction coefficients of complexes **1** and **3** were determined by linear fits to plots of concentration vs. absorbance. The average extinction coefficient of complex **1** at 439 nm is 184.3 $cm^{-1}M^{-1}$. The extinction coefficient of complex **3** at 450 nm is 1514 $cm^{-1}M^{-1}$.

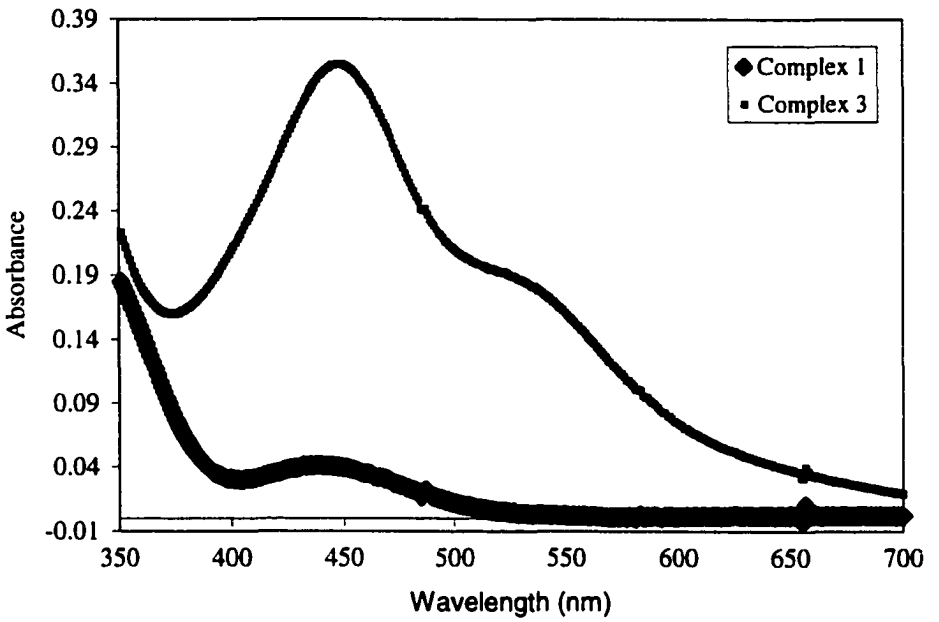

Figure 3.9. UV-Vis spectra of Complex **1** and Complex **3** in CH_3CN.

Low Temperature Stopped-flow Studies of the Protonation of $Re(O)(I)(H_3CC{\equiv}C(CH_2)_3C{\equiv}CCH_3)$ with CF_3SO_3H in Acetonitrile. Stock solutions of complex **1** and CF_3SO_3H were cooled to -40 °C and mixed in the mixing chamber in the stopped-flow apparatus. Dramatic changes occurred. In the first eight seconds of reaction, a broad peak centered at 422 nm appeared (Figure 3.10). The spectrum recorded in the stopped-flow apparatus at early time (at 128 ms) matched the UV-Vis spectrum of complex **1** (the concentration of complex **1** in the stopped-flow is half of the

concentration of the stock solution). The spectrum of the solution in the mixing chamber eventually matched the UV-Vis spectrum of complex **3**.

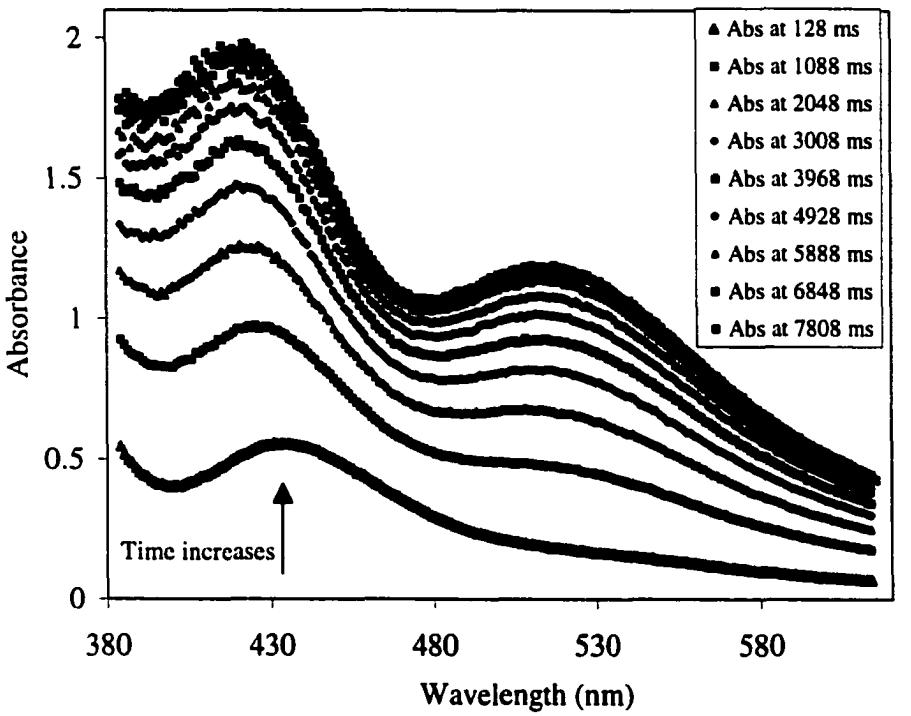

Figure 3.10. Stopped-flow traces of the reaction of the reactions of complex **1** with CF_3SO_3H in CH_3CN at -40 °C.

The rate constants for the protonation of complex **1** with CF_3SO_3H in CH_3CN were obtained by single wavelength fits with the OLIS software at two different wavelengths. The stopped-flow single wavelength trace was best fitted with a two-exponential process. The average values from seven or eight parallel experiments at each concentration of acid were used as the rate constants at that acid concentration. The plot of the observed first-order rate constants, k_{obs}, against concentration of acid used is linear, $k_{obs} = k[H^+]$ (Figure 3.11-12). The slopes of these lines, 11.9 $M^{-1}s^{-1}$ and 3.8 $M^{-1}s^{-1}$, are

the values of the second-order rate constants of the protonation reactions of complex **1** with CF_3SO_3H in CH_3CN at -40 °C. The rate constants obtained at different wavelength (422 nm and 517 nm) were the same.

Figure 3.11. Linear relationship between the observed first-order rate constants

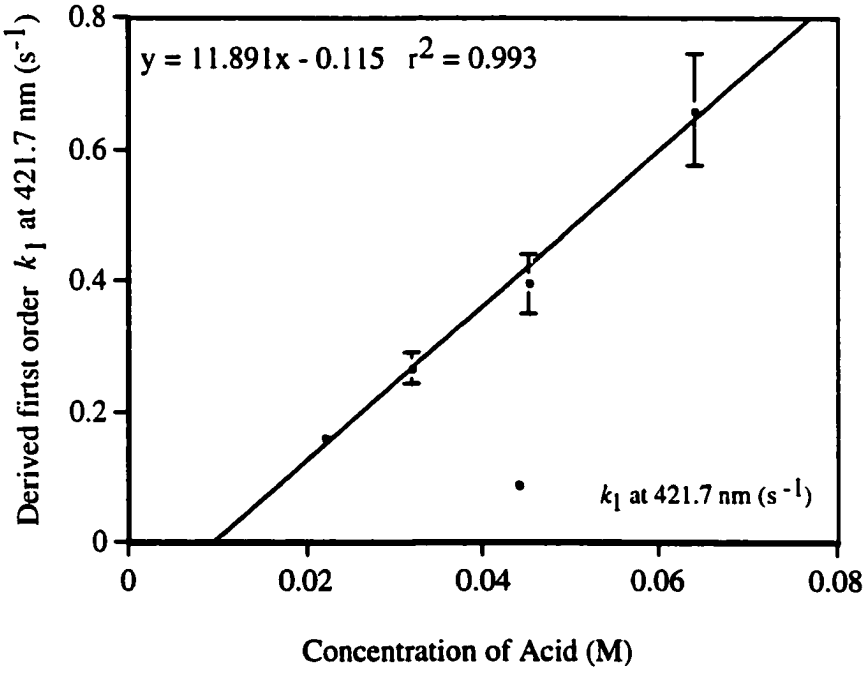

of the first step (k_1) from stopped-flow and the acid concentration for the reaction of complex **1** with CF_3SO_3H in CH_3CN at -40 °C. The second-order rate constant, which is the slope of the plot, is 11.9 $s^{-1}M^{-1}$. Acid concentration plotted is half that of the stock solution, i.e., the concentration in the mixing chamber.

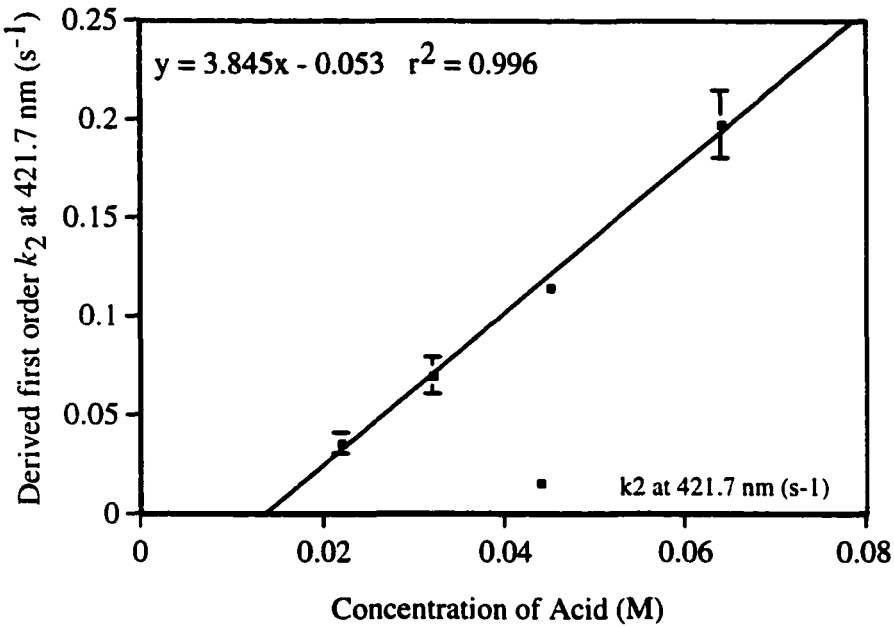

Figure 3.12. Linear relationship between the observed first-order rate constants of the second step (k_2) from stopped-flow and the acid concentration for the reaction of complex **1** with CF_3SO_3H in CH_3CN at -40 °C. The second-order rate constant, which is the slope of the plot, is 3.8 $s^{-1}M^{-1}$. Acid concentration plotted is half that of the stock solution, i.e., the concentration in the mixing chamber.

Global fits with the OLIS software were used to obtain the calculated spectra of the starting material, the intermediate, and the product by using the scheme of A→B→C (Figure 3.13). The calculated spectrum of A matched the spectrum of **1**, the starting material of the protonation reaction. The calculated spectrum of C was close to the spectrum of **3**, the final product of the reaction. The calculated spectrum of B, which had a peak at 422 nm, agreed with the intermediate observed.

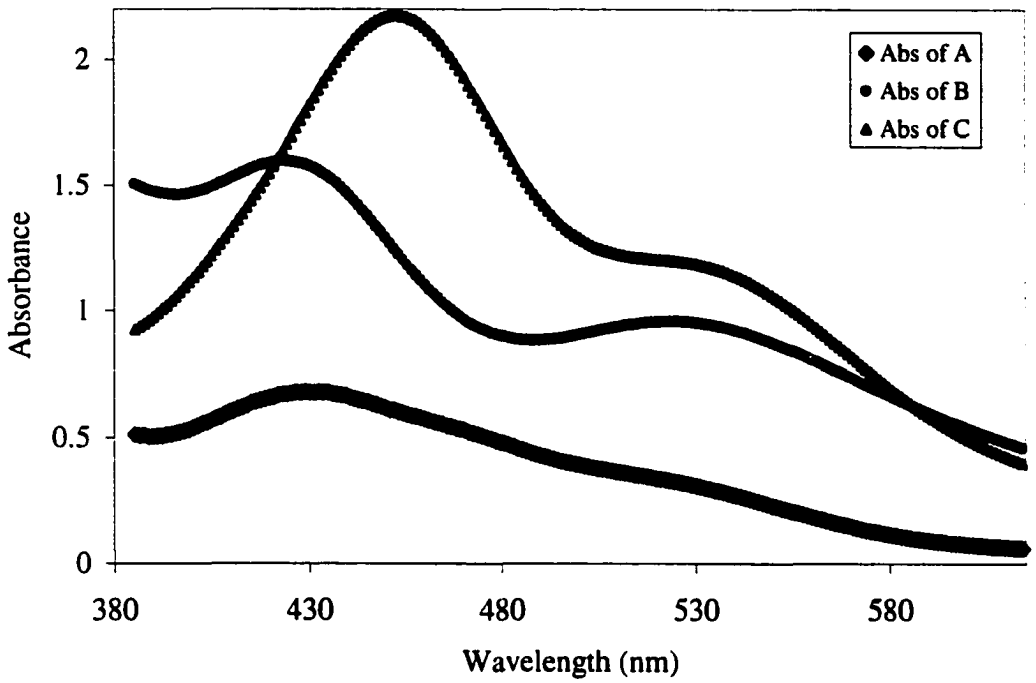

Figure 3.13. The calculated spectra of the starting material (A), the intermediate (B), and the product (C) of the reaction of **1** with CF_3SO_3H.

The sequence of the observed rate constants, k_1 then k_2, was verified. "Dual solution" in consecutive reactions means that the sequence of the rate constants for the two steps cannot be determined only by the kinetics.[141] One way to determine the sequence of the rate constants is to exchange the order of the two steps, k_2 and k_1, and to compare the calculated spectrum of the intermediate with the observed one. The alternative order produced an intermediate spectrum with unreasonably large extinction coefficients, ruling out a k_2 then k_1 sequence. The correct sequence of the protonation reactions had a faster first step followed by a slower second step.

Thus a two-step process, A→B→C, is observed in the stopped-flow apparatus when **1** reacts with CF_3SO_3H; **1** is the A. The fact that the two observed first-order rate constants are acid dependent implies that the reactions observed in the stopped-flow apparatus are indeed *protonations*. As the oxo ligand is eventually lost, it is reasonable to propose that the protonations occur on the terminal oxo ligand. The fact that only three equivalents of CF_3SO_3H were needed to convert **1** to **3** (two for the protonations of **1** and one for the protonation of produced water) indicated that the protonated forms of **1** were weaker acids than CF_3SO_3H. So the protonations of **1** with CF_3SO_3H are thermodynamically downhill although it is impossible to say by how much. The fact that the second-order rate constants of the protonation reactions are so much slower than a diffusion-controlled rate constant provides direct evidence for the slow proton transfer process to a terminal oxo ligand. There could be a sizable kinetic barrier associated with these processes, caused by the substantial electronic and structural rearrangements that can be deduced by comparing the structure of complex **4** to that of **1**.

2. Two Intermediates Observed in the Low Temperature ^{1}H NMR Studies of the Reaction of Re(O)(I)($H_3CC{\equiv}C(CH_2)_3C{\equiv}CCH_3$) with CF_3SO_3H in Acetonitrile and the Related Kinetic Studies of the Conversions of These Two Intermediates.

Two Intermediates Observed in the Low Temperature ^{1}H NMR Spectra of the Reactions of Re(O)(I)($H_3CC{\equiv}C(CH_2)_3C{\equiv}CCH_3$) (1) with CF_3SO_3H in

---

[141] Espenson, J. H. *Chemical Kinetics and Reaction Mechanisms*, 2nd Ed., McGraw-Hill: New York, 1995.

Acetonitrile. Three complexes (with ratio of 3:1:0.8 for **3**:X:Y) were observed by ^1H NMR when the solution of complex **1** at 233 K was treated with CF_3SO_3H and the NMR tube was rapidly placed in the pre-cooled NMR probe. The major one of the three complexes was the final product, complex **3**. The other two species (designated as X and Y) were converted to complex **3** when the temperature was raised to room temperature. Thus, the two complexes, X and Y, observed at 233 K were intermediates in the formation of **3** from **1**.

The chemical shift assignments of the ^1H NMR spectra of X and Y were completed by a COSY experiment (Figure 3.14). They have chelating dialkyne ligand structures similar to that of complex **3** with mirror planes, indicating that the dialkyne ligands have not changed in the reactions.

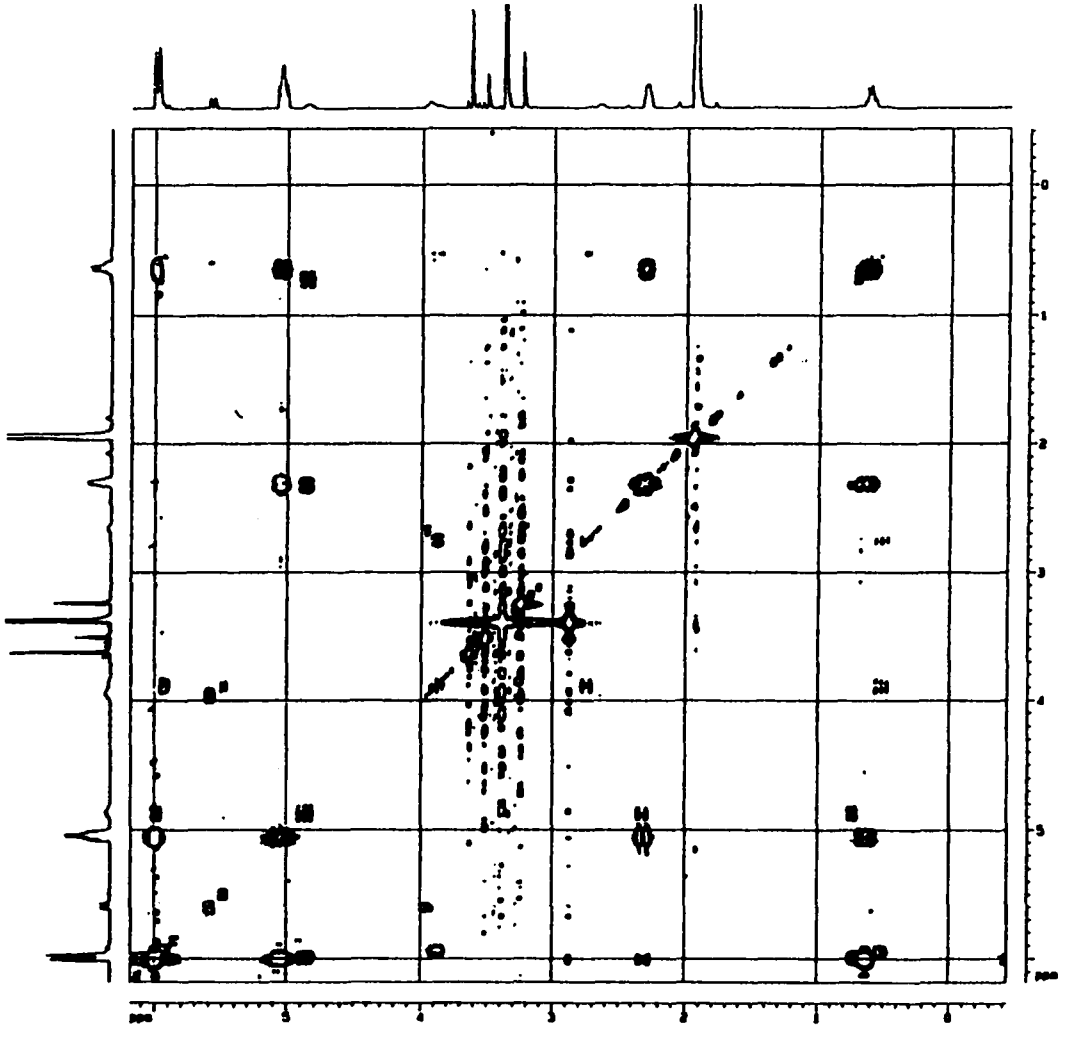

Figure 3.14. COSY spectrum of the reaction of complex **1** with excess CF_3SO_3H in CD_3CN at 233 K just after mixing. Two intermediates (X and Y) and the final product appeared.

Kinetic Studies of the Conversions of the Two Intermediates. The conversions of two NMR intermediates (X and Y) to the final product were followed by ^{1}H NMR at low temperature over a period of two and half hours. The time-dependent ^{1}H NMR integrals for each intermediate were fitted with one exponential (Figure 3.15-16). The rate constants of the conversions were obtained at various acid concentrations at 243 K.

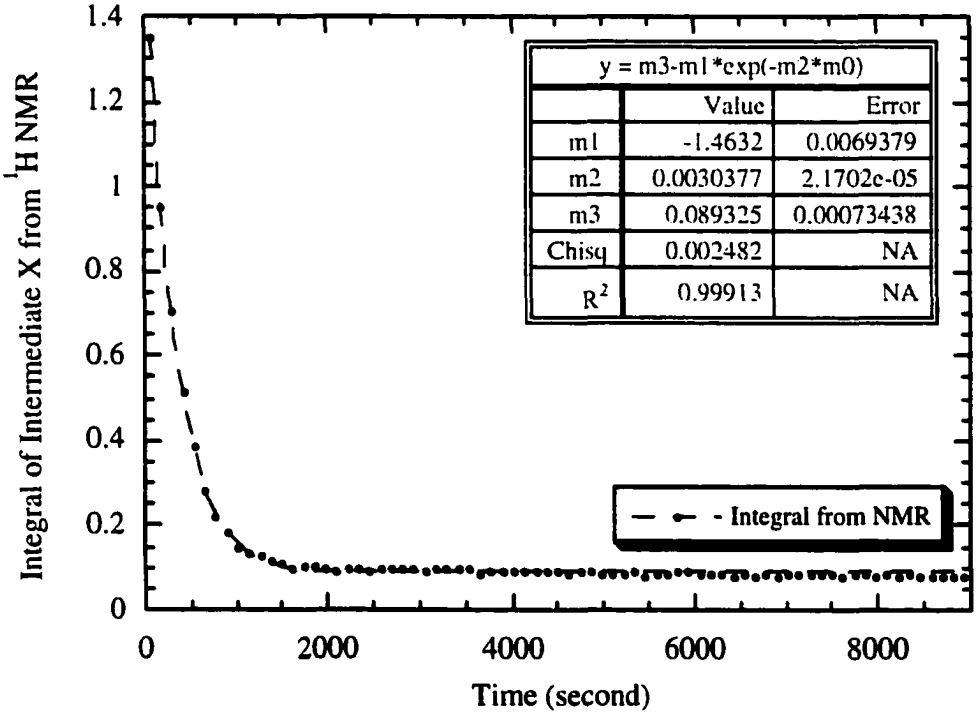

Figure 3.15. Time-dependent integrals from ^{1}H NMR of Intermediate X in CD_3CN, fitted with one exponential. The first-order rate constant of the conversion of X to **3** is 3×10^{-3} s^{-1} at 243 K.

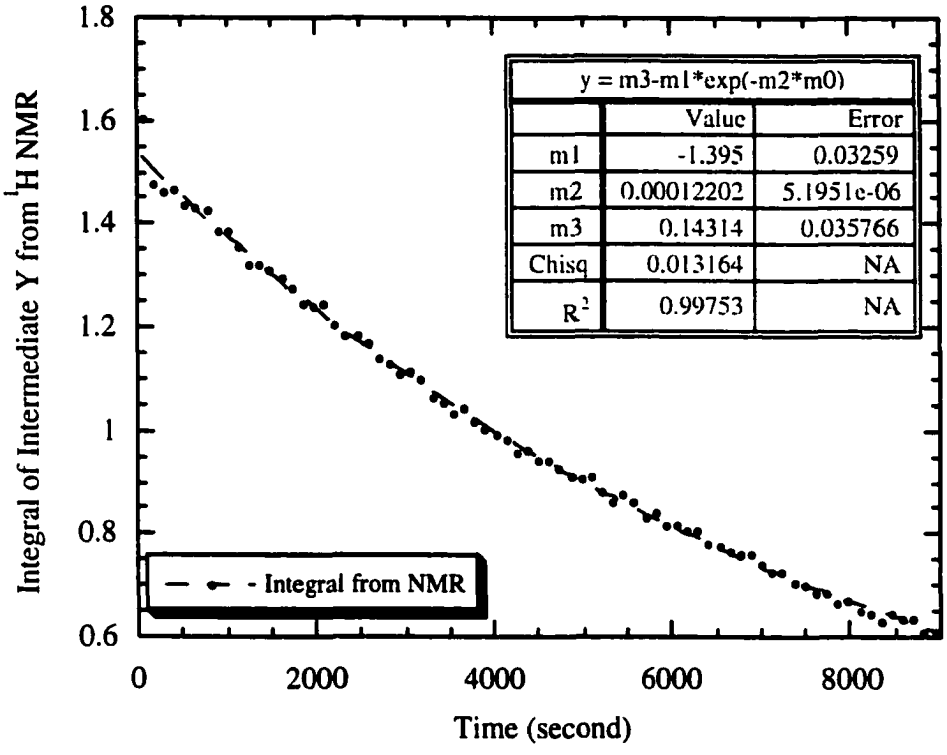

Figure 3.16. Time-dependent integrals from ^{1}H NMR of Intermediate Y in CD_3CN, fitted with one exponential. The first-order rate constant of the conversion of Y to **3** is 1.2×10^{-4} s^{-1} at 243 K.

No apparent correlation between the conversion of X to **3** and the conversion of Y to **3** was found; they both followed one-exponential decay. Kinetically, this means that either they independently converted to **3** or Y converted to **3** through X. (If the conversion of X to **3** had gone through Y, the buildup of Y would have been observed since the conversion of X to **3** was faster than the conversion of Y to **3**.) Kinetic simulation with MacKinetics showed that both pathways below were possible in the conversion of intermediates X and Y to **3** (Figure 3.17).

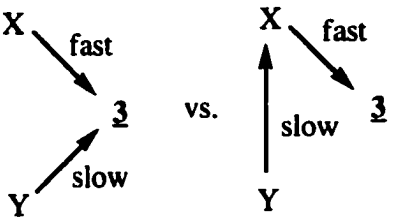

Figure 3.17. Two possible kinetic schemes for conversion of X and Y to **3**.

There was no correlation between the acid concentrations and the rate constants of the conversion of the two intermediates (Figure 3.18-19). The averaged first-order rate constants of conversion of X and Y to **3** were approxiately 3×10^{-3} s^{-1} and 8×10^{-4} s^{-1} respectively at 243 K. This implies that the conversion of these intermediates to the final product, complex **3**, is not acid dependent. So protonation is not rate-limiting in these reactions

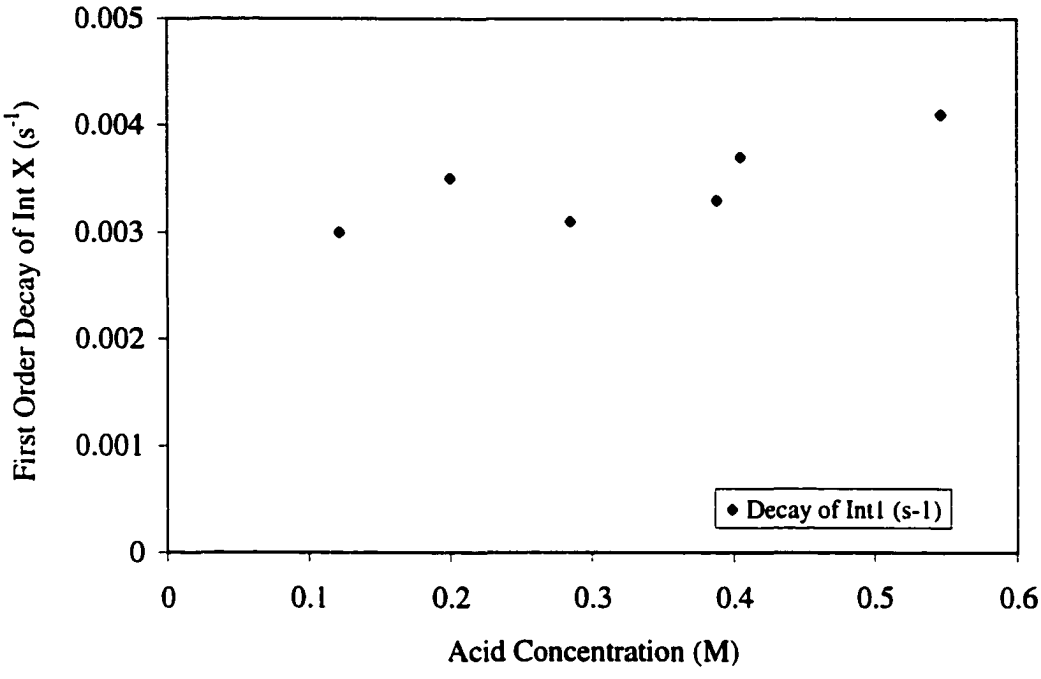

Figure 3.18. Absence of the correlation between the first-order rate constants for the conversion of intermediate X to complex **3** and the concentrations of CF_3SO_3H used in CD_3CN at 243 K.

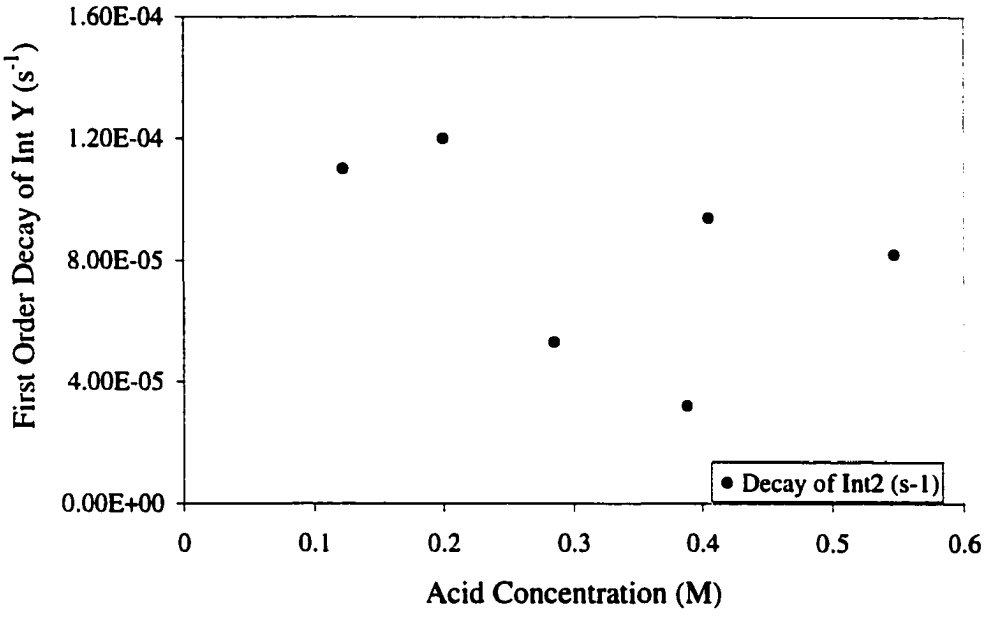

Figure 3.19. Absence of the correlation between the first-order rate constants for the conversion of intermediate Y to complex **3** and the concentrations of CF_3SO_3H used in CD_3CN at 243 K.

The Initial Ratios of the Intermediate X and Y. In order to further understand the nature of X and Y, in particular the number of acid-derived protons they carried, the ratios of X and Y at the start of the ^1H NMR experiments were calculated and plotted against the concentration of acid used. The fact that these ratios did not vary with acid concentration indicated that intermediates X and Y carried the same numbers of acid-derived protons (Figure 3.20).

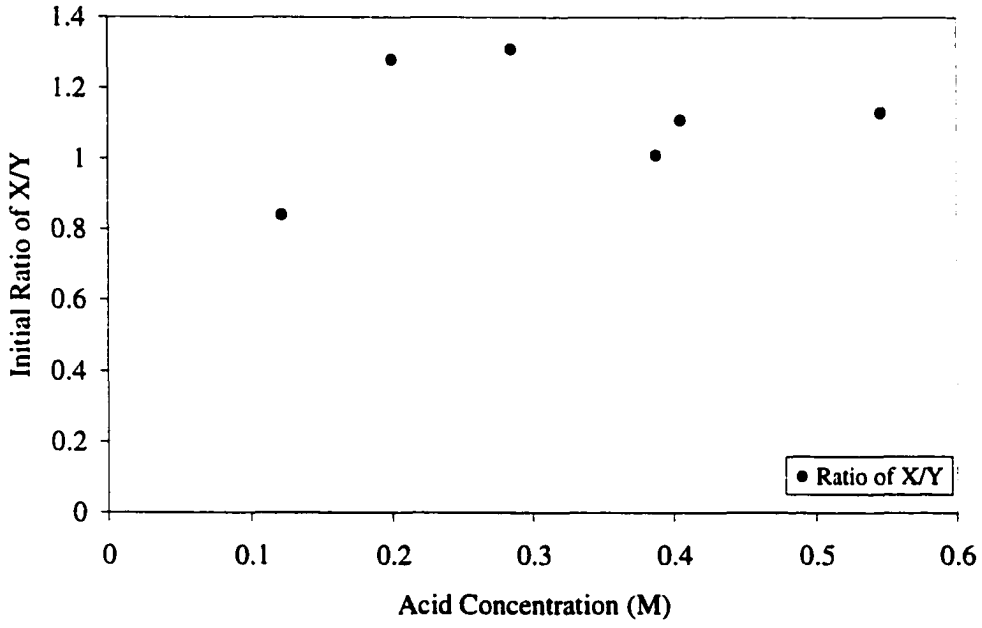

Figure 3.20. Absence of correlation between the ratios of X and Y at the start of the ^{1}H NMR experiments and the concentration of CF_3SO_3H used in CD_3CN at 243 K.

UV-Vis Studies of Reaction of Re(O)(I)($H_3CC{\equiv}C(CH_2)_3C{\equiv}CCH_3$) (1) with CF_3SO_3H in Acetonitrile at Low Temperature. In order to relate the two processes observed in stopped-flow experiment, A→B→C, and the two intermediates, X and Y, observed in ^{1}H NMR experiments (especially the relationship between X and Y and the final product observed in the stopped-flow experiments), low temperature UV-Vis experiments were carried out under conditions similar to those of the ^{1}H NMR experiments. A solution of complex **1** was treated with CF_3SO_3H at -78 °C in a NMR tube. The UV-Vis spectrum of the solution in the tube was recorded at -40 °C with a spectrometer locally designed by the group of Prof. Marilyn Gunner at City College of CUNY. The spectrum just after mixing was similar to the spectrum of the product, C, in

the stopped-flow experiments (Figure 3.21). The spectrum did not change after the reaction had been followed for one hour at -40 °C, one hour at -15 °C, and one hour at 25 °C.

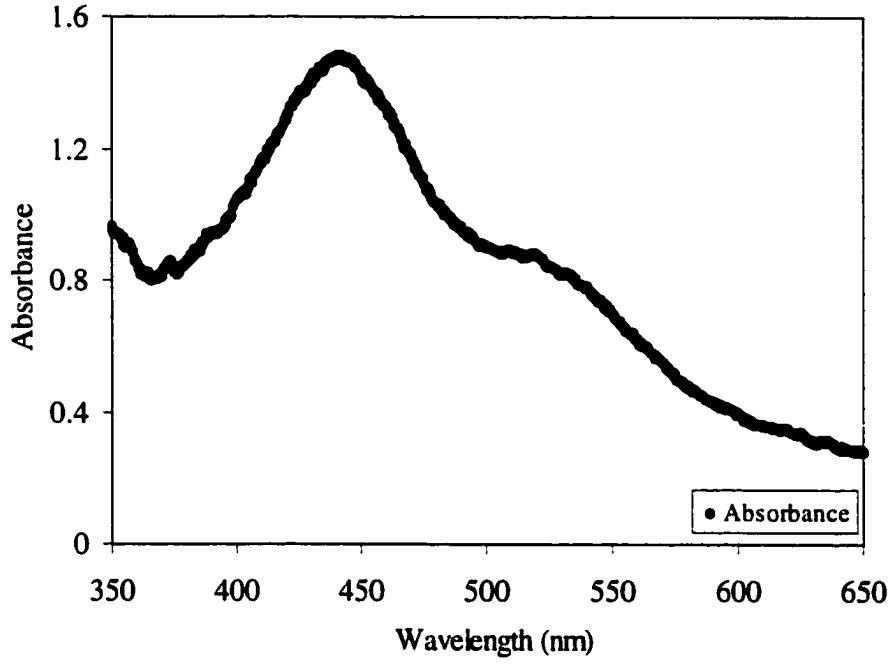

Figure 3.21. UV-Vis spectrum of complex **1** with CF_3SO_3H in CD_3CN at -40 °C just after mixing.

D. Mechanism of the Reaction of Re(O)(I)($H_3CC{\equiv}C(CH_2)_3C{\equiv}CCH_3$) (1) with CF_3SO_3H in Acetonitrile.

Relationship Between Observed Stopped-flow Processes and ^1H NMR Process at Low Temperature. Two acid-dependent consecutive processes, A→B→C, were observed in stopped-flow experiments at -40 °C; two intermediates, X and Y, were observed in ^1H NMR spectra taken at the same temperature. The processes converting

intermediates X and Y to **3** observed in the ^{1}H NMR experiments can hardly be the same processes as those observed in the stopped-flow experiments. From the second-order rate constants derived from the stopped-flow experiments it can be estimated that the half-life of species A and B would be about 0.2 and 0.6 second respectively under the conditions of the ^{1}H NMR experiments; in practice the half-life of intermediate X was about 200 s in the ^{1}H NMR experiment and intermediate Y had a half-life longer than that of X. Thus the intermediates X and Y cannot be the species A and B in the stopped-flow experiments (Figure 3.22). Also the ^{1}H NMR spectra of X and Y are different from that of **1**, the confirmed A in the stopped-flow experiments. So X and Y have to be C in the stopped-flow experiments. As the UV-Vis spectrum of C is similar to that of **3**, the final product, X, Y, and **3** must have similar UV-Vis spectra. This is confirmed by the low temperature UV-Vis experiments. Under conditions that should generate X, Y, and **3** at the same time, the UV-Vis spectra did not change while (as shown by the NMR spectra) the X and the Y converted to **3**.

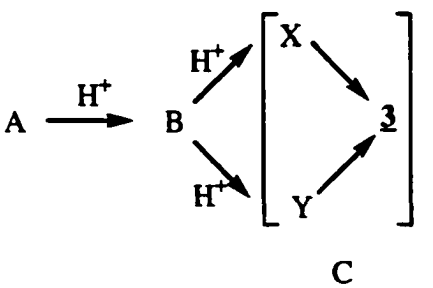

Figure 3.22. Proposed reaction scheme based on stopped-flow experiments and ^{1}H NMR experiment.

Mechanistic Implication of the Protonation Reaction of $Re(O)(I)(H_3CC{\equiv}C(CH_2)_3C{\equiv}CCH_3)$ (1) with CF_3SO_3H in Acetonitrile. The reversal of protonation of **1** with pyridine and $H_2{}^{18}O$ shows that two protonations on the terminal oxo ligand must be involved in the overall transformation of complex **1** to complex **3**; the aqua ligand formed is eventually replaced by solvent acetonitrile under strong acidic conditions.

The two acid-dependent steps observed in the low temperature stopped-flow experiments support the proposal that *the overall transformation begins with two consecutive proton transfers from added acid to the oxo ligand.*

The two intermediates X and Y observed in the low temperature ^1H NMR experiments are very puzzling. As the chelating dialkyne ligands are not protonated the only available protonation sites on complex **1** are the oxo ligand, the iodo ligand, and the rhenium itself.

The acid-independent conversions of the two intermediates X and Y to the final product, complex **3** imply that proton transfer from acid is not involved in the these processes. So either the two intermediates X and Y still carry two acid-derived protons, or the aqua ligand must have left the rhenium center before the formation of these two intermediates. The latter possibility is unlikely to be correct, as there would be no remaining change required for the formation of **3** from **1** that would explain why the transformation of X and Y is so slow.

If both X and Y contain two acid-derived protons, these intermediates must be two of the following three species: an aqua complex, a hydroxo metal hydride complex, or a hydroxo HI complex (Figure 3.23).[142]

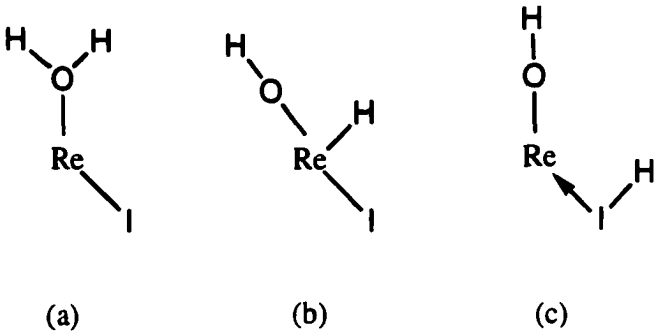

(a) (b) (c)

Figure 3.23. Three possible structures for the two intermediates in the low temperature ^{1}H NMR spectra.

^{1}H NMR studies were carried out to search for a hydride signal at 233 K just after mixing complex **1** and CF_3SO_3H. Mayer and coworkers have reported the synthesis of Re(O)(H)(MeC≡CMe)$_2$ with an Re-*H* chemical shift of 6.18.[34] No signal was found in the range from 0 to - 40 ppm. Small peaks in the range of 0 to 10 ppm might have been a hydride signal, but could not be positively identified

In the hydroxo HI complex the HI ligand would be a good leaving group so that it could easily be replaced by an acetonitrile molecule, the solvent of reaction, once it is formed in the solution.

---

[142] Example of HX complex: (a) Aullón, G.; Bellamy, D.; Brammer, L.; Bruton, E. A.; Orpen, A. G. *J. Chem. Soc.; Chem. Commun.* **1998**, 653. (b) Murphy, V. J.; Hascall, T.; Chen, J. Y.; Parken, G. *J. Am. Chem. Soc.* **1996**, *118*, 7428. (c) Peris, E.; Lee Jr., J. C.; Crabtree, R. H. *J. Chem. Soc., Chem. Commun.* **1994**, 2573. (d) Murphy, V. J.; Rabinovich, D.; Hascall, T.; Klooster, W. T.; Koetzle, T. F.; Parkin, G. *J. Am. Chem. Soc.* **1998**, *120*, 4372.

Overall this leads to the possibility of an aqua complex as X, and a hydroxo metal hydride complex or hydroxo HI complex as Y, in the ^{1}H NMR spectra. The rearrangement of the hydroxo metal hydride or the hydroxo HI complex to the aqua complex is likely to be the slower step (Y→X) of the observed conversion of the intermediates to the final product. The loss of the aqua ligand will be the faster step (X→3) of the observed conversion of the intermediates to the final product.

III. Conclusions and Future Work.

Even a seemingly simple proton transfer reaction can be very complicated. The tentative mechanistic scheme is shown in Figure 3.24. The intermediates could have one or two coordinated acetonitrile molecules.

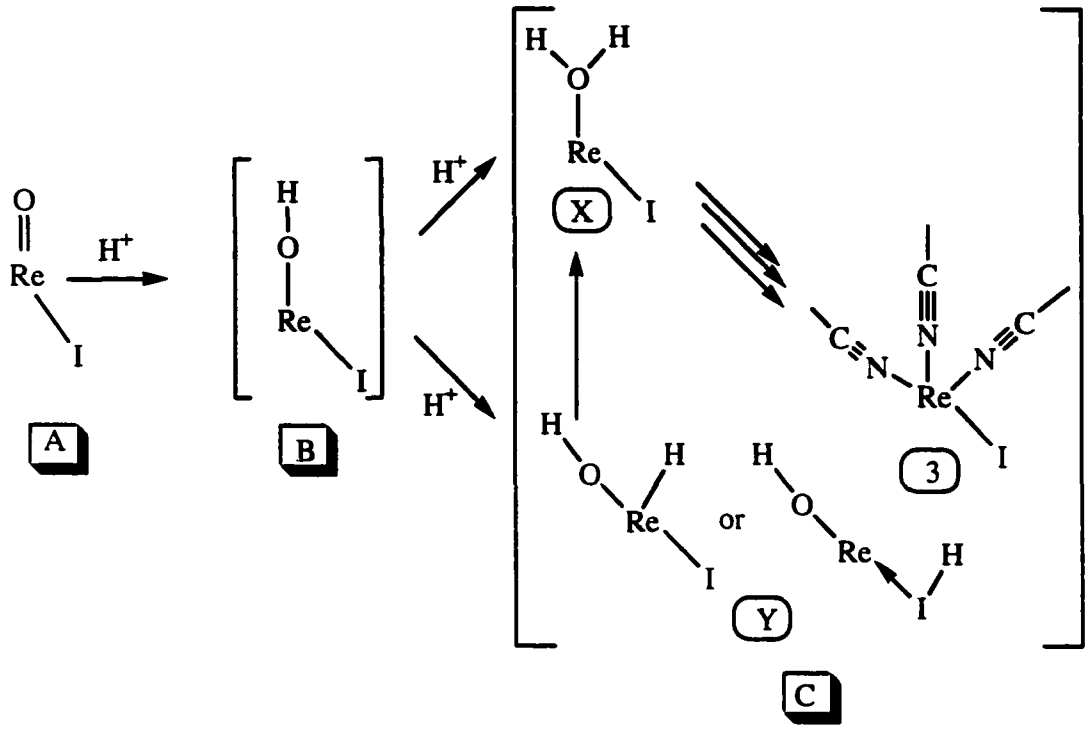

Figure 3.24. Tentative mechanism for the overall transformation of complex **1** to complex **3** with CF_3SO_3H in CH_3CN.

This study offers the quantitative evidence (but without clear proof of the nature of the products) that a proton transfer to a terminal oxo ligand can be much slower than a diffusion-controlled rate constant despite a favorable thermodynamic driving force. The second-order rate constants for proton transfer to the terminal oxo ligand in **1** are on the order of 10 $s^{-1}M^{-1}$ with CF_3SO_3H. Extensive structural and electronic rearrangements have been indicated for the protonation by the model study of the coordination of a Lewis acid to the oxo ligand. The Re-O bond distance increases, while the distances between the rhenium and the other ligands decreases when $B(C_6F_5)_3$ is coordinated to the terminal oxo ligand.

There are still interesting experiments to be done to further understand this proton transfer process. Kinetic isotope effects will be useful in understanding the conversion of the two intermediates X and Y, found in low temperature ^1H NMR experiments, to the final product. A significant kinetic isotope effect would imply that there are bond-breaking steps with hydrogen involved in the conversion. However preliminary result indicates that only a small kinetic isotope effect (1.3) is found at -40 °C.

Low temperature *in situ* IR experiments would give some clues about the nature of the two intermediates X and Y. Is there an observable Re-O stretching mode just after the mixing of complex **1** with CF_3SO_3H at low temperature?

The X-ray structure of **1** shows that the oxo ligand stands away from the dialkyne ligand. Bulky substituents on the dialkyne carbons would have little effect on the rate constants for the proton transfer process to the oxo ligand but would be expected to slow down or even stop the protonation of the rhenium center and iodo ligand. This would simplify the kinetic scheme and might allow us to evaluate the proton transfer to the oxo ligand exclusively.

It is always worth trying to find a better terminal oxo complex to study. It should be stable and soluble in organic solvents. Ideally the hydroxyl complex should be stable and its X-ray structure available.

IV. Experimental Section

Materials. Reactions and manipulations were performed under an atmosphere of nitrogen purified by passing through BTS catalyst (BASF) and molecular sieves (3Å

Linde), either using standard Schlenk techniques or in an inert atmosphere box (Vacuum Atmospheres Co.; Model HE-553-2). Complexes $Re(O)(I)_3(PPh_3)_2$,[143] $Et_3SiB(C_6F_5)_4$,[144] $(C_6Me_3H_4)B(C_6F_5)_4$,[145] and $NaBArF'_4$[146] were prepared according to published procedures.

Benzene, tetrahydrofuran (THF), hexane, pentane and pyridine were distilled from sodium-benzophenone ketyl in the presence of tetraglyme. Dichloromethane was distilled from P_4O_{10}. Acetonitrile was stirred with $CuSO_4$. The solid was filtered. It was then distilled from P_4O_{10} and CaH_2. Acetonitrile (DriSolv™, water: 50 ppm max) purchased from EM Science was used as received. There was no difference found between the purified acetonitrile and the purchased DriSolv acetonitrile in the reaction performed. Toluene was distilled from sodium-benzophenone ketyl. Trifluoromethanesulfonic acid and trifluoromethanesulfonic acid-*d* were stored in vacuum bulbs in an inert atmosphere box upon receiving. They were purified by three freeze/pump/thaw cycles at -196 °C and transferred into flame-dried vacuum bulbs when they turned dark after stored for some time.

Dichloromethane-d_2, benzene-d_6, chloroform-*d*, and acetonitrile-d_3 were purchased from Cambridge Isotopes Laboratories. Dichloromethane-d_2, chloroform-*d* and acentonitrile-d_3 were stirred with P_4O_{10}, degassed by three freeze/pump/thaw cycles at -196 °C and transferred into flame-dried vacuum bulbs. They were stored in an inert

---

[143] Manion, A. B.; Erikson, T. K. G.; Spaltenstein, E.; Mayer, J. M. *Organometallics*, **1989**, *8*, 1871.

[144] Lamber, J. B.; Zhang, S.; Ciro, S. M. *Organometallics*, **1994**, *13*, 2430.

[145] Reed, C. A.; Fackler, N. L. P.; Kim, K.-C.; Stasko, D.; Evans, D. R.; Boyd, P. D.; Rickard, C. E. F. *J. Am. Chem. Soc.* **1999**, *121*, 6314.

[146] Brookhart, M.; Grant, B.; Volpe, Jr., A. F. *Organometallics*, **1992**, *11*, 3920.

atmosphere box. Benzene-d_6 was distilled from sodium-benzophenone ketyl and stored in an inert atmosphere box.

$B(C_6F_5)_3$ (Boulder Scientific) was used as received or purified via recrystallization from hexane or sublimation at 60 °C. $CH_3C_6H_4SO_3H$ was dried by heating it at 50 °C under vacuum overnight. Alternatively benzene was distilled from a solution of the acid using a Dean-Stark trap until the distillate became clear; addition of hexane to the solution caused the precipitation of fine powder. The mixture was transferred to another pre-dried flask via cannula; the solvent was evaporated. All other reagents employed were used without further purification.

Instruments. ^1H NMR spectra were recorded at 300 MHz on a Bruker spectrometer unless otherwise noted; ^{13}C NMR spectra were recorded at 75 MHz.; ^{19}F NMR spectra were recorded at 282 MHz. HMQC and COSY experiments were performed on a Bruker 400 MHz or 500 MHz spectrometer. NMR spectra were recorded at room temperature unless otherwise noted. HMQC results were reported as $\delta\ ^{13}C/\delta\ ^1H$. Residual ^1H shifts in the deuterated solvents were used as internal standards in the ^1H NMR spectra. ^{13}C shifts in the solvents were used as internal standards in the ^{13}C NMR spectra. ^{19}F shifts were relative to $CFCl_3$. ^{31}P shifts were relative to 85% H_3PO_4.

Infrared spectra were recorded on a Perkin-Elmer FT-IR spectrophotometer Spectrum 2000 and reported in cm^{-1}. UV-Vis spectra were recorded on a Hewlett Packard HP8453 diode array spectrophotometer controlled by HP ChemStation (Rev. A.02.05) software system. Elemental analyses of C, H, and N were performed on a Perkin-Elmer 2400 CHN elemental analyzer. Conductivity measurements were

performed on a YSI conductivity bridge (Yellow Springs Instrument Co., Inc. Model 31) with conductivity cell (YSI model 3402, cell K = 0.1/cm). Mass spectra were obtained on a VG 7070 EQ-HF and a VG Autospec mass spectrometer. Chromatography with less than 1 g material was performed on a Chromatotron (Harrison Research Inc.) with silica gel (Merck, TLC grade 7749) as the adsorbent. Otherwise flash chromatographies were performed on silica gel 60 (Merck, 230-400 mesh).

The rapid scan stopped-flow system used was a Hi-Tech Canterbury SF-41 with OLIS RSM-1000 rapid scanning device (On-Line Instrument Systems) with temperature control of ±0.1 °C. It could obtain one thousand spectra per second with each spectrum up to 300 nm wide. The noise level of the RSM-1000 was about 0.001 au. The software used to control the apparatus and to analyze the data was OLIS System Version 6.2.4. Parameter settings for the RSM were as follows: scans were collected in dual beam mode, 1000 scan/second, with a stopped-flow delay of 20 ms and sampling time of 4 μs. The monochromater grating was 400 lines with a blaze wavelength of 500 nm. The speed of the 16-slit scanning disk was 62.50 Hz with the step motor set at 4.0 steps/nm.

Low temperature UV-Vis absorption spectra were obtained on a spectrometer of local design belonging to the group of Prof. Marilyn Gunner at City College of CUNY, with the help of Mr. Qiang Xu. The measuring beam was provided by a xenon flash lamp (IBH Model 500XeF). The flashes had typical t_{hwfm} of about 460 ns and power of 50 mJ. The use of this flash lamp as the light source enabled investigation of kinetics with much faster time scale (~μs) than a normal lamp and shutter apparatus.

The temperature of the sample was controlled by a closed cycle helium cryostat system (APD cryogenics Inc., Model CSW202A) with a programmable temperature

controller. The temperature resolution was 0.1 K and controllability was ± 0.4 K. During sample change, helium gas was blown through the sample chamber to keep the temperature and to prevent frost from being formed inside the chamber or on the quartz window where the probe light was transmitted.

The transmitted light was sent through an optical fiber to a spectrometer (Instrument SA HR460). A liquid nitrogen cooled CCD detector (Princeton Instruments, LN/CCD-1024-EHRB/1) operating at -80 °C was used to collect the spectrum. The CCD detector contained 1024 by 256 pixels; each pixel converted the light it observed to a charge, which was subsequently read. The 256 pixels in Y dimension were binned together in this measurement. The detector and the flash lamp were controlled by a delay generator (Stanford research DG535) for synchronization.

To measure the absorbance of the sample, the spectrum of the transmitted light through a reference, I_0, was recorded first. After the spectrum of the sample, I_1, was recorded, the absorption spectrum of the sample was calculated using the following equation.

$$A = \log(\frac{I_0}{I_1})$$

MacKinetics[147] was used to analyze the kinetic data obtained from low temperature NMR experiments. MacKinetics is a kinetics program which takes a set of chemical equations, starting concentrations of the reactants, time-dependent data, any known rate constants, and initial guesses for the unknown rate constants, all provided by the user, and iteratively optimizes those rate constants and calculates the concentrations

[147] Written by and obtained from: Leipold, W. S., III; Weiher, J. F.; McKinney, R. J. E. I. du Pont de Nemours, Inc.

of any or all species in the system during the course of the reaction for the system in question. One can also simulate reactions simply by integrating the model with a rate constant and the initial concentrations in order to decide on an initial guess for optimization, or to plan benchtop experiments in such a manner that they have a higher probability of working.

Nonadiyne-2,7 ($H_3CC{\equiv}C(CH_2)_3C{\equiv}CCH_3$). Heptadiyne-1,6 (4.61 g, 0.05 mol) and THF (40 ml) were added via syringe to a 500 mL three-neck round-bottom flask sealed with a septum, an additional funnel and a nitrogen/vacuum inlet. At –40 °C *n*-BuLi (1.6 M, 68.75 mL) was added dropwise via the additional funnel. At –30 °C iodomethane (15.6 g, 0.11 mol) in THF (15 mL) was added dropwise. THF (25 mL) was added again. The reaction mixture was stirred overnight. The reaction mixture was then added to a 1 L separatory funnel with ice/water mixture (150 mL). The water portion was washed with hexane (3 × 50 mL). The hexane portion was combined, washed with water (3 × 50 mL) and dried by $MgSO_4$ overnight. The solid was filtered. The filtrate was evaporated. Yield: 3.9 g (65%). ^{1}H NMR ($CDCl_3$): δ 1.61 ($CH_2CH_2CH_2$, qn, J = 7.0 Hz, 2 H), 1.75 (CH_3, t, J = 2.5 Hz, 6 H), 2.21 (CH_2CH_2, tq, 4 H). ^{13}C NMR ($CDCl_3$): δ 3.67 (CH_3), 18.1 (CH_2), 28.7 (CH_2), 76.1, 78.6.

Re(O)(I)($H_3CC{\equiv}C(CH_2)_3C{\equiv}CCH_3$) (1a). $Re(O)I_3(PPh_3)_2$ (4.0 g, 3.61 mmol) in benzene (40 mL) was treated with $H_3CC{\equiv}C(CH_2)_3C{\equiv}CCH_3$ (1.3 g, 10.8 mmol). The mixture was stirred overnight. The reaction mixture was then filtered through silica gel. The silica gel was washed with benzene (3 × 20 mL). The filtrate was evaporated. The

resulting dark red solution was loaded on the chromatotron and eluted with ethyl acetate/hexane (10:90). The yellow portion was collected. The solvent was evaporated. The solid was dried overnight under vacuum. Yield: 0.43 g (27%). The product can be further purified by recrystalization with ether/pentane or sublimation at 60 °C under dynamic vacuum. Crystals suitable for X-ray diffraction were obtained via diffusion of hexane into THF solution. ^{1}H NMR (CD_3CN): δ 2.05 ($CH_2CH_2CH_2$, m, 1 H), 2.46 ($CH_2CH_2CH_2$, m, 1 H), 2.59 (CH_2CH_2, m, 2 H), 3.08 (CH_3, t, 6H), 3.50 (CH_2CH_2, m, 2 H). ^{13}C NMR (CD_3CN): δ 16.57 (CH_3), 22.80 (CH_2), 31.49 (CH_2), 138.5, 143.4. IR (Nujol): 2925, 1456, 1360, 1313, 1240, 1140, 1055, 974, 956, 864, 768, 633. MS: 448, 450.

Re(O)Me($H_3CC{\equiv}C(CH_2)_3C{\equiv}CCH_3$) (2). Re(O)I($H_3CC{\equiv}C(CH_2)_3C{\equiv}CCH_3$) (0.5 g, 1.11 mmol) in benzene (40 mL) was cooled to 10 °C and treated with $CH_3Li{\bullet}LiBr$(1.5 M, 0.9 mL). The solution was stirred overnight, and filtered through silica gel. The silica gel was washed with benzene (3 × 20 mL). The filtrate was evaporated. The concentrated solution was loaded on the chromatotron and eluted with ethyl acetate/hexane (15:85). The correct portion (R_f value = 0.32) was collected. The solvent was evaporated. The solid was dried overnight under vacuum. Yield: 0.15g (40%). To further purify the product, the product was sublimed at 10^{-3} torr under dynamic vacuum at 45 °C. Crystals suitable for X-ray diffraction were obtained via diffusion of hexane into ether solution. ^{1}H NMR (CD_3CN): δ 2.04 ($ReCH_3$, s, 3 H), 2.09 ($CH_2CH_2CH_2$, m, 1 H), 2.38 ($CH_2CH_2CH_2$, m, 1 H), 2.42 (CH_2CH_2, m, 2 H), 2.50 (CH_3, t, 6 H), 3.38 (CH_2CH_2, m, 2 H). ^{13}C NMR (CD_3CN): δ 5.6 ($ReCH_3$), 9.30 (CH_3), 22.90 (CH_2), 32.4

(CH_2), 141.6, 148.5. Anal. Calcd for $C_{10}H_{15}ORe$ (337.4): C, 35.6; H, 4.48; N, 0.00. Found: C, 35.1; H, 4.21; N, -0.08. MS: 337, 339.

$[Re(I)(CH_3CN)_3(H_3CC{\equiv}C(CH_2)_3C{\equiv}CCH_3)][BF_4]_2$ (3). A solution of $Re(O)(I)(H_3CC{\equiv}C(CH_2)_3C{\equiv}CCH_3)$ (0.012 g, 0.027 mmol) in CH_2Cl_2 (0.4 mL) and CH_3CN (0.2 mL) was treated with $HBF_4 \cdot (CH_3)_2O$ (24 mmol, 30 μL). Toluene (ca. 1 mL) was added and the solution was cooled to -35 °C overnight, yielding red needles. Yield: 0.0071 g (36%). ^1H NMR (CD_3CN, -15 °C): δ 0.64 ($CH_2CH_2CH_2$, m, 1 H), 2.31 ($CH_2CH_2CH_2$, m, 1 H), 3.39 (CH_3, s, 6 H), 5.05 (CH_2CH_2, m, 2 H), 6.00 (CH_2CH_2, m, 2 H). ^{13}C NMR (CD_3CN, -15 °C): δ 17.0 (CH_3), 20.9 ($CH_2CH_2CH_2$), 35.9 (CH_2CH_2), 175.5, 188.3. ^{19}F (CD_3CN, -15 °C): δ -150. IR (KBr): 2937, 2297, 1809, 1052, 522.

$Re(O)(I)(H_3CC{\equiv}C(CH_2)_3C{\equiv}CCH_3){\cdot}B(C_6F_5)_3$ (4). A solution of $Re(O)(I)(H_3CC{\equiv}C(CH_2)_3C{\equiv}CCH_3)$ (0.057 g, 0.13 mmol) in C_6D_6 (0.2 mL) was treated with a solution of $B(C_6F_5)_3$ (0.072 g, 0.14 mmol) in C_6D_6 (0.3 mL), forming a dark red solution. Hexane (1.5 mL) was added and the solution was cooled to -20 °C overnight, yielding large red blocks. Yield: 93 mg (74 %). ^1H NMR (CD_2Cl_2): δ 2.21 (m, 1 H), 2.55 (m, 1 H), 2.69 (m, 2 H), 3.40 (s, 6 H) 3.68 (m, 2 H). ^{13}C NMR (CD_2Cl_2): δ 18.1, 24.3, 29.3, 154.8, 162.2. Anal. Calcd for $C_{27}H_{12}BF_{15}IORe$ (961.3): C, 33.74; H, 1.26; N, 0.00. Found: C, 33.87; H, 0.64; N, 0.00. The analysis for H was consistently below the calculated value in numerous runs, while that for C was consistently near the calculated value. IR: 979, 951.

[Re(O)(P(CH$_3$)$_3$)(H$_3$CC≡C(CH$_2$)$_3$C≡CCH$_3$)]I (5). A solution of Re(O)(I)(H$_3$CC≡C(CH$_2$)$_3$C≡CCH$_3$) (0.052 g, 0.12 mmol) in CD$_3$C$_6$D$_5$ (0.4 mL) and CD$_2$Cl$_2$ (0.2 mL) was treated with two drops of PMe$_3$, causing an immediate change from orange to pale yellow and yielding the precipitation of a pale yellow powder. The precipitate was isolated by decantation, washed with C$_6$H$_6$ (1.0 mL), and dried under vacuum. Yield: 20 mg (32%). Crystals suitable for X-ray diffraction were obtained via cooling of the supernatant (– 20 °C). ^{1}H NMR (CD$_2$Cl$_2$, -45 °C): δ 2.19 (m, 1 H), 2.39 (d, 9 H), 2.59 (m, 1 H), 2.82 (s, 3 H), 2.87 (m, 2 H), 3.60 (m, 2 H). ^{13}C NMR (CD$_2$Cl$_2$, -45 °C): δ 14.1, 16.2(d), 22.1, 29.7, 130.8, 148.3. Anal. Calcd for C$_{12}$H$_{21}$IOPRe (525.4): C, 27.43; H, 4.03; N, 0.00. Found: C, 27.65; H, 4.09; N, -0.04.

Re(^{18}O)(I)(H$_3$CC≡C(CH$_2$)$_3$C≡CCH$_3$) (1b). Two methods were employed: (a). A solution of Re(O)(I)(H$_3$CC≡C(CH$_2$)$_3$C≡CCH$_3$) (0.2 g, 0.4 mmol) in C$_6$H$_6$ (5 mL) and CH$_2$Cl$_2$ (5 mL) was treated with H$_2$^{18}O (98% enriched, 9 μL, 0.5 mmol). The solution was stirred for two weeks. The solvent was evaporated. IR (Nujol): 975(s), 959(s). (b). A solution of [Re(I)(CH$_3$CN)$_3$(H$_3$CC≡C(CH$_2$)$_3$C≡CCH$_3$)][BF$_4$]$_2$ (0.0086 g, 0.012 mmol) in CD$_3$CN (0.6 mL) was treated with H$_2$^{18}O (98% enriched, 5 μL, 0.28 mmol). ^{1}H NMR (CD$_3$CN): same as Re(O)(I)(H$_3$CC≡C(CH$_2$)$_3$C≡CCH$_3$). IR (CD$_3$CN): 916 (s) [ν(Re^{18}O)].

NMR Studies of the Protonation of Re(O)Me(H$_3$CC≡C(CH$_2$)$_3$C≡CCH$_3$) with MeC$_6$H$_4$SO$_3$H. A 5 mm NMR tube was charged with Re(O)Me(H$_3$CC≡C(CH$_2$)$_3$C≡CCH$_3$) (0.0234 g, 0.069 mmol) and MeC$_6$H$_4$SO$_3$H (0.042 g,

0.22 mmol). CD_3CN (0.6 mL) was added at -20 °C. A ^1H NMR spectrum was obtained at -20 °C. Various amounts of acid were used, 0.22 and 0.037 mmol.

Reversibility Studies of the Protonation of $Re(O)Me(H_3CC{\equiv}C(CH_2)_3C{\equiv}CCH_3)$ with $MeC_6H_4SO_3H$. A 5 mm NMR tube was charged with $Re(O)Me(H_3CC{\equiv}C(CH_2)_3C{\equiv}CCH_3)$ (0.023 g, 0.069 mmol) in CD_3CN (0.6 mL) and treated with CF_3SO_3H (6.4 μl, 0.072 mmol) at low temperature. A ^1H NMR spectrum was obtained at -20 °C. The solution was then treated with pyridine (7 μl, 0.086 mmol). Another ^1H NMR spectrum was taken at -20 °C.

General Procedures for the Protonation of $Re(O)(I)(H_3CC{\equiv}C(CH_2)_3C{\equiv}CCH_3)$ under Various Conditions. (a) A 5 mm NMR tube was charged with $Re(O)(I)(H_3CC{\equiv}C(CH_2)_3C{\equiv}CCH_3)$ (0.008 g, 0.018 mmol) in CD_3CN (0.6 mL) and treated with CF_3SO_3H (8 μL, 0.09 mmol). A ^1H NMR spectrum was obtained. The acids used were $CH_3C_6H_4SO_3H$, $HBF_4\cdot(CH_3)_2O$, and $(C_6Me_3H_4)B(C_6F_5)_4$. The solvents used were CD_3CN, CD_2Cl_2, CD_2Cl_2/CD_3CN and CD_2Cl_2/THF-d_8. (b) $Re(O)(I)(H_3CC{\equiv}C(CH_2)_3C{\equiv}CCH_3)$ (0.1g, 0.22 mmol) and $LiB(C_6F_5)_4$ (0.16 g, 0.23 mmol) in $CH_3C_6H_5$ (3 mL) were treated with CF_3SO_3H (60 μL, 0.68 mmol). The solid formed was separated from the solution and dried under vacuum. A ^1H NMR spectrum was taken. The solvent was evaporated from the saved solution. A ^1H NMR spectrum was obtained. The salts used were $LiB(C_6F_5)_4$ and $NaBArF'_4$. (c) $Re(O)(I)(H_3CC{\equiv}C(CH_2)_3C{\equiv}CCH_3)$ (0.1g, 0.22 mmol) and $Et_3SiB(C_6F_5)_4$ (0.17 g, 0.23 mmol)in $CH_3C_6H_5$ (3 mL) were treated with HCl gas for 15 minutes, generated by

addition of H_2SO_4 to solid NaCl. The solvent was evaporated. A ^1H NMR spectrum was obtained for the oily material. The salts used were $Et_3SiB(C_6F_5)_4$ and $LiB(C_6F_5)_4$. The solvents used were $CH_3C_6H_5$ and CH_2Cl_2/CH_3CN. (d) A 100 mL flask was filled with HCl gas (100 mL, 4.1 mmol), generated as above. $Re(O)(I)(H_3CC{\equiv}C(CH_2)_3C{\equiv}CCH_3)$ (0.1g, 0.22 mmol) and $LiB(C_6F_5)_4$ (0.2 g, 0.29 mmol) in CD_3CN (0.5 mL) and CD_2Cl_2 (2 mL) were transferred to that flask via syringe. The solution was stirred for 5 minutes. A ^1H NMR spectrum was obtained.

Reversion of the Protonation of $Re(O)(I)(H_3CC{\equiv}C(CH_2)_3C{\equiv}CCH_3)$. A 5 mm NMR tube was charged with $Re(O)(I)(H_3CC{\equiv}C(CH_2)_3C{\equiv}CCH_3)$ (0.008 g, 0.018 mmol) in CD_3CN (0.6 mL) and treated with CF_3SO_3H (8 μL, 0.09 mmol). A ^1H NMR spectrum was obtained. Pyridine (8.1 μL, 0.1 mmol) was added to the solution via syringe. A ^1H NMR spectrum was recorded.

Titration of $Re(O)(I)(H_3CC{\equiv}C(CH_2)_3C{\equiv}CCH_3)$ with CF_3SO_3H. A 5 mm NMR tube was charged with $Re(O)(I)(H_3CC{\equiv}C(CH_2)_3C{\equiv}CCH_3)$ (0.012 g, 0.027 mmol) in CD_3CN (0.6 mL) and treated with CF_3SO_3H (1.2 μL, 0.014 mmol) at -15 °C. A ^1H NMR spectrum was obtained at -15 °C. CF_3SO_3H (1.2 μL, 0.014 mmol) was added to the solution 7 more times at -15 °C. Each time the ^1H NMR spectrum was recorded at -15 °C.

Solution IR Study of the Protonation of $Re(O)(I)(H_3CC{\equiv}C(CH_2)_3C{\equiv}CCH_3)$ by CF_3SO_3H. A solution of $Re(O)(I)(H_3CC{\equiv}C(CH_2)_3C{\equiv}CCH_3)$ (0.0075 g, 0.017 mmol)

in CH_3CN (0.8 mL) was treated with CF_3SO_3H (5 μL, 0.057 mmol). A solution IR spectrum was recorded in a KBr cell. The same procedure was repeated with CF_3SO_3D (5 μL, 0.057 mmol).

Conductivity of Re(O)(I)($H_3CC{\equiv}C(CH_2)_3C{\equiv}CCH_3$). The conductivity of the solution of Re(O)(I)($H_3CC{\equiv}C(CH_2)_3C{\equiv}CCH_3$) (0.0171 g, 0.038 mmol) in CH_3CN (10 mL) was measured using the conductivity bridge, which was tested using the reported solution. The conductivity readout was 0.45 $cm^2ohm^{-1}mol^{-1}$.

Exchange Reaction Between the Bonded and the Free CH_3CN in [Re(I)(CH_3CN)$_3$($H_3CC{\equiv}C(CH_2)_3C{\equiv}CCH_3$)][$BF_4$]$_2$. A 5 mm NMR tube was charged with [Re(I)(CH_3CN)$_3$($H_3CC{\equiv}C(CH_2)_3C{\equiv}CCH_3$)][$BF_4$]$_2$ (0.009 g, 0.012 mmol) in CD_2Cl_2 (0.6 mL) and CD_3CN (0.2 mL). A ^1H NMR spectrum was obtained. The solution was treated with CH_3CN (8 μL). A ^1H NMR spectrum was recorded again. The intensity of the peak corresponding to the free CH_3CN increased. All the other peaks did not change.

General Procedure of the Reaction of Re(O)(I)($H_3CC{\equiv}C(CH_2)_3C{\equiv}CCH_3$) with Electrophiles. A solution of Re(O)(I)($H_3CC{\equiv}C(CH_2)_3C{\equiv}CCH_3$) (0.008 g, 0.018 mmol) in CD_3CN (0.6 mL) was treated with $CF_3SO_3SiEt_3$ (16 μL, 0.072 mmol). A ^1H NMR spectrum was obtained. The electrophiles used were $Et_3SiB(C_6F_5)_4$, $CF_3SO_3CH_3$, CH_3I, $CF_3SO_3Si(CH(CH_3)_2)_3$, and $CF_3SO_3SiEt_3$. The solvents used were CD_3CN, CD_2Cl_2, and $CDCl_3$. Clean product was only found in the reaction with $CF_3SO_3SiEt_3$ in CD_3CN. ^1H NMR (CD_3CN): δ 2.78 (m, 2 H), 3.24 (s, 6 H), 3.25 (m, 2 H), 3.53 (m, 2

H). ^{13}C NMR (CD_3CN): δ 23.5, 31.8, 33.8, 93.6, 122.9. COSY spectrum showed that the peaks at 2.78, 3.25, 3.53 in ^1H NMR were coupled to each other. HMQC: 33.8/3.24, 31.8/2.78, 23.5/(3.53, 3.25).

Determination of the Extinction Coefficients of $Re(O)(I)(H_3CC{\equiv}C(CH_2)_3C{\equiv}CCH_3)$ and $[Re(I)(CH_3CN)_3(H_3CC{\equiv}C(CH_2)_3C{\equiv}CCH_3)][BF_4]_2$ in CH_3CN. For $Re(O)(I)(H_3CC{\equiv}C(CH_2)_3C{\equiv}CCH_3)$: A bulb was charged with $Re(O)(I)(H_3CC{\equiv}C(CH_2)_3C{\equiv}CCH_3)$ (0.041 g, 0.091 mmol) and CH_3CN (10 mL). A portion of the above solution (0.6 mL) was transferred to a 5 mL volumetric flask, which was then filled with CH_3CN. A UV-Vis spectrum was recorded. The process was repeated five more times with different amounts of the original solution. The absorbances at 439 nm were recorded from each spectrum. The concentrations of $Re(O)(I)(H_3CC{\equiv}C(CH_2)_3C{\equiv}CCH_3)$ solutions were plotted against the absorbance recorded at that concentration. The whole procedure was repeated with $Re(O)(I)(H_3CC{\equiv}C(CH_2)_3C{\equiv}CCH_3)$ (0.052 g, 0.12 mmol) in CH_3CN (10 mL). For $[Re(I)(CH_3CN)_3(H_3CC{\equiv}C(CH_2)_3C{\equiv}CCH_3)][BF_4]_2$: A bulb was charged with $Re(O)(I)(H_3CC{\equiv}C(CH_2)_3C{\equiv}CCH_3)$ (0.0155 g, 0.034 mmol) and CH_3CN (10 mL). A portion of the above solution (0.5 mL) was transferred to a 2 mL volumetric flask, which was then filled with CH_3CN. Excess CF_3SO_3H was added to protonate the complex completely. A UV-Vis spectrum was recorded. The process was repeated three more times with different amounts of the original solution. The absorbances at 450 nm were recorded from each spectrum. The concentrations of

$[Re(I)(CH_3CN)_3(H_3CC{\equiv}C(CH_2)_3C{\equiv}CCH_3)][BF_4]_2$, assured same as initial concentrations of $Re(O)(I)(H_3CC{\equiv}C(CH_2)_3C{\equiv}CCH_3)$ solutions, were plotted against the absorbance recorded at that concentration.

General Procedure for the Rapid Scan Stopped-flow Studies of the Protonation of $Re(O)(I)(H_3CC{\equiv}C(CH_2)_3C{\equiv}CCH_3)$ with CF_3SO_3H. One solution contained $Re(O)(I)(H_3CC{\equiv}C(CH_2)_3C{\equiv}CCH_3)$ (0.0355 g, 0.079 mmol) in CH_3CN (25 mL); the other contained CF_3SO_3H (0.145 mL, 1.64 mmol) in CH_3CN (10 mL). These solutions were placed in the two reservoirs in the stopped-flow apparatus. The temperature of the mixing chamber was set to -40 °C. A change in spectrum was observed when these solutions were mixed at -40 °C. The data were best fit with a two-step process, A→B→C. The *pseudo* first-order rate constants ($k_{obs} = k[H^+]$) were obtained from the single wavelength fits.

General Procedure for the Kinetic Studies of the Protonation of $Re(O)(I)(H_3CC{\equiv}C(CH_2)_3C{\equiv}CCH_3)$ with CF_3SO_3H by NMR. A 5 mm NMR tube was charged with $Re(O)(I)(H_3CC{\equiv}C(CH_2)_3C{\equiv}CCH_3)$ (0.008 g, 0.018 mmol) in CD_3CN (0.6 mL) and treated with CF_3SO_3H (8 μL, 0.09 mmol) at 233 K. ^1H NMR spectra were recorded every minute for two hours at 233 K using Bruker macro program *kineticzg*. The integrals of individual species were plotted against time. The rate constants of the decay of the intermediates were obtained by non-linear least-square fitting.

Low Temperature UV-Vis Studies of the Protonation of $Re(O)(I)(H_3CC{\equiv}C(CH_2)_3C{\equiv}CCH_3)$ with CF_3SO_3H in CD_3CN. A shortened NMR tube was charged with $Re(O)(I)(H_3CC{\equiv}C(CH_2)_3C{\equiv}CCH_3)$ (0.0006 g, 0.0013 mmol) in CD_3CN (1.1 mL). The solution was frozen at -78 °C and treated with CF_3SO_3H (1 μL, 0.011 mmol). The solid was melted quickly, mixed with acid, and placed in the pre-cooled probe. UV-Vis spectra were recorded at -40 °C.

General Procedure for X-Ray Determination of Structure. Crystal data were collected on a Bruker P4 diffractometer equipped with a SMART CCD detector. The structures were solved using direct methods and standard difference map techniques, and refined by full matrix least-squares procedures using SHELXTL.[148] Hydrogen atoms on carbon were included in calculated positions.

[148] Sheldrick, G. M. *SHELXTL*, An Integrated System for Solving, Refining and Displaying Crystal Structures from Diffraction Data; University of Göttingen, Göttingen, Federal Republic of Germany, 1981.

Table 3.2. Summary of Crystal Data for Re(O)(I)($H_3CC{\equiv}C(CH_2)_3C{\equiv}CCH_3$).

Empirical formula	$C_9H_{12}IORe$
Formula weight	449.29
Temperature (K)	228 (2)
Crystal system	Monoclinic
Space Group	$P2_1/n$
a (Å)	10.0184 (15)
b (Å)	7.1551 (10)
c (Å)	15.790 (2)
α, deg	90
β, deg	108.326 (2)
γ, deg	90
Volume ($Å^3$), Z	1074.5 (3), 4
Wavelength (Å)	0.71073
Reflections collected	7028
Independent reflections	2381
Data/restraints/parameters	2381/0/112
Absorption coefficient (mm^{-1})	14.137
GOF on F^2	1.109
*R*1, w*R*2 [$I>2\sigma(I)$]	0.0293, 0.0772
*R*1, w*R*2 (all data)	0.0304, 0.0780

Table 3.3. Atomic coordinates ($\times 10^4$) and equivalent isotropic displacement parameters ($Å^2 \times 10^3$) for Re(O)(I)($H_3CC{\equiv}C(CH_2)_3C{\equiv}CCH_3$).

	x	y	z	U (eq)
Re	4312 (1)	2135 (1)	1198 (1)	22 (1)
I	1839 (1)	3925 (1)	620 (1)	41 (1)
O	5571 (5)	3250 (6)	885 (3)	35 (1)
C (1)	3625 (8)	3820 (11)	3014 (5)	45 (2)
C (2)	4292 (6)	2702 (8)	2476 (4)	29 (1)
C (3)	5090 (6)	1282 (9)	2478 (4)	30 (1)
C (4)	5921 (7)	-357 (10)	2930 (4)	37 (1)
C (5)	6406 (7)	-1570 (10)	2301 (4)	39 (1)
C (6)	5243 (9)	-2217 (8)	1497 (5)	43 (2)
C (7)	4376 (6)	-640 (8)	991 (4)	29 (1)
C (8)	3311 (6)	-17 (8)	372 (4)	30 (1)
C (9)	2061 (7)	-551 (12)	-367 (5)	46 (2)

Table 3.4. Summary of Crystal Data for Re(O)Me($H_3CC{\equiv}C(CH_2)_3C{\equiv}CCH_3$).

Empirical formula	$C_{10}H_{15}ORe$
Formula weight	337.42
Temperature (K)	163 (2)
Crystal system	Tetragonal
Space Group	$P42_1c$
a (Å)	16.56890 (10)
b (Å)	16.56890 (10)
c (Å)	7.45200 (10)
α, deg	90
β, deg	90
γ, deg	90
Volume ($Å^3$), Z	2045.79 (3), 8
Wavelength (Å)	0.71073
Reflections collected	9010
Independent reflections	1460
Data/restraints/parameters	1460/0/110
Absorption coefficient (mm^{-1})	11.832
GOF on F^2	1.133
*R*1, w*R*2 [$I>2\sigma(I)$]	0.0351, 0.0645
*R*1, w*R*2 (all data)	0.0511, 0.0681

Table 3.5. Atomic coordinates ($\times 10^4$) and equivalent isotropic displacement parameters ($Å^2 \times 10^3$) for Re(O)Me($H_3CC{\equiv}C(CH_2)_3C{\equiv}CCH_3$).

	x	y	z	U (eq)
Re	2393 (1)	4632 (1)	9457 (1)	17 (1)
O	2832 (4)	4808 (4)	7408 (11)	26 (2)
C (1)	2318 (6)	2647 (5)	10573 (20)	33 (2)
C (2)	2622 (5)	3502 (5)	10510 (17)	21 (2)
C (3)	3082 (5)	4029 (5)	11271 (16)	20 (2)
C (4)	3675 (6)	4273 (6)	12664 (18)	26 (3)
C (5)	3895 (5)	5162 (6)	12578 (17)	24 (2)
C (6)	3150 (6)	5717 (6)	12722 (16)	24 (2)
C (7)	2528 (6)	5512 (6)	11285 (14)	17 (2)
C (8)	1818 (5)	5605 (5)	10618 (19)	23 (2)
C (9)	1035 (6)	6053 (7)	10774 (20)	37 (3)
C (10)	1157 (5)	4147 (6)	9170 (16)	23 (2)

Table 3.6. Summary of Crystal Data for

$[Re(I)(CH_3CN)_3(H_3CC{\equiv}C(CH_2)_3C{\equiv}CCH_3)][BF_4]_2$.

Empirical formula	$C_{15}H_{21}B_2F_8IN_3Re$
Formula weight	730.07
Temperature (K)	228 (2)
Crystal system	Tetragonal
Space Group	I4/m
a (Å)	23.889 (2)
b (Å)	23.889 (2)
c (Å)	9.7525 (11)
α, deg	90
β, deg	90
γ, deg	90
Volume ($Å^3$), Z	5565.6 (9), 8
Wavelength (Å)	0.71073
Reflections collected	18516
Independent reflections	3438
Data/restraints/parameters	3438/0/158
Absorption coefficient (mm^{-1})	5.534
GOF on F^2	1.073
*R*1, w*R*2 [$I>2\sigma(I)$]	0.0588, 0.1696
*R*1, w*R*2 (all data)	0.0810, 0.1932

Table 3.7. Atomic coordinates ($\times 10^4$) and equivalent isotropic displacement parameters ($Å^2 \times 10^3$) for $[Re(I)(CH_3CN)_3(H_3CC{\equiv}C(CH_2)_3C{\equiv}CCH_3)][BF_4]_2$.

	x	y	z	U (eq)
Re	43 (1)	2465 (1)	0	42 (1)
I	249 (1)	1330 (1)	0	69 (1)
N (1)	262 (4)	3310 (5)	0	48 (2)
N (2)	752 (3)	2442 (3)	-1413 (9)	51 (2)
C (1)	-417 (5)	3193 (5)	2631 (12)	66 (3)
C (2)	-382 (4)	2716 (4)	1694 (10)	49 (2)
C (3)	-564 (4)	2235 (4)	1332 (11)	53 (2)
C (4)	-1026 (5)	1803 (5)	1331 (13)	66 (3)
C (5)	-1372 (7)	1875 (7)	0	78 (5)
C (11)	584 (9)	4327 (7)	0	97 (7)
C (12)	411 (6)	3741 (6)	0	59 (4)
C (21)	1598 (5)	2609 (6)	-3001 (11)	73 (3)
C (22)	1121 (4)	2514 (4)	-2111 (10)	50 (2)
F (11)	2501 (5)	3433 (4)	-1181 (13)	137 (4)
F (12)	1694 (5)	3417 (6)	0	100 (4)
F (13)	2258 (6)	2672 (4)	0	98 (4)
F (21)	1706 (6)	5655 (6)	0	117 (5)
F (22)	857 (6)	5633 (5)	1040 (20)	208 (8)
F (23)	1176 (5)	6411 (5)	0	98 (4)
B (1)	2257 (8)	3233 (8)	0	62 (4)
B (2)	1184 (10)	5822 (9)	0	88 (7)

Table 3.8. Summary of Crystal Data for

$[Re(O)(P(CH_3)_3)(H_3CC{\equiv}C(CH_2)_3C{\equiv}CCH_3)]I$.

Empirical formula	$C_{12}H_{21}IOPRe$
Formula weight	525.36
Temperature (K)	228 (2)
Crystal system	Monoclinic
Space Group	$P2_1/n$
a (Å)	8.9812 (16)
b (Å)	18.417 (3)
c (Å)	9.7160 (17)
α, deg	90
β, deg	94.068 (3)
γ, deg	90
Volume ($Å^3$), Z	1603.0 (5), 4
Wavelength (Å)	0.71073
Reflections collected	11017
Independent reflections	3638
Data/restraints/parameters	3638/0/151
Absorption coefficient (mm^{-1})	9.588
GOF on F^2	1.083
*R*1, w*R*2 [$I>2\sigma(I)$]	0.0219, 0.0415
*R*1, w*R*2 (all data)	0.0301, 0.0428

Table 3.9. Atomic coordinates ($\times 10^4$) and equivalent isotropic displacement coefficients (Å $\times 10^3$) for [Re(O)(P(CH$_3$)$_3$)(H$_3$CC≡C(CH$_2$)$_3$C≡CCH$_3$)]I.

	x	y	z	U (eq)
Re	12435 (1)	4329 (1)	19483 (1)	27 (1)
I	6753 (1)	3231 (1)	14093 (1)	49 (1)
P	13222 (1)	4193 (1)	17171 (1)	34 (1)
O	12666 (3)	5214 (1)	19962 (3)	42 (1)
C (1)	15528 (5)	3221 (2)	19754 (5)	48 (1)
C (2)	14159 (4)	3619 (2)	20078 (4)	35 (1)
C (3)	13180 (4)	3634 (2)	20980 (4)	36 (1)
C (4)	12543 (5)	3341 (2)	22228 (4)	51 (1)
C (5)	11063 (5)	3684 (3)	22500 (4)	51 (1)
C (6)	9912 (5)	3609 (2)	21282 (4)	47 (1)
C (7)	10472 (4)	3908 (2)	19990 (4)	33 (1)
C (8)	10339 (4)	4004 (2)	18684 (4)	36 (1)
C (9)	9264 (5)	3844 (3)	17479 (4)	60 (1)
C (11)	13261 (6)	3274 (2)	16546 (4)	53 (1)
C (12)	15046 (5)	4584 (2)	17064 (4)	47 (1)
C (13)	12103 (5)	4696 (3)	15872 (4)	54 (1)

Table 3.10. Summary of Crystal Data for

$Re(O)(I)(H_3CC{\equiv}C(CH_2)_3C{\equiv}CCH_3)\cdot B(C_6F_5)_3$.

Empirical formula	$C_{33}H_{18}BF_{15}IORe$
Formula weight	1039.38
Temperature (K)	228 (2)
Crystal system	Monoclinic
Space Group	$P2_1/n$
a (Å)	10.6281 (6)
b (Å)	10.6867 (6)
c (Å)	29.8237 (15)
α, deg	90
β, deg	95.7890 (10)
γ, deg	90
Volume ($Å^3$), Z	3370.1 (3), 4
Wavelength (Å)	0.71073
Reflections collected	23579
Independent reflections	7805
Data/restraints/parameters	7805/0/472
Absorption coefficient (mm^{-1})	4.633
GOF on F^2	1.008
*R*1, w*R*2 [$I>2\sigma(I)$]	0.0379, 0.0614
*R*1, w*R*2 (all data)	0.0798, 0.0684

Table 3.11. Atomic coordinates ($\times 10^4$) and equivalent isotropic displacement coefficients ($Å \times 10^3$) for $Re(O)(I)(H_3CC{\equiv}C(CH_2)_3C{\equiv}CCH_3)\cdot B(C_6F_5)_3$.

	x	y	z	U (eq)
Re	3953 (1)	2088 (1)	1393 (1)	34 (1)
I	4599 (1)	3085 (1)	2192 (1)	74 (1)
O	2983 (3)	3072 (3)	1045 (1)	40 (1)
F (12)	3228 (3)	2203 (3)	143 (1)	53 (1)
F (13)	4310 (3)	2892 (3)	-585 (1)	65 (1)
F (14)	4390 (3)	5332 (3)	-820 (1)	60 (1)
F (15)	3330 (3)	7078 (3)	-315 (1)	60 (1)
F (16)	2191 (3)	6434 (3)	392 (1)	53 (1)
F (22)	-749 (3)	4592 (3)	730 (1)	62 (1)
F (23)	-1565 (3)	6528 (4)	1158 (1)	83 (1)
F (24)	76 (4)	7992 (3)	1686 (1)	77 (1)
F (25)	2560 (3)	7373 (3)	1802 (1)	63 (1)
F (26)	3422 (3)	5458 (3)	1354 (1)	61 (1)
F (32)	760 (3)	2285 (3)	1385 (1)	61 (1)
F (33)	-904 (4)	432 (3)	1231 (1)	89 (1)
F (34)	-1831 (3)	-147 (3)	372 (2)	96 (1)
F (35)	-1043 (3)	1164 (3)	-326 (1)	77 (1)
F (36)	645 (3)	2953 (3)	-184 (1)	57 (1)
C (1)	7045 (5)	2752 (6)	1503 (2)	65 (2)
C (2)	5842 (5)	2160 (5)	1327 (2)	40 (1)
C (3)	5319 (5)	1322 (5)	1062 (2)	39 (1)
C (4)	5357 (6)	261 (5)	747 (2)	52 (2)
C (5)	4090 (5)	-382 (5)	643 (2)	47 (1)
C (6)	3524 (5)	-777 (5)	1064 (2)	49 (2)
C (7)	3391 (5)	308 (5)	1376 (2)	41 (1)
C (8)	3079 (5)	761 (5)	1745 (2)	43 (1)
C (9)	2551 (7)	482 (6)	2179 (2)	76 (2)

C (11)	2629 (4)	4261 (4)	307 (2)	32 (1)
C (12)	3210 (5)	3450 (5)	38 (2)	39 (1)
C (13)	3794 (5)	3754 (5)	-338 (2)	42 (1)
C (14)	3827 (5)	4990 (5)	-458 (2)	41 (1)
C (15)	3286 (5)	5863 (5)	-203 (2)	39 (1)
C (16)	2704 (5)	5483 (5)	167 (2)	37 (1)
C (21)	1388 (5)	4875 (4)	1031 (2)	35 (1)
C (22)	131 (5)	5221 (5)	999 (2)	41 (1)
C (23)	-320 (6)	6250 (6)	1215 (2)	51 (2)
C (24)	485 (6)	6967 (5)	1487 (2)	49 (1)
C (25)	1745 (6)	6657 (5)	1540 (2)	46 (1)
C (26)	2161 (5)	5639 (5)	1308 (2)	41 (1)
C (31)	857 (5)	2660 (4)	614 (2)	38 (1)
C (32)	384 (5)	1984 (5)	949 (2)	46 (1)
C (33)	-504 (6)	1061 (6)	880 (2)	59 (2)
C (34)	-983 (6)	790 (5)	445 (3)	62 (2)
C (35)	-579 (6)	1430 (5)	99 (2)	53 (2)
C (36)	320 (5)	2359 (5)	183 (2)	44 (1)
C (41)	6720 (30)	9770 (20)	2378 (11)	280 (20)
C (42)	6877 (19)	9110 (30)	2030 (8)	206 (16)
C (43)	6514 (19)	7940 (20)	1925 (5)	180 (9)
C (44)	5641 (14)	7444 (12)	2193 (7)	157 (5)
C (45)	5341 (11)	8143 (19)	2515 (5)	130 (4)
C (46)	5809 (18)	9240 (20)	2596 (5)	162 (7)
B	1923 (5)	3752 (5)	734 (2)	32 (1)